10
50
45
2
Copy

Journal of Research

of the

National Bureau of Standards

SEPTEMBER 1950

VOLUME 45 NUMBER 3

U. S. DEPARTMENT OF COMMERCE
Charles Sawyer, Secretary
NATIONAL BUREAU OF STANDARDS
E. U. Condon, Director

SEPTEMBER 1950
VOLUME • 45
NUMBER 3

JOURNAL OF RESEARCH

of the

NATIONAL BUREAU OF STANDARDS

PERIODICALS OF THE NATIONAL BUREAU OF STANDARDS

As the principal agency of the Federal Government for fundamental research in physics, chemistry, mathematics, and engineering, the National Bureau of Standards conducts projects in fourteen fields: electricity, optics, metrology, heat and power, atomic and radiation physics, chemistry, mechanics, organic and fibrous materials, metallurgy, mineral products, building technology, applied mathematics, electronics, and radio propagation. The Bureau has custody of the national standards of measurement and conducts research leading to the improvement of scientific and engineering standards and of techniques and methods of measurement. Testing methods and instruments are developed; physical constants and properties of materials are determined; and technical processes are investigated.

JOURNAL OF RESEARCH

Internationally known as a leading scientific periodical, the Journal presents research papers by authorities in the specialized fields of physics, mathematics, chemistry, and engineering. Complete details of the work are presented, including laboratory data, experimental procedures, and theoretical and mathematical analyses. Each of the monthly issues averages 85 two-column pages; illustrated. Annual subscription: domestic, $4.50; foreign, $5.50.

TECHNICAL NEWS BULLETIN

Summaries of current research at the National Bureau of Standards are published each month in the Technical News Bulletin. The articles are brief, with emphasis on the results of research, chosen on the basis of their scientific or technologic importance. Lists of all Bureau publications during the preceding month are given, including Research Papers, Handbooks, Applied Mathematics Series, Building Materials and Structures Reports, and Circulars. Each issue contains 12 or more two-column pages; illustrated. Annual subscription: domestic, $1.00; foreign $1.35.

BASIC RADIO PROPAGATION PREDICTIONS

The Predictions provide the information necessary for calculating the best frequencies for communication between any two points in the world at any time during the given month. The data are important to all users of long-range radio communications and navigation, including broadcasting, airline, steamship, and wireless services, as well as to investigators of radio propagation and ionosphere. Each issue, covering a period of one month, is released three months in advance and contains 16 large pages, including pertinent charts, drawings, and tables. Annual subscription: domestic, $1.00; foreign, $1.25.

Order all publications from the Superintendent of Documents
U. S. Government Printing Office, Washington 25, D. C.

The printing of this publication has been approved by the Director of the Bureau of the Budget, April 6, 1950.

W

B
wor
wor
mo
circ
pro
cap
var
wid
tio
as
imp
tio
resi

ϵ_i

co
ca
cir

wl

Journal of Research of the National Bureau of Standards Vol. 45, No. 3, September 1950 Research Paper 2123

Wide-Range Phase Control with Constant Attenuation by Adjustable Impedance in a Resistance-Loaded Bridged-Tee Network

By Myron G. Pawley

Phase may be shifted through a wide range without change in attenuation by means of a properly designed bridged-tee network. Equations are presented, and the necessary relations between circuit constants are deduced for phase control using an adjustable resistance, inductance, or capacitance located in a suitably selected branch of a bridged-tee network.

I. Introduction

Bridged-tee circuits are widely used as null networks [1].[1] This paper shows that bridged-tee networks may be devised for phase shifting or phase modulating and gives the necessary relations between circuit constants when the phase displacement is produced by an adjustable resistance, inductance, or capacitance in the proper branch of the tee. Advantages of these circuits will be seen to include: wide-range phase shift without change in attenuation; common ground for input and output circuits, as well as for one end of a single adjustable control impedance; large change in phase with small variation in control reactance; ability to work into a low resistance load; stability; and simplicity.

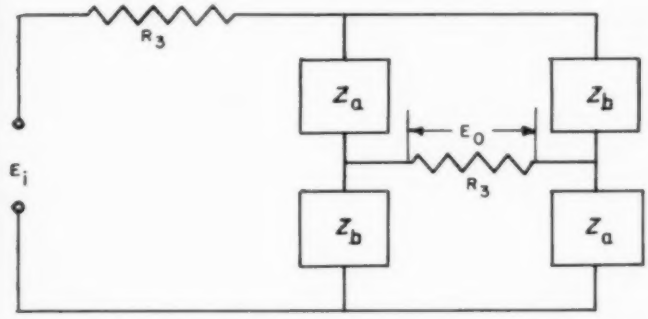

FIGURE 1. *Symmetrical lattice network with resistive load.*

A good general approach to the problem is to first consider the lattice network shown in figure 1. It can be shown that the transfer function [2] for this circuit can be written [3] as

$$\frac{E_o}{E_i}=\frac{R_3}{2}(y_{ao}-y_{bo}), \tag{1}$$

where

$$\left.\begin{aligned} y_{ao}&=\frac{1}{Z_{ao}}; \qquad y_{bo}=\frac{1}{Z_{bo}};\\ Z_{ao}&=R_3+Z_a; \qquad Z_{bo}=R_3+Z_b. \end{aligned}\right\} \tag{2}$$

[1] Figures in brackets indicate the literature references at the end of this paper.

For constant attenuation, α, with phase shift produced by variation in resistance or reactance in the circuit, one may write

$$\frac{E_0}{E_i}=\alpha\epsilon^{j\beta}, \tag{3}$$

where α is a constant independent of the variable that changes the phase angle β. Hence, one may represent this transfer function geometrically as a circular locus with pole at the center.

II. Variable Reactance Control of Phase with Constant Attenuation

If we desire to use an adjustable reactance as the control element, we can examine the expressions in terms of the components that Z_a and Z_b of figure 1 require to preserve the form of eq 3.

Referring to figure 1 and to eq 2, if

$$\left.\begin{aligned} &Z_a=R_a\\ \text{and}\qquad &\\ &Z_b=R_b+jX, \end{aligned}\right\} \tag{4}$$

where X may be inductive or capacitative, we obtain the lattice network of figure 2, a. Here,

$$\left.\begin{aligned} y_{ao}&=\frac{1}{R_3+R_a}\\ \text{and}\qquad &\\ y_{bo}&=\frac{1}{(R_3+R_b)\sqrt{1+\left(\frac{X}{R_3+R_b}\right)^2}}\epsilon^{-j\ \arctan\frac{X}{R_3+R_b}}\\ &=\frac{1}{R_3+R_b}\cos\theta\cdot\epsilon^{-j\theta}, \end{aligned}\right\} \tag{5}$$

where

$$\theta=\arctan\frac{X}{R_3+R_b}.$$

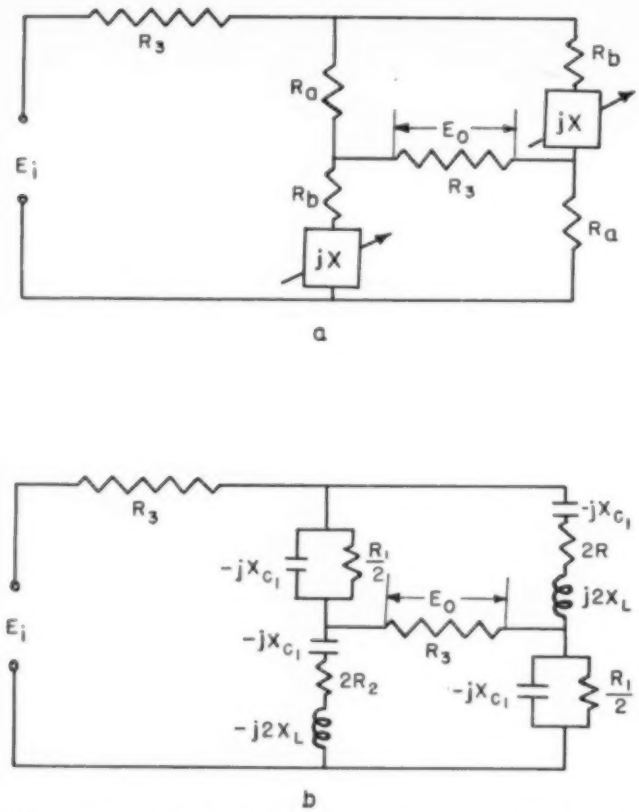

FIGURE 2. *Lattice networks for variable reactance control of phase with constant attenuation.*

A study of the geometry of the vectors representing the admittances y_{ao} and y_{bo} shows that the desired phase shift characteristics will be obtained in the circuit of figure 2, a, provided

$$R_a = R_3 + 2R_b. \tag{6}$$

In this case,

$$y_{ao} - y_{bo} = \frac{1}{R_3 + R_b}\left[\frac{1}{2} - \cos\theta\,(\cos\theta - j\sin\theta)\right]$$

$$= -\frac{1}{2(R_3 + R_b)}\,[\cos 2\theta - j\sin 2\theta]$$

$$= -\frac{1}{2(R_3 + R_b)}\,\epsilon^{-j2\theta},$$

and eq 1, which represents the transfer function for the circuit of figure 1, and for that of figure 2, a, may be written

$$\left.\begin{aligned} &\frac{E_o}{E_i} = -\frac{R_3}{4(R_3 + R_b)}\,\epsilon^{-j2\theta}, \\ &\text{where} \\ &\theta = \text{arc tan}\,\frac{X}{R_3 + R_b}. \end{aligned}\right\} \tag{7}$$

Equation 7 is now in the form of eq 3, and therefore represents the transfer function for a lattice network giving constant attenuation when the phase is shifted by variation in reactance X.

Hence, the circuit of figure 1 becomes the desired phase shift network, shown in figure 2, a, provided Z_a and Z_b are as given by eq 4 and *provided the circuit constants are related as given in eq 6*.

The circuit shown in figure 2, b, also will be shown to satisfy these conditions, and hence will represent an example with the desired characteristics. Although lattice networks cannot always be converted to equivalent bridged-tee networks, this particular circuit was chosen because it may be converted to an equivalent bridged-tee. The lattice network is not generally convenient as a phase shifter, with constant attenuation, because simultaneous variation of the reactances in two arms would be required. The equivalent bridged-tee has the advantage of requiring the variation of only one reactance element for shifting the phase and of having the ground common to one side of the input and output, as well as to one end of the variable control reactance.

Examination of figure 2, b, shows that if we make $X_{C_1} \gg R_1$,

$$\left.\begin{aligned} &Z_a \doteq \frac{R_1}{2}, \\ &Z_b = 2R_2 + j(2X_L - X_{C_1}). \end{aligned}\right\} \tag{8}$$

These forms for Z_a and Z_b correspond to those given by eq 4. If, in addition,

$$\frac{R_1}{2} = R_3 + 4R_2, \tag{9}$$

the condition given in eq 6 is satisfied, and the circuit of figure 2, b, provides an example of the desired phase shift network. From eq 4, 7, 8, and 9, the transfer function may now be written

$$\left.\begin{aligned} &\frac{E_o}{E_i} = -\frac{R_3}{4(R_3 + 2R_2)}\,\epsilon^{-j2\theta}, \\ &\text{where} \\ &\theta = \text{arc tan}\,\frac{2X_L - X_{C_1}}{R_3 + 2R_2}. \end{aligned}\right\} \tag{10}$$

Equation 10, therefore, represents the transfer function for the circuit of figure 2, b, provided

$$\left.\begin{aligned} &X_{C_1} \gg R_1, \\ &\text{and} \\ &\frac{R_1}{2} = R_3 + 4R_2. \end{aligned}\right\} \tag{11}$$

Under these conditions, simultaneous variation of the reactances in the circuit of the symmetrical lattice network of figure 2, b, shifts the phase without varying the attenuation.

An equivalent bridged-tee network [4] shown in figure 3 may be derived from the lattice of figure 2, b. The variable shunt capacitor, shown connected with a dashed line, shows one means of varying the effec-

ive reactance for producing phase shift. This will be described more fully later in this paper. The transfer function for this bridged-tee network (not including the added capacitative reactance X_{C_2}) is the same as that given in eq 10 for the corresponding lattice network of figure 2, b.

In the bridged-tee circuit of figure 3, the phase may be shifted by varying the inductance, for example, with an adjustable core reactor or with a saturable reactor. The attenuation will not remain constant unless the resistance R_2 of the reactor remains constant. In laboratory tests, R_2 was found not to change appreciably when the circuit reactance was changed by varying an external capacitance across the high-Q inductor. With this mode of operation, the circuit performed closely to theoretical predictions.

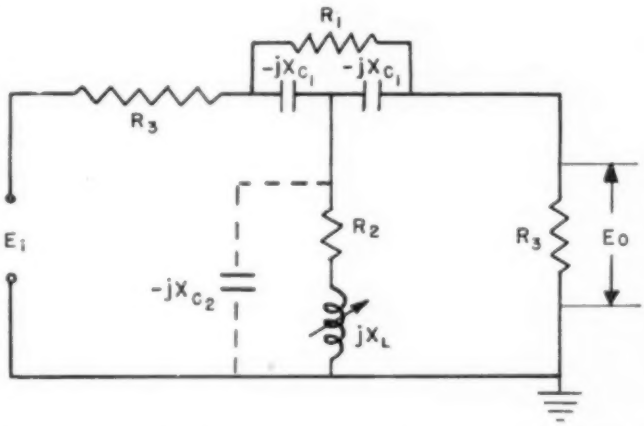

FIGURE 3. *Bridged-tee equivalent to lattice network of figure 2, b.*

Examination of the transfer function, eq 10, for the bridged-tee of figure 3 shows that as the resistance R_2 of the inductor approaches zero, (Q approaches ∞) the attenuation approaches a minimum of one-fourth, and the phase sensitivity, with variation in reactance, approaches a maximum.

When X_L is considered the variable in figure 3, with $C_2=0$, it is convenient to write eq 10 in a different form:

Let

$$\delta L=\frac{2X_L}{X_{C_1}}=2\omega^2C_1L. \tag{12}$$

In this case, eq 10 becomes

$$\left.\begin{aligned}&\frac{E_o}{E_i}=-\frac{R_3}{4(R_3+2R_2)}\epsilon^{-j2\theta},\\ \text{where}\quad&\theta=\text{arc tan}\frac{(\delta_L-1)X_{C_1}}{R_3+2R_2},\end{aligned}\right\} \tag{13}$$

Equation 13, therefore, represents the transfer function for the bridged-tee of figure 3, with $C_2=0$, and with δ_L proportional to L, as indicated by eq 12. As explained previously, for constant attenuation with variable phase shift, the conditions given with eq 11 are necessary.

When X_{C2} is considered the variable in figure 3, it is convenient to write eq 10 in another form:

Assume the Q of the inductor to be high, and that the network is adjusted for $X_L=X_{C1}/2$. Let

$$\delta_C=\frac{X_L}{X_{C_2}}=\frac{X_{C_1}}{2X_{C_2}}=\omega^2LC_2\ll 1. \tag{14}$$

If we replace X_L in eq 10 by the parallel combination of X_L and X_{C2} in figure 3, then make $X_L=X_{C1}/2$, and substitute for X_{C2} from eq 14, eq 10 becomes

$$\left.\begin{aligned}&\frac{E_o}{E_i}=-\frac{R_3}{4(R_3+2R_2)}\epsilon^{-j2\theta},\\ \text{where}\quad&\theta=\text{arc tan}\frac{X_{C_1}\delta_C}{R_3+2R_2}\\ &\delta_C\ll 1.\end{aligned}\right\} \tag{15}$$

Equation 15 then represents the transfer function for the bridged-tee of figure 3, with δ_C proportional to C_2, as indicated by eq 14. As in the preceding case, for constant attentuation with variable phase shift, the conditions given with eq 11 are necessary.

Attenuation and phase characteristic curves, with phase shift and attenuation shown as functions of shunt capacitance C_2, are given in figure 4, a, for the bridged-tee network of figure 4, c, operating at a frequency of 4,170 c/s. Figure 5, a, shows similar curves for the bridged-tee phase modulator of figure 5, b, operating at 29.1 Mc/s. These curves show the large changes in phase that may be secured by small changes in capacitance, particularly at the higher frequency. Figure 4, a, shows that, even at 4,170 c/s, 90° phase shift is produced by a shunt capacitance change of only 25 $\mu\mu$f. As shown in figure 5, a, at 29.1 Mc/s, a phase shift of 90° is produced by a capacitance change of only 2 $\mu\mu$f.

Inspection of eq 10, giving the transfer function for the networks of figures 2, b, and 3, shows that the attenuation is independent of frequency in the lattice network as well as in its equivalent bridged-tee network. Figure 4, b, shows the attenuation and phase curves for the bridged-tee of figure 4, c, when $C_2=0$ and the frequency is varied.

III. Variable Resistance Control of Phase with Constant Attenuation

If we desire to use a variable resistor as the control element for shifting phase, we can examine the components of Z_a and Z_b of figure 1 that will make eq. 1 assume the form of eq. 3.

Referring to figure 1 and to eq. 2, if

$$\left.\begin{aligned}&Z_a=jX_a\\ \text{and}\quad&Z_b=R_b+jX_b\end{aligned}\right\}, \tag{16}$$

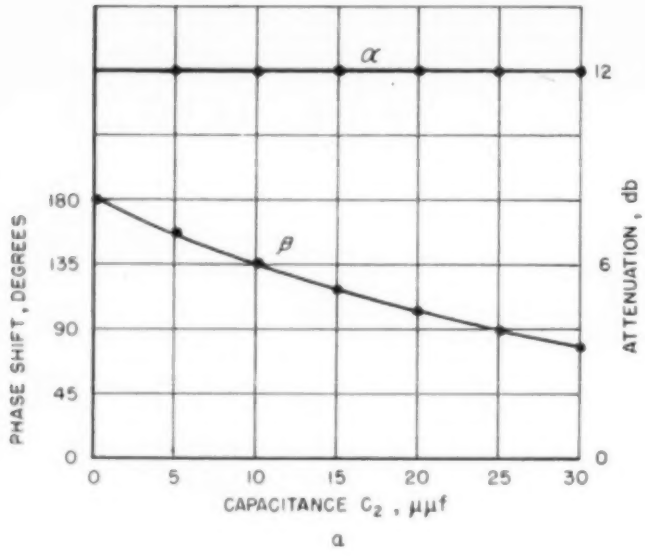

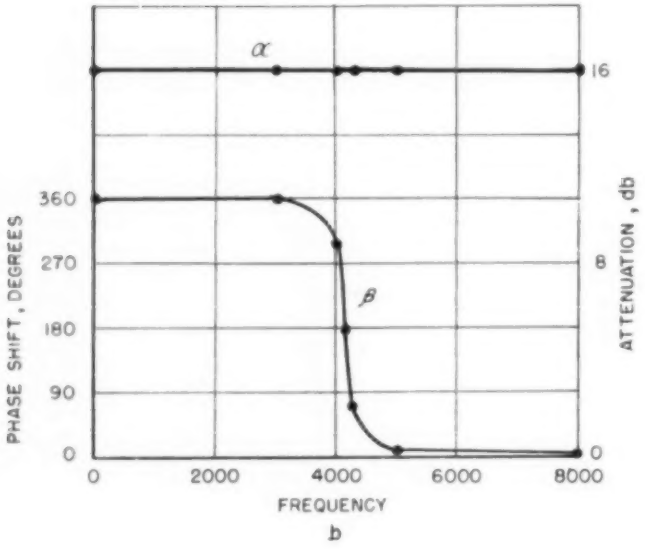

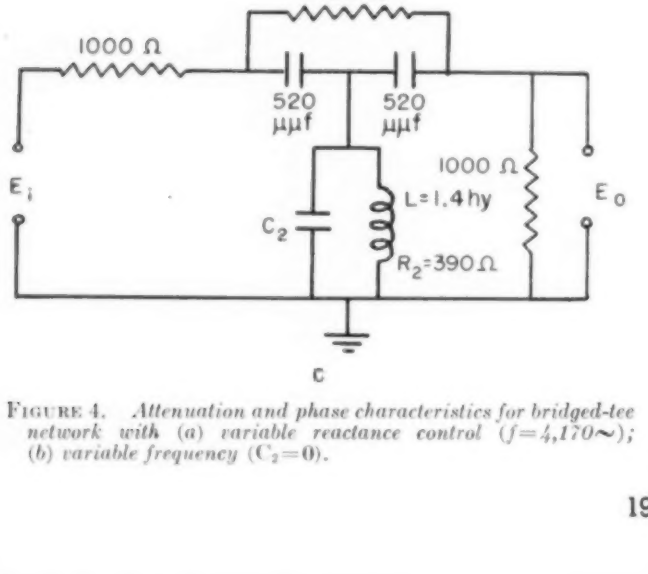

FIGURE 4. *Attenuation and phase characteristics for bridged-tee network with (a) variable reactance control (f=4,170∼); (b) variable frequency (C_2=0).*

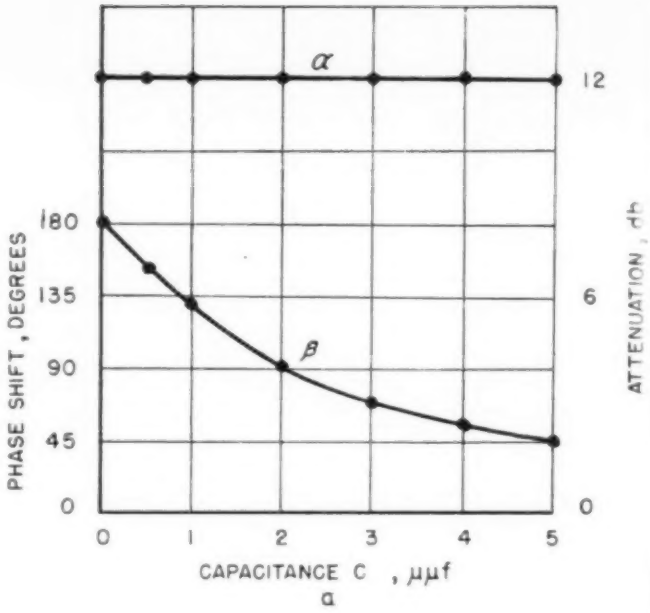

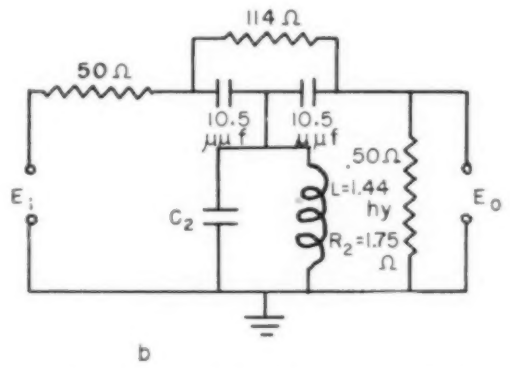

FIGURE 5. *Attenuation and phase characteristics for bridged-tee network with variable reactance control (f=29.1 Mc).*

where X_a and X_b are of the same sign, we obtain the lattice network of figure 6, a. If we assume $|X_a| \gg R_3$,

$$\left.\begin{aligned} y_{ao} &= -j\frac{1}{X_a} \\ \text{and} \\ y_{bo} &= \frac{1}{X_b\sqrt{\left(\frac{R_3+R_b}{X_b}\right)^2+1}}\,\epsilon^{-j \arctan \frac{X_b}{R_3+R_b}} \\ &= \frac{1}{X_b}\sin\theta\cdot\epsilon^{-j\theta}, \end{aligned}\right\} \quad (17)$$

where

$$\theta = \arctan X_b/(R_3+R_b).$$

A study of the geometry of the vectors representing the admittances y_{ao} and y_{bo} shows that the desired

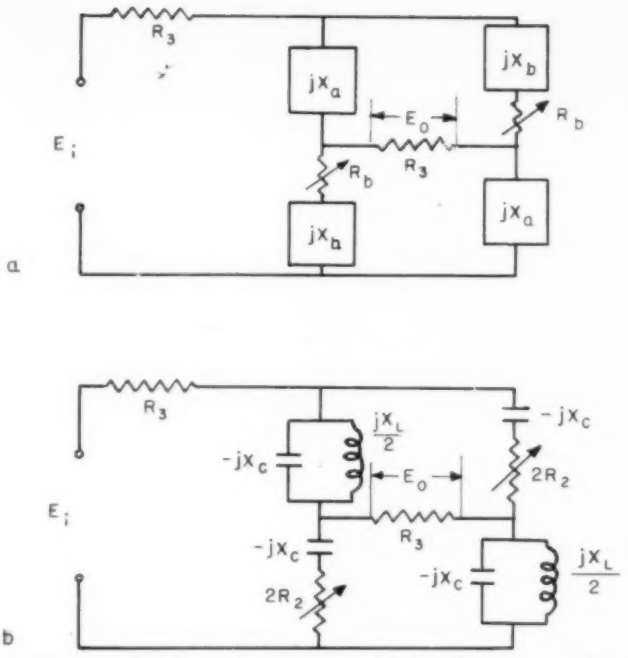

FIGURE 6. *Lattice networks for variable resistance control of phase with constant attenuation. (a) X_a and X_b have same sign.*

phase shift characteristics will be obtained in the circuit of figure 6, a, provided

$$X_a = 2X_b. \tag{18}$$

In this case,

$$y_{ao} - y_{bo} = \frac{1}{2X_b}\left[-j - 2\sin\theta\,(\cos\theta - j\sin\theta)\right]$$

$$= -\frac{j}{2X_b}\left[\cos 2\theta - j\sin 2\theta\right]$$

$$= -j\,\frac{1}{2X_b}\epsilon^{-j2\theta},$$

and eq. 1, which represents the transfer function for the circuit of figure 1, and for that of figure 6, a, may be written

$$\left.\begin{aligned} &\frac{E_o}{E_i} = -j\,\frac{R_3}{4X_b}\,\epsilon^{-j2\theta}, \\ &\text{where} \\ &\theta = \text{arc tan}\,\frac{X_b}{R_3 + R_b}. \end{aligned}\right\} \tag{19}$$

Equation 19 is now in the form of eq 3, and therefore represents the transfer function for a lattice network giving constant attenuation when the phase is shifted by adjusting the resistance R_b.

Hence, the circuit of figure 1 becomes the desired phase shift network, shown in figure 6a, provided the necessary relation in equation 18 as fulfilled and Z_a and Z_b are as given in eq 16.

The circuit shown in figure 6b, also will be shown to satisfy these conditions, and hence will represent an example with the desired transfer function. Although, as mentioned before, lattice networks cannot always be converted to equivalent bridged-tee networks, this particular circuit was chosen because it may be converted to an equivalent bridged-tee. As in the previous case, this lattice network is not generally convenient for use in phase shifting because for constant attenuation, simultaneous proportional adjustment of the resistance in two arms would be required. The equivalent bridged-tee has the advantage that the phase may be shifted by adjusting only one resistance element. It also offers the advantage of a common ground for one side of the input and output and one end of the adjustable phase-control resistor.

Examination of figure 6b, shows that, if we assume the Q of the inductor to be high,

$$\left.\begin{aligned} &Z_a \doteq j\,\frac{X_L X_C}{2X_C - X_L}, \\ &\text{and} \\ &Z_b = 2R_2 - jX_C. \end{aligned}\right\} \tag{20}$$

These forms for Z_a and Z_b correspond to those given by eq 16. If, in addition,

$$\left.\begin{aligned} &\frac{X_L X_C}{X_L - 2X_C} = 2X_C, \\ &\text{or} \\ &X_L = 4X_C, \end{aligned}\right\} \tag{21}$$

the condition given in eq 18 is satisfied, and the circuit of figure 6b, provides an example of the desired phase shift network. From eq 16, 19, 20, and 21, the transfer function may now be written

$$\left.\begin{aligned} &\frac{E_o}{E_i} = j\,\frac{R_3}{4X_C}\,\epsilon^{+j2\theta}, \\ &\text{where} \\ &\theta = \text{arc tan}\,\frac{X_C}{R_3 + 2R_2} \end{aligned}\right\} \tag{22}$$

Equation 22, therefore, represents the transfer function for the circuit of figure 6, b, provided

$$\left.\begin{aligned} &Q\ (\text{inductor}) \gg 1, \\ &\text{and} \\ &X_L = 4X_C \gg 2R_3. \end{aligned}\right\} \tag{23}$$

Under these conditions, simultaneous variation of the resistances R_2 in the circuit of figure 6, b, shifts the phase without varying the attenuation.

Figure 7 shows the equivalent bridged-tee network [4] corresponding to the lattice of figure 6, b. The transfer function for this bridged-tee network is the same as that given in eq 22 for the corresponding lattice network of figure 6, b. In this bridged-tee network (fig. 7), the phase may be shifted, without variation in attenuation, by varying the single resistance R_2. Examination of eq 22 shows that the magnitude of the attenuation is proportional to the ratio $R_3/4X_C$. This ratio must, however, be consistent with the relation given with eq 23, in order

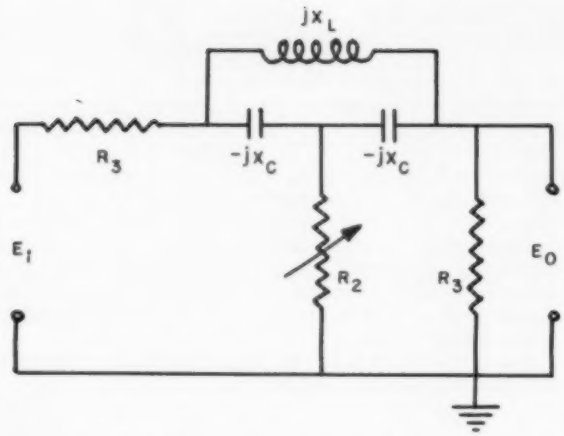

FIGURE 7. *Bridged-tee equivalent to lattice network of figure 6, b.*

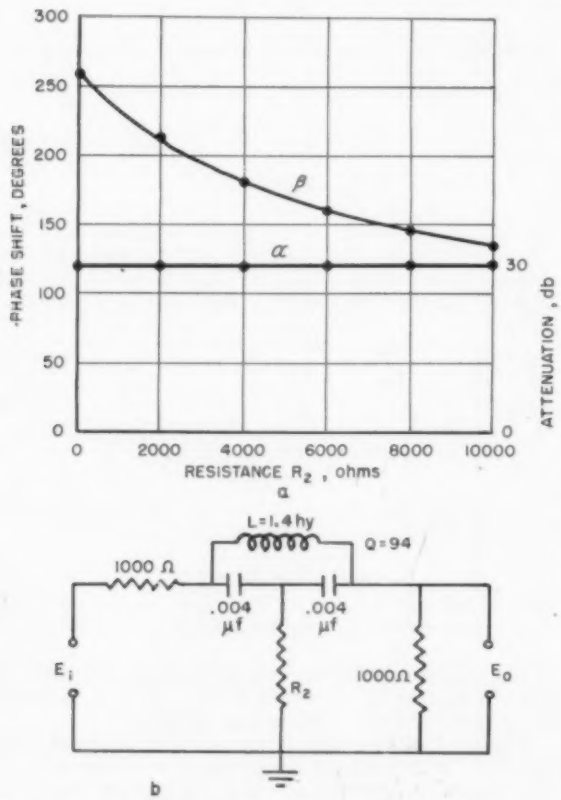

FIGURE 8. *Attenuation with phase characteristics for bridged-tee network with variable resistance control ($f=4{,}170$) ~.*

that the attenuation remain constant with variatiou in phase when R_2 is varied.

Attenuation and phase characteristic curves, with phase shift and attenuation shown as functions of control resistance R_2, are given in figure 8, a, for the bridged-tee network of figure 8, b, operating at 4,170 c/s.

IV. Geometrical Interpretation

Equation 1 shows that the transfer function for the phase shift networks discussed in this paper may be considered as the difference between two admittances, except for a constant multiplier.

Figure 9, a, shows plots of the admittance loci y_{ao} and y_{bo} for the bridged-tee circuit of figure 3, wherein the phase is shifted by varying the reactance without producing any change in attenuation. Examination of eq 5 shows that, for this circuit, y_{ao} is a constant vector independent of reactance X, whereas y_{bo} is a vector whose origin rests at the extremity of the horizontal diameter of a circular locus and whose terminus moves along the circle as the reactance X is varied. Examination of figure 9, a, shows that if the length of the vector y_{ao} is made equal to the radius of the circular locus for y_{bo}, the difference $y_{ao}-y_{bo}$, representing the transfer function for the circuit of figure 3, will appear as a vector of constant length rotating in a circle, as pictured in figure 9, b. The attenuation is thus seen to remain constant when the phase is changed by adjusting the value of the reactance X. These relations are represented analytically in eq 5 to 7, inclusive. Equation 6 gives the analytical relation corresponding to the equality in length of the vector y_{ao} with the radius of the circular locus for y_{bo}, as pictured in figure 9, a, and, b.

Figure 10, a, shows plots of the admittance loci y_{ao} and y_{bo} for the bridged-tee circuit of figure 7, wherein the phase is shifted without variation in attenuation by changing the value of the resistance. Examination of eq 17 shows that for this circuit, y_{ao} is a constant vector (along the axis of imaginaries) independent of resistance R_b, whereas y_{bo} is a vector whose origin rests at the extremity of the vertical diameter of a circular locus and whose terminus moves along the circle as the resistance R_b is varied. Examination of figure 10, a, shows that if the length of the vector y_{ao} is made equal to the radius of the circular locus for y_{bo}, the difference $y_{ao}-y_{bo}$, representing the transfer function for the circuit of figure

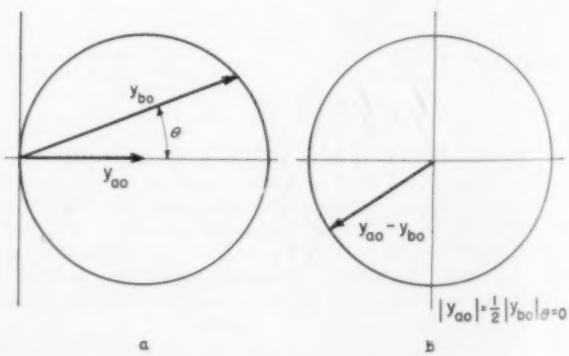

FIGURE 9. *Admittance loci for bridged-tee of figure 3.*

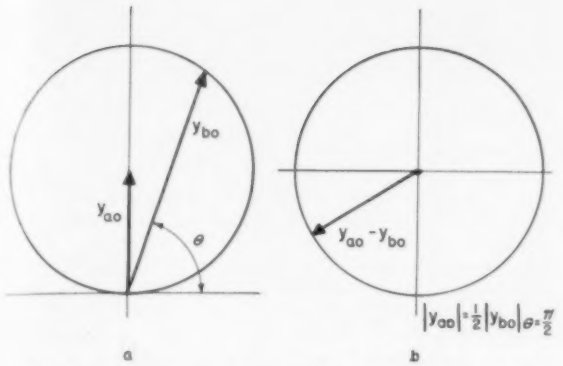

FIGURE 10. *Admittance loci for bridged-tee of figure 7.*

7, will appear as a vector of constant length rotating in a circle, as pictured in figure 10, b. The attenuation is thus seen to remain constant for change in phase produced by changing the value of resistance R_b. These relations are represented analytically in eq 17 to 19, inclusive. Equation 18 gives the analytical relation corresponding to the equality in length of the vector y_{ao} with the radius of the circular locus for y_{bo}, as pictured in figure 10, a, and b.

V. Related Null Network

Referring to figure 9a, which shows plots of admittance loci related to the bridged-tee circuit of figure 3, it can be seen that if y_{ao} is made equal in magnitude to the diameter of the circular locus for y_{bo}, as shown by the dashed line of figure 9, a, the difference $y_{ao}-y_{bo}$ will be a circular locus with the pole at the extremity of the horizontal diameter. Hence, as the reactance X is varied continuously, the resultant vector will shrink to a null when the vectors for y_{ao} and y_{bo} become equal. The corresponding analytical conditions can be derived readily from the relations given in eq 5. This manipulation results in the well-known relations for this bridged-tee when used as a null network.

It is interesting to observe that the only adjustment required to change the null network to the phase shift network of figure 3 is to change R_1 from $R_1=4R_2$, for the null condition, to the value given by eq 9 for the bridged-tee phase shift network.

VI. Impedance of Bridged-Tee Networks

The image impedance of the symmetrical lattice of figure 1 (with R_3 omitted) is

$$z_o=\sqrt{Z_aZ_b}. \tag{24}$$

For the lattice network of figure 2,b, and its equivalent bridged-tee shown in figure 3 (with R_3 omitted), the image impedance may be determined from the values of Z_a and Z_b given in eq 8. If $2X_L=X_{C1}$,

$$z_o=\sqrt{R_1R_2}. \tag{25}$$

This is the input impedance the bridged-tee of figure 3 would have if R_3 *in the input* were shorted, and the load were given the value

$$R_3=z_o=\sqrt{R_1R_2}. \tag{26}$$

Solving eq 9 and 26 simultaneously, we obtain

$$R_1=R_3=4R_2, \tag{27}$$

for the input impedance of the bridged-tee of figure 3 if R_3 *in the input* were shorted. The impedance looking back into this network from the load is

$$R_o=R_3=4R_2, \tag{28}$$

if the source impedance is equal to R_3. The input and output impedances given by eq 27 and 28 for the bridged-tee of figure 3 are minimum values existing when $2X_L=X_{C1}$. These impedances become reactive when the phase is shifted by varying the circuit reactance from this value.

The input and output impedances of the bridged-tee of figure 7 may be shown to vary from $-j4X_C/3$ when $R_2=0$ to $-j4X_C$ when $R_2=\infty$. For intermediate values of R_2, these impedances include a resistive component.

VII. Applications

The bridged-tee phase shifting circuits described in this paper were developed originally for use with variable-resistance, or variable-reactance telemetering pickup devices to produce phase modulation in multiplex time-division telemetering systems and frequency modulation in multiplex frequency-division telemetering systems. Other possible applications include use as a phase shifter in servo loops including two-phase motors, and use as a phase modulator at high frequencies. The circuit of figure 5, b, with phase and attenuation characteristics shown in figure 5, a, was demonstrated successfully in the laboratory as a phase modulator at 29 Mc/s. In this application, modulation was effected by variation of shunt capacitance with a reactance modulator. Alternately, the shunt capacitance could be varied by utilizing a barium-strontium titanate element whose capacitance changes with variation in modulating voltage.

For voltage modulation of phase, the bridged-tee of figure 7 was tested with the variable resistance R_2 replaced by a biased varistor as shown in figure 11, b. Static tests at 7,250 kc indicated excellent linearity of phase versus bias voltage over a 90° phase shift, as shown in the experimental curve of figure 11, a. The nonlinear characteristic of the biased varistor compensates for the nonlinear phase characteristic of the bridged-tee network, resulting in a remarkably linear phase response over the 90° range. As seen from the theory of the bridged-tee phase shifter above, this range of modulation is effected with no change in attenuation. The loading effect of the net-

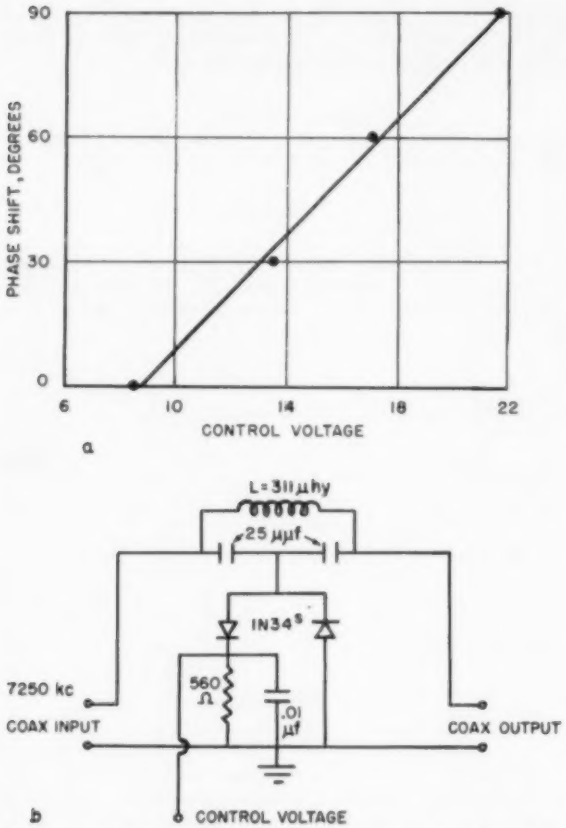

FIGURE 11. *Phase shift versus control voltage for bridged-tee phase modulator (f=7,250 kc).*

work during modulation is not generally serious, since the input reactance of the network decreases to only $-j4X_C/3$ ohms when R_2 becomes zero.

Another application of the bridged-tee of figure 3 is suggested by the previously mentioned property of this network of giving constant attenuation with variation in frequency as shown in figure 4, b. Two bridged-tee networks in tandem, properly adjusted, result in a constant phase shift independent of frequency over a wide range. This combination of bridged-tee networks may have advantages over lattice networks that have been described recently [5, 6] for this purpose, particularly since the bridged-tee is single-ended and functions when loaded. Hence, no phase-inverting and isolating vacuum tube amplifiers should be required with this bridged-tee arrangement, although the attenuation through the two bridged-tee networks may be a disadvantage in some applications.

VIII. References

[1] F. E. Terman, Radio engineers' handbook, p. 918 (McGraw-Hill Book Co., New York, N. Y., 1943).

[2] I. A. Greenwood, Jr., J. V. Holdam, Jr., and D. MacRae, Jr., Electronic instruments, Radiation Laboratory Series **21,** 230 (McGraw-Hill Book Co., Inc., New York, N. Y., 1948).

[3] E. A. Guillemin, A method of representing the insertion loss and angle of symmetrical networks (manuscript circulated to staff members of Radiation Laboratory during World War II).

[4] H. Lauer, R. Lesnick, and L. Matson, Servomechanism fundamentals, 1st ed., p. 158 (McGraw-Hill Book Co., Inc., New York, N. Y., 1947).

[5] R. B. Dome, Wide-band phase shift networks, Electronics **19,** 112 to 115 (Dec. 1946).

[6] David G. C. Luck, Properties of some wide-band phase-lifting networks, Proc. IRE **37,** 147 to 151 (Feb. 1949).

WASHINGTON, March 28, 1950.

Journal of Research of the National Bureau of Standards Vol. 45, No. 3, September 1950 Research Paper 2124

Stability of Dextrose Solutions of Varying pH

By Emma J. McDonald

A study has been made of the rate of the initial decomposition reaction taking place in dextrose solutions of varying pH. From the change in direct optical rotation over a period of time velocity constants have been calculated for eight values of pH. The results indicate that dextrose solutions are most stable at about pH 4.

I. Introduction

A great deal of work has been reported in the literature concerning the decomposition of reducing sugars in acid and in alkaline solutions. However, there is little to be found that gives an explanation or measure of the relation that exists between the pH and the stability of aqueous dextrose solutions. The wide use of dextrose solutions as standards in methods of sugar analysis has led to this investigation. In addition, aqueous solutions of dextrose find application in the practice of medicine where the solutions are stored in a sterile condition in ampoules or in bottles. A great variety of food products, both naturally occurring and manufactured, contain dextrose, often as one of the main constituents. Fruit juices, honey, table sirups, and molasses are examples of this group.

In the presence of aqueous acids, dextrose undergoes condensation reactions, forming disaccharides and possibly higher oligosaccharides. The products of this primary reaction, as is to be expected, are of great variety as the mode of attachment of two dextrose molecules is unselective and depends upon the

particular hydrogen and hydroxyl removed during the condensation. Some authors have grouped the products together under the name isomaltose.[1]

From this mixture, as well as from "hydrol," the molasses of the dextrose industry, the disaccharide gentiobiose [1],[2] has been isolated.

By evaporating a 10-percent solution of dextrose in 1 percent of hydrochloric acid, Levene and Ulpts [2] obtained a disaccharide not further identified but having a specific rotation of 95° and only 12 percent of the reducing power of dextrose. More drastic action of acids on dextrose causes further dehydration. In general, hydroxymethylfurfural is formed by the removal of three molecules of water, and further loss of water results in the formation of formic acid and levulinic acid.

In alkaline solution, the familiar Lobry de Bruyn-Van Ekenstein transformation [3] occurs leading to an equilibrium between dextrose, levulose, and mannose, established by rearrangement of the common enediol. Kusin [4] reports that after 24 hours a glucose solution made alkaline with sodium hydroxide contained fructose and very little mannose. He found that the equilibrium composition is dependent upon the alkaline reagent used. Nef [5] has shown that the prolonged action of relatively strong alkali leads to a complete disintegration of the dextrose molecule with the possible formation of about 116 products. The discoloration of dextrose solutions and particularly that related to the initial decomposition is of interest to the canning industry. Therefore studies have been made concerning the color produced when dextrose solutions are heated under conditions used in preserving fruits and vegetables. Kroner and Kathe [6] have related the intensity of discoloration of 40-percent-dextrose solutions to pH. The values of the extinction coefficient (as measured with a Zeiss Pulfrich photometer) rapidly decreases from pH 1 to pH 2 and passes thru a minimum at approximately pH 2.5. After this point the color increases with pH. The minimum of discoloration therefore takes place between pH 2 and pH 3.

The present investigation is to be interpreted as qualitative in its findings; however, it does denote the relative stability of dextrose solutions where the rate of reaction can be followed. As to that range between pH 1 and pH 7 where decomposition takes place very slowly at 30° C, it is to be expected that the rate of decomposition continues in the trend indicated by the measured values. Experiments run at 100° and 70° C show this to be the case at these temperatures.

II. Method

In this work measurements have been made of the initial rate of decomposition of dextrose solutions of varying pH. This requires the determination of small changes in dextrose content. Except in the range of high acidity or alkalinity, these changes take place over a considerable period of time. The calculations involved in this study are based upon the change in optical rotation of a solution rather than on the determination of accurate specific rotations. Polariscopic measurements have the advantage of being a direct measurement of the change taking place with less error in reproducibility than one obtains with chemical methods. In some instances the products of decomposition alter the pH of the solution during the time of study. The pH of each solution was tested at various intervals and the adjustments required to obtain approximate constancy made. As it is impractical to follow the reaction until equilibrium is established, the procedure described by Jackson and Matthews [3] [7] in their study of the stability of levulose has been used in determining the equilibrium toward which this initial reaction is progressing. It is assumed that the decomposition reaction under consideration is unimolecular. The fact that essentially the same velocity constant is obtained for two solutions of different concentrations at a given pH substantiates this assumption. Uncertainties introduced by the complex nature of the reactions and the method of analysis limit the accuracy of the determination of velocity constants to ±50 percent.

In alkaline solution the period of time during which the reaction can be followed polariscopically is limited by discoloration. In acid solution there is no limit, but the time required to reach equilibrium is prohibitive. The results are therefore applicable only for comparing the stability of dextrose solutions during the initial decomposition period. In considering the keeping qualities of a dextrose solution, whether for use as a standard solution or for other purposes as discussed above, the chemist is concerned with the initial changes and hence with the decomposition reaction before the side reactions begin.

Pure dextrose hydrate was dissolved in buffer solutions of systematically varying pH to form solutions of about 10 percent with respect to anhydrous sugar.[4] For studying the more rapid reactions, a 50-percent solution of sugar was prepared that permitted rapid mixing after both the buffer and sirup solutions has acquired the temperature of the bath. The buffer solutions were prepared according to Clark and Sørensen [8]. When it was practical,

[1] The term isomaltose has also been provisionally used to designate 6-α-D-glucopyranosyl-β-D-glucopyranose. Although this sugar has not been obtained in crystalline form it has been identified by means of its crystalline octaacetate. (M. L. Wolfrom, L. W. Georges and I. L. Miller, J. Am. Chem. Soc. **71**, 125 (1949).

[2] Figures in brackets indicate the literature references at the end of this paper.

[3] The following details for calculating the equilibrium are quoted from [7].

"Polarizations are observed or read from a curve at exactly equal intervals of time. If a, b, c, d, etc. are the polarizations at the times, t_1, t_2, t_3, t_4, etc., the time intervals between observations being equal, we can set up a series of equations of the form,

$$k=\frac{1}{t_2-t_1}\log\frac{a-x}{b-x} \qquad (1)$$

in which k is the unknown velocity constant and x the polarization at equilibrium. Elimination of k between two of these equations gives

$$\frac{1}{t_2-t_1}\log\frac{a-x}{b-x}=\frac{1}{t_4-t_3}\log\frac{c-x}{d-x}$$

But as $t_2-t_1=t_4-t_3$,

$$\frac{a-x}{b-x}=\frac{c-x}{d-x}$$

Solving for x,

$$x=\frac{ad-bc}{a+d-b-c}. \qquad (2)"$$

[4] When necessary mercuric iodide was used to prevent the growth of mold.

898894—50——2

TABLE 1. *Hydrochloric acid and buffer solutions*

Average pH	Range of pH	Buffer	Average pH	Range of pH	Buffer
−2.61	Not measured.	14.5 M HCl.	8.0	8.0	KH_2PO_4, NaOH.
			8.6	9.1 to 8.1	glycine, NaOH.
−1.80	do	8.83 M HCl.	9.6	9.8 to 9.4	Do.
−1.43	do	6.81 M HCl.	10.7	10.8 to 10.6	Do.
+0.10	do	1 M HCl.	12.1	12.2 to 12.0	Na_2HPO_4, NaOH.

the dry constituents were added to the sugar solution. The pH of the resulting solution was measured with a glass electrode, and the measured value was used in the tabulation. The buffers used in the individual experiments are given in table 1.

The pH of the hydrochloric acid solutions were calculated from the work of Harned and Ehlers [9] and of Akerlof and Teare [10]. If one assumes that the activity of the hydrogen ion is equal to that of the hydrochloric acid, the pH of the solution may be calculated by the following formula:

$$pH = -\log m_H \cdot \gamma_{HCl} = -(\log m_H + \log \gamma_{HCl}),$$

where m=molality, γ=activity coefficient.

The reactions were followed by observing the change in optical rotation that took place over a period of time. These measurements were made with a Bates-type quartz wedge saccharimeter in a water jacketed polariscope tube. All polarizations at a given pH were measured under identical conditions in order to avoid errors that might enter if corrections had to be made for temperature and volume.

The decomposition of a dextrose solution at 70° C, in 5 molal hydrochloric acid (pH−0.92) was followed by observing polarization, by Munson and Walker's method [11] for reducing sugars, and by Somogyi's selective fermentation method in order to be assured that the value of k was independent of the method used in following the reaction. Table 2 shows the results of this comparison. It was concluded that in the acid region change of polarization might be used as a criterion of the initial rate of decomposition.

The details of the fermentation method are given since some modifications of the author's procedure were used. Somogyi [12] showed that in dextrose-maltose mixtures the fermentation of maltose can be completely suppressed during a period of time sufficient for the complete fermentation of dextrose if the pH of the solution is held at 7.2 to 7.4. The difference in reducing sugar before and after fermentation is then a measure of dextrose. In using the method, it was assumed that any other sugar likely to have been formed in the mixture was at least as resistant to fermentation as maltose.

TABLE 2. *Decomposition of dextrose at 70° C in 5 M HCl pH−0.92*

Time	Polarization		Munson and Walker reducing sugar method		Somogyi fermentation method	
	Percentage of initial reading	$k \times 10^3$	Percentage of initial reading	$k \times 10^3$	Percentage of initial reading	$k \times 10^3$
min						
0	100		100		100	
46	101.7	5.2	96.5	6.7	96.81	4.1
121	103.1	5.2	94.7	5.3	93.62	4.4
182	103.5	5.1	93.8	5.6		
283			93.3	5.6	93.09	4.1
Average		5.2		5.8		4.2

It was found convenient to use ordinary yeast cakes for the fermentation. These were washed by suspension in water and centrifugal sedimentation. In the sediment first obtained the starch settled out in a clearly visible layer at the bottom of the conical centrifuge tube. About two-thirds of the yeast, essentially free from starch, was scraped off and washed in the same manner three times more. From each yeast cake (13 grams) about 9 grams of moist sedimented yeast was obtained. To this was added an equal weight of water, which yielded a suspension thin enough to be drawn into a pipette and roughly measured. Four milliliters corresponding to 2 grams of moist yeast was used for an analysis.

Test tubes (17×150 mm) were graduated with indelible ink at the 25-ml volume point. Two identical samples of the sugar solution were taken, each containing about 7 mg of sugar. One sample was transferred to a calibrated test-tube, the other to a 25-ml volumetric flask. The sample in the test-tube was diluted to about 15 ml, and 4 ml of the yeast suspension was added. One drop of phenol red was added and the solution was kept perceptibly pink by dropwise addition of 0.2 N sodium hydroxide. A rubber stopper was inserted and the test-tube was inverted after each addition to insure thorough mixing. The fermentation proceeded rapidly and was usually practically complete in 6 to 7 minutes. It was allowed, however, to continue for 25 minutes. The tube was then filled to the 25-ml mark, mixed, and sedimented. A 5-ml aliquot was taken for analysis.

Reducing sugar was determined in the samples by Somogyi's modification of Shaffer and Hartmann's micro method [11].

In the alkaline region, a 12.5-molal sodium hydroxide solution of pH 12.1 containing dextrose was kept at 5° C, and the change followed by direct polarization measurements and by Munson and Walker's method for reducing sugar. Although the latter method is not selective for dextrose in the presence of levulose and mannose, the difference in the reducing effect of these sugars on the reagent was sufficient that it could be used as a measure of the change that was taking place. At this temperature the change was slow, making a considerable number of observations possible. The agreement in the values for k arrived at by the two methods is well within the experimental error as shown in table 3.

III. Experimental Data and Conclusions

Thirty degrees centigrade was selected as the most suitable temperature at which to carry on the series of reactions. The solutions were prepared as

described previously, and the polarization observations were made at time intervals depending upon the rate of the reaction in question. Table 4 gives the

TABLE 3. *Decomposition of dextrose at 5° C in 12.5 M NaOH (pH —12.1)*

Time	Polarization		Dextrose by Munson and Walker reducing sugar method	
	Percentage of initial reading	$k \times 10^5$	Percentage of initial reading	$k \times 10^5$
min				
0	100		100	
4,595	82.4	1.8	99.18	1.0
11,375	59.5	1.9	98.10	1.0
30,181	26.1	1.8	95.5	1.2
43,260	11.1	1.9	95.2	.9
60,810	4.5	1.8	92.4	2.1
Average		1.8		1.2

TABLE 4. *Experimental data at 30° C*

Time	Rotation °S
pH −2.6	
min	
0	30.53
3	30.59
72	31.34
150	31.96
225	32.33
310	32.80
439	33.31
$k=2.2\times10^{-2}$, $\log 1/k=1.6$	
pH −1.78	
min	
0	31.74
1,364	33.23
3,015	33.89
4,345	34.50
8,940	35.05
$k=1.6\times10^{-4}$, $\log 1/k=3.8$	
pH −1.44	
min	
0	31.02
1,360	32.10
4,506	32.85
7,236	33.03
$k=2.2\times10^{-4}$, $\log 1/k=3.6$	
pH 0	
min	
0	29.05
191,660	30.10
289,550	30.29
423,530	30.38
$k=3.9\times10^{-6}$, $\log 1k=5.4$	

Time	Rotation °S
pH 8	
min	
0	26.81
50,040	26.39
94,985	26.33
$k=7.7\times10^{-7}$, $\log 1/k=6.1$	
pH 8.6	
min	
0	27.83
1,463	27.56
11,360	27.04
71,760	25.08
215,926	25.10
$k=5.4\times10^{-6}$, $\log 1k=5.3$	
pH 9.6	
min	
0	30.07
710	28.65
1,361	28.33
6,044	26.68
15,840	22.76
$k=5.2\times10^{-5}$, $\log 1/k=4.3$	
pH 10.7	
min	
0	29.78
1,450	22.06
2,873	17.05
4,636	12.82
5,993	10.62
9,960	7.48
12,812	6.50
20,460	6.05
$k=1.3\times10^{-4}$, $\log 1/k=3.9$	

TABLE 5. *Calculated equilibrium rotations expressed as percent of initial rotation*

pH	Equilibrium rotation	pH	Equilibrium rotation
−2.6	108.5	8	76.6
−1.78	107.0	8.6	70.0
−1.44	106.6	9.6	65.0
0	104.6	10.7	25.0

experimental data. The calculated equilibrium rotations are given in table 5.

At each pH a different reaction or series of reactions is being considered. However, as the equilibrium rotation (table 5) toward which the individual reactions are proceeding has been calculated, the values of k [5] are independent of the reaction taking place. The values of log $1/k$ have been plotted against pH and a curve of the form indicated by measurements at higher temperatures drawn through the points. This curve (fig. 1) indicates that dextrose solutions are most stable at some point between pH 3 and pH 5.

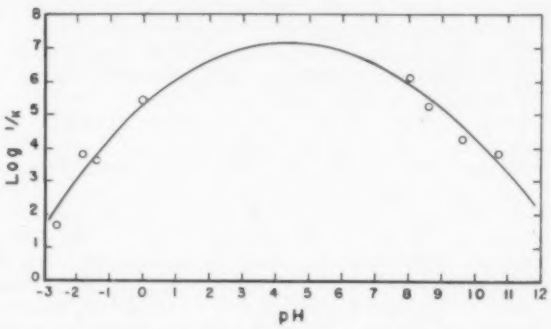

FIGURE 1. *Relation between the initial rate of decomposition of aqueous dextrose solutions and their pH.*

[1] H. Berlin, J. Am. Chem. Soc. **48,** 2627 (1926).
[2] P. A. Levene and R. Ulpts, J. Biol. Chem. **64,** 475 (1925).
[3] C. A. Lobry de Bruyn and W. A. Van Ekenstein, Rec. trav. chim. **14,** 156, 203 (1895); **16,** 256 (1897).
[4] A. Kusin, Ber. **69,** 1041 (1936).
[5] J. U. Nef, Liebigs Ann. Chem. **335,** 191 (1904); **357,** 214 (1907); **376,** 1 (1910); **403,** 204 (1914).
[6] W. Kroner and H. Kathe, Ind. Eng. Chem. **31,** 248 (1939).
[7] R. F. Jackson and J. A. Matthews, J. Research NBS **11,** 619 (1933) RP611.
[8] W. M. Clark, The determination of hydrogen ions (The Williams and Wilkins Co., Baltimore, Md., 1928).
[9] H. S. Harned and R. W. Ehlers, J. Am. Chem. Soc. **54,** 1350 (1932); **55,** 652, 2179 (1933).
[10] G. Akerlof and J. W. Teare, J. Am. Chem. Soc. **59,** 1855 (1937).
[11] Official and Tentative Methods of the Association of Official Agricultural Chemists. 6th ed. (1945).
[12] M. Somogyi, J. Biol. Chem. **119,** 741 (1937).

WASHINGTON, April 18, 1950.

[5] All values of k are expressed in units of min^{-1}

Journal of Research of the National Bureau of Standards Vol. 45, No. 3, September 1950 Research Paper 2135

Infrared Spectrum of Chlorofluoromethane

By Earle K. Plyler and Mary A. Lamb

In order to compare its spectrum with that of other halogenated methanes, the infrared spectrum of chlorofluoromethane has been measured in the gaseous state from 2 to 30 microns. The longest wavelength band was observed at 26 microns. Twenty-five bands have been observed with cells of 5, 60, and 100 centimeters in length and with gas pressures up to 60 centimeters of mercury. Nine of the observed bands have been classified as fundamentals, and the remaining bands are attributed to harmonics and combinations. Several bands in the region from 1.5 to 2.5 microns were measured on a high resolution grating instrument, and it was possible to resolve each of seven bands into a series of lines in this region. These bands are located at 1.657, 1.682, 1.700, 1.755, 2.229, 2.287, and 2.436 microns; the separation of the rotational lines is of the order of 2.3 cm^{-1} for these bands.

The infrared spectra of a number of substituted methanes have been measured by many observers.[1] The change in the spectrum when the halogens are substituted for the hydrogen atoms is marked, and there is a general shift of all the corresponding fundamental bands to longer wavelengths. When all the hydrogens of methane are substituted by the halogens, no fundamental bands occur at wavelengths less than 7μ. In the case of chlorofluoromethane the vibrations of the two hydrogens give rise to strong bands in the region of 3.5 μ, and the contributions of the halogen to the vibrations occur in the region from 7 to 26 μ. Of the nine fundamental bands, the one with longest wavelength is observed at 26 μ. Seventeen harmonic and overtone bands are present in the spectrum when moderate amounts of the gas are measured. Thirteen of these bands were observed in the short wavelength region. The spectrum of chlorofluoromethane is similar to that of dichloromethane and difluoromethane. The locations of the nine fundamentals of these three compounds are compared, and it is found that the bands of chlorofluoromethane have characteristics similar to those of the corresponding bands of dichloromethane and difluoromethane.

The spectrum of chlorofluoromethane was measured from 2 to 30 μ on a Perkin-Elmer infrared spectrometer using prisms of sodium chloride, lithium fluoride, potassium bromide, and thallium bromide-iodide. In the region of 1.5 to 2.6 μ the spectrum was observed by the use of a grating spectrometer. A 15,000 line per inch grating with the ruling surface 7¼ in. in width and 4½ in. in height was used in the spectrometer, and a 1-m off-axis mirror was used for collimating the radiation. A PbS cell was used for the detector. The high resolution available with this instrument permitted observation of fine structure in some of the bands. The angular position of the grating was noted by a Veeder counter, and the readings were related to wavelengths by use of the higher orders of the emission lines of mercury. A Cetron mercury lamp, similar to the S–1 sun lamp, was used as the source. The image of one of the hot electrodes was focussed on the entrance slit, and the absorption spectrum was measured. Superimposed on the recorder trace of the chlorofluoromethane absorption spectrum were the mercury emission lines. With these observations the wavelengths of the absorption bands could be located accurately. The wavelength determinations for separate trials checked to about one part in 24,000. For higher resolution a tungsten ribbon lamp with a quartz window was used as the source. When it was operated at 2,700° K, it was possible to use slits of 0.025 mm in the 1.6-μ region.

Three cells with thicknesses of 5, 60, and 100 cm were used for containing the gas. The different pressures of gas are recorded on the figures. The 100-cm cell, which was used in observing the 26-μ band, had polyethylene windows, and could not be evacuated. It was filled by flushing with the gas, and the precise amount in the cell was not determined.

The chlorofluoromethane was supplied by Kinetic Chemicals, Inc. That it was of sufficient purity for absorption measurements was indicated by tests on the mass spectrometer. It was found to consist of 97.3 percent of chlorofluromethane; the 2.7 percent is made up of related methanes. Comparison also was made with the infrared spectra of other substituted methanes, and none of the strong bands of these compounds were present in the spectrum of chlorofluoromethane with the cell thicknesses used in this investigation.

In figure 1 is shown the spectrum of chlorofluoromethane from 2 to 31 μ. The region from 15 to 22 μ, measured with a potassium bromide prism, has not been included in the figure since no bands were observed in this region when a 5-cm cell with a gas pressure of 50 cm of mercury was used. Two inserts of the bands at 4.72 and 7.40 μ are included on an enlarged scale. The zero branches can be seen for both of these bands. The two CH_2 vibrations in the region of 3.5 μ are sufficiently separated so that there is not a serious overlapping. Two small bands were observed in the region of 2.3 μ with the 5-cm cell. When a 60-cm cell was employed, eight bands were found in this region and are shown in figure 2. The two bands at 2.4719 and 2.4840 μ are not shown in the figure, They are of very low intensities, and only the zero branches appeared. At high resolution the rotational structure of the band at 2.2291 μ is shown in the lower part of figure 2. In figure 3 the absorption bands in the region of 1.6 μ, as observed

[1] G. Herzberg, Infrared and Raman spectra of polyatomic molecules (D. Van Nostrand Co., Inc., New York, N. Y., 1945).

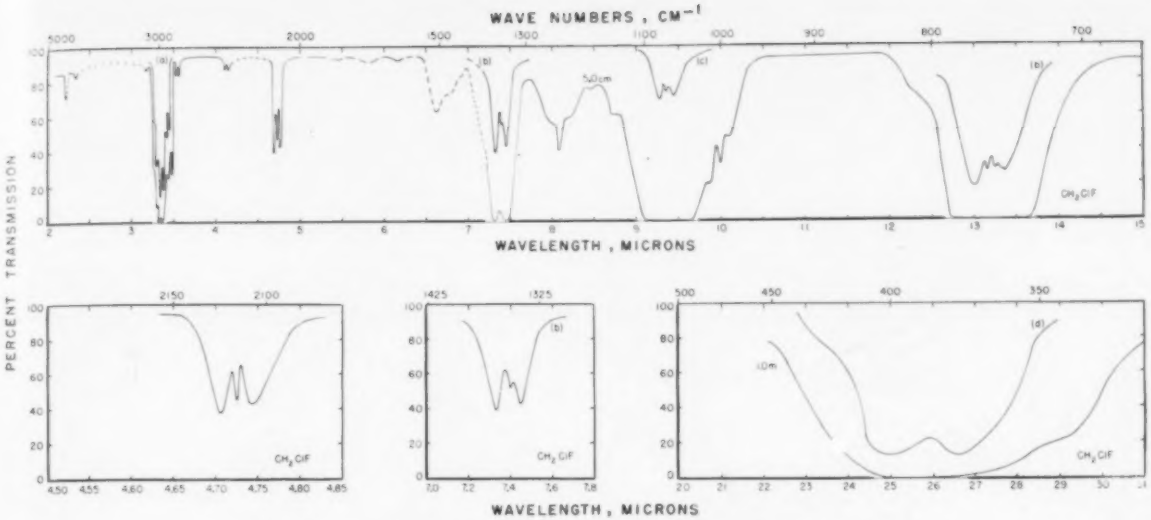

FIGURE 1. *Absorption spectrum of chlorofluoromethane from 2 to 31 μ.*

A 5-cm cell with a gas pressure of 50 cm of mercury was used from 2 to 15 μ. The gas pressure for insert (a) was 20 cm, (b) 4 cm, and (c) 0.5 cm of mercury, all in a 5-cm cell. From 22 to 31 μ, a 1-m cell with polyethylene windows was used. Since the gas pressure could not be measured in this cell, gas was flushed through it and thus the gas was at atmospheric pressure. For insert (d) some gas was removed from the 1-m cell. The bands at 4.72 and 7.40 μ are repeated on an enlarged scale.

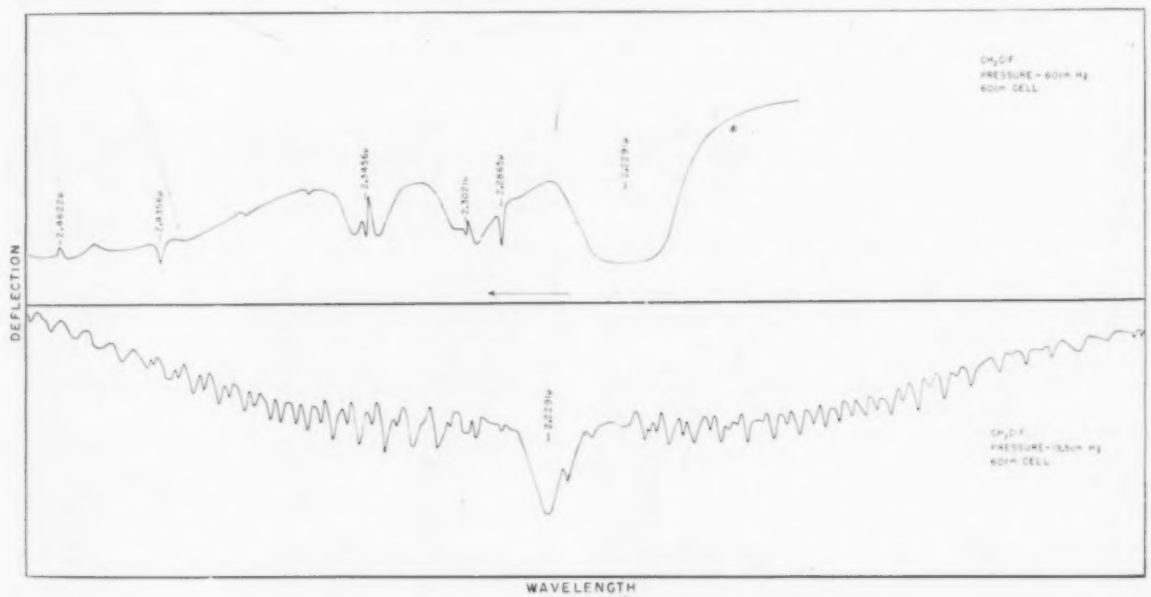

FIGURE 2. *Absorption spectrum of chlorofluoromethane from 2.15 to 2.48 μ.*

The lower curve is the band at 2.229 μ, as observed under high resolution.

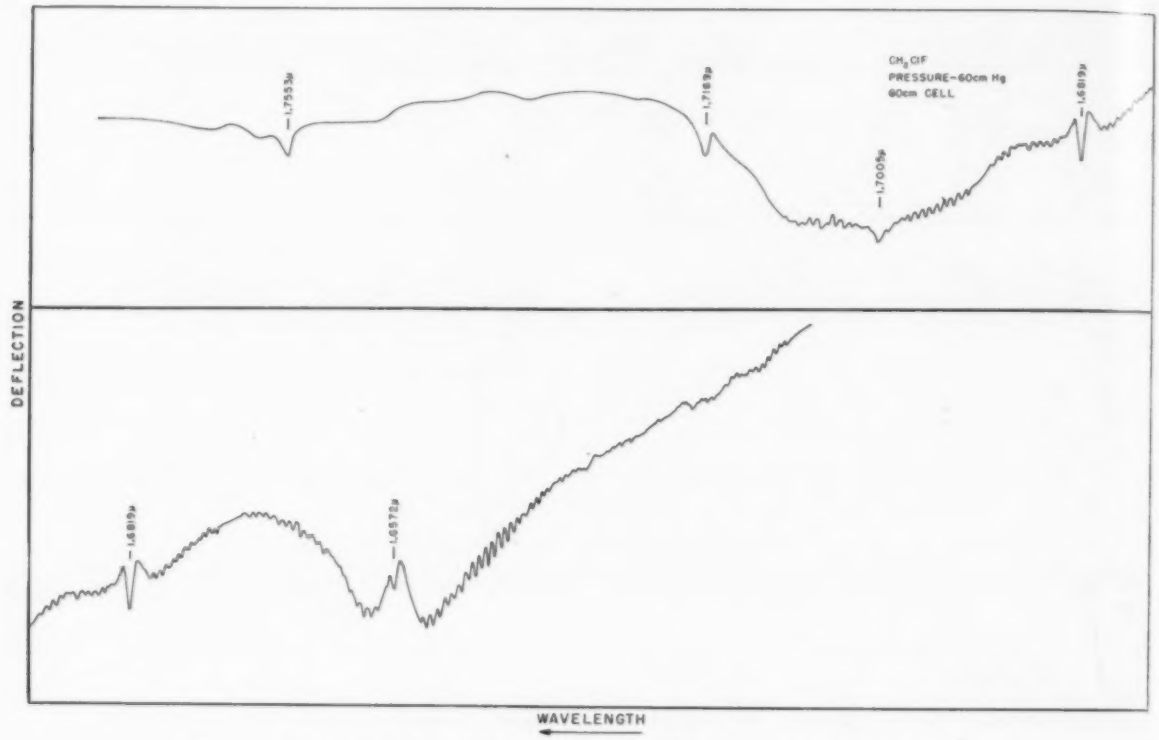

FIGURE 3. *Absorption spectrum of chlorofluoromethane in the region of 1.60 to 1.78 μ.*

The wavelengths of the centers of the six bands in this region are indicated on the figure.

with rapid scanning of the grating instrument, are shown. The low intensity band at 1.7880 μ is not shown in the figure. All the bands in this region include the 3.4- and 3.5-μ bands as combinations or harmonics. In figure 4 are shown the bands at 1.6572 and 1.7005 μ under high resolution. The emission lines at 1.6921, 1.7074, and 1.7110 μ on the lower part of figure 4 are from the mercury spectrum. The region between 2.5 and 3.0 μ should contain several combination bands. This region was not measured on the grating instrument, because of intense absorption due to atmospheric water vapor.

The nine fundamentals have been selected from the observed bands by making a comparison with the spectra of dichloromethane and difluoromethane. Except for the two bands in the region of 3.5μ, all the fundamentals of chlorofluoromethane should have longer wavelengths than those for difluoromethane and smaller wavelengths than those for dichloromethane. The Raman spectrum also has been compared with the infrared spectrum, and it is found that the infrared band at 1,236 cm^{-1} was not observed in the Raman spectrum. The Raman value of 1,468 cm^{-1} is somewhat smaller than the wave number of the infrared band at 1,475 cm^{-1}, but because of the water vapor absorption in this region it was not possible to make an accurate determination of the center of the band. The nine fundamental vibrations of chlorofluoromethane may be classified as two stretching vibrations of CH_2 (ν_1 symmetrical and ν_6 antisymmetrical) and the deformation of CH_2, ν_2. The C–FCl will have corresponding motions, which are ν_9, ν_3, and ν_4 bending or deformation. In addition there are three other vibrations, the torsional, ν_5, and two rocking vibrations, ν_7 and ν_8.

There is a close parallel between the infrared spectra of dichloromethane, difluoromethane, and chlorofluoromethane. In table 1 the fundamental frequencies of the three molecules are listed for the nine

TABLE 1. *A comparison of the fundamental bands of dichloromethane, chlorofluoromethane, and difluoromethane*

Assignment	Wave number (cm^{-1})		
	CH_2Cl_2	CH_2ClF	CH_2F_2
ν_4	283	385	529
ν_5	704	760	1,060
ν_9	737	1,000	1,120
ν_7	899	1,068	1,176
ν_3	1,155	1,236	1,262
ν_8	1,266	1,351	1,435
ν_2	1,429	[a]1,468	[a]1,508
ν_1	2,984	2,993	2,949
ν_6	3,048	3,048	3,012

[a] Raman value.

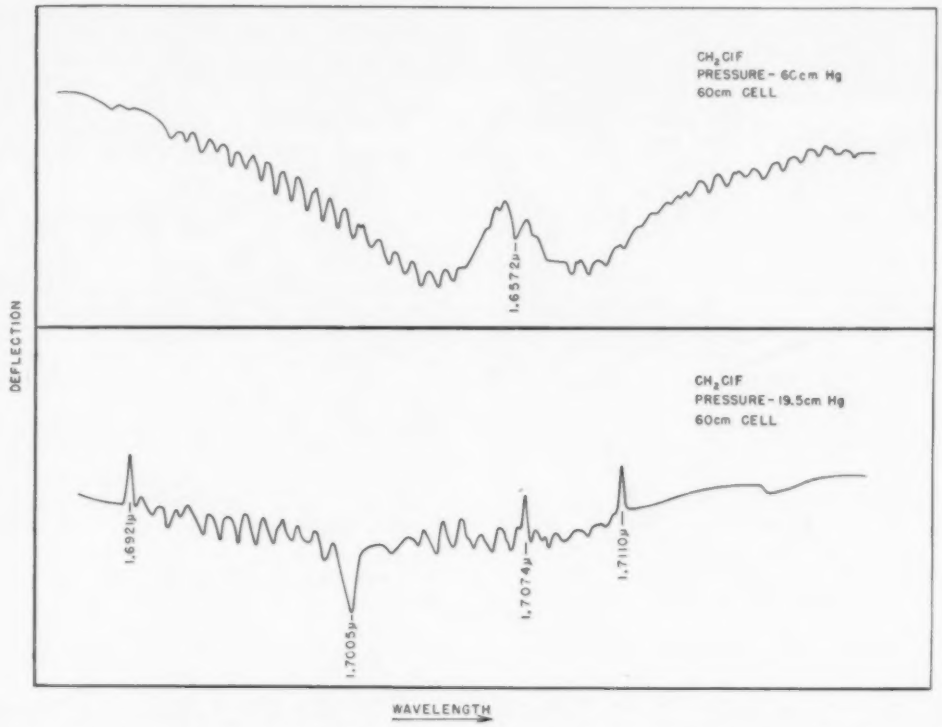

FIGURE 4. *Absorption spectrum of chlorofluoromethane in the region of 1.6572 and 1.7005 μ under high resolution.*

The emission lines on the lower curve, 1.6921, 1.7074, and 1.7110 μ, are produced by the mercury spectrum and are used for reference wavelengths.

types of vibrations involved. The classification of the bands of dichloromethane follows the assignments of Herzberg [2] from the data of C. Corin and G. B. B. M. Sutherland.[3] The classification of chlorofluoromethane and difluoromethane have been made on the basis of assignments for dichloromethane.

The experimental values were obtained on the same instruments for the three molecules. H. B. Stewart and H. H. Nielsen [4] have recently classified the bands of difluoromethane and assigned the torsional frequency as 1,511 cm^{-1}, instead of 1,262 cm^{-1} as in this work, and the band at 1,262 cm^{-1} observed in this work is missing in Stewart and Nielsen's data (see footnote 4). All bands involving the motions of the fluorine atom in chlorofluoromethane should be found at wave numbers between those of the corresponding bands in difluoromethane and dichloromethane. This is true for the assignments in table 1.

It is interesting to note that the CH_2 stretching vibrations of difluoromethane have wave numbers that are less than in chlorofluoromethane. This indicates that the fluorine atoms may decrease the binding force in the CH_2 group. The CH_2 deformation vibration in difluoromethane is of very low intensity and was not observed, and the value 1,508 cm^{-1} is used from Raman data. This mode of vibration appears as a weak band at 1,475 cm^{-1} in chlorofluoromethane in the infrared spectrum.

In table 2 is given a list of the observed bands and their classifications. After the fundamentals were selected, the harmonic bands were classified. It was found that fairly large anharmonic terms caused the observed bands in the region of 1.6 μ to vary by 50 cm^{-1} or more from being twice the wave number of the fundamental. However, the band shapes were of assistance in the classification. For example, the small zero branch shows that the band at 1.7005 μ is the harmonic of the ν_1 band, which is the symmetric motion of the two hydrogens. The other intense band is classified as $2\nu_8$, and the combination band, $\nu_1+\nu_8$, has a wave number between the values for the two harmonic bands. On the short wavelength side of the strong bands in the 3.4-μ region is a small band that arises from the second harmonic of ν_7, $3\nu_7$. This

[2] See p. 317 of footnote 1.
[3] C. Corin and G. B. B. M. Sutherland, Proc. Roy. Soc. (London) **165**, 43 (1938).
[4] H. B. Stewart and H. H. Nielsen, Phys. Rev. **75**, 640 (1949).

TABLE 2. *Classification of observed bands in chlorofluoromethane*

Assignment	Intensity	Wavelength	Wave number (vacuum)
		μ	cm^{-1}
ν_4	M	26.0	385
ν_5	VS	13.16	760
ν_3	M	9.99	1,001
ν_7	VS	9.36	1,068
ν_2	M	8.09	1,236
ν_6	S	7.40	1,351
ν_1	W	6.78	1,475
$\nu_6+\nu_7$	M	4.725	2,115
$\nu_3+\nu_7+2\nu_4$	VW	4.141	2,414
$\nu_2+\nu_6$	VW	3.544	2,821
$2\nu_2$	M	3.434	[a] 2,911
ν_1	MS	3.340	[a] 2,993
ν_6	M	3.280	[a] 3,048
$3\nu_7$	VW	3.184	3,140
$\nu_1+\nu_7$	VVW	2.4841	4,025
$\nu_6+\nu_7$	VW	2.4719	4,044
$\nu_1+\nu_3+\nu_5$	VVW	2.4622	4,060
$\nu_6+\nu_3+\nu_5$	W	2.4356	4,105
$\nu_6+\nu_3$	W	2.3456	4,262
$\nu_2+\nu_6$	VW	2.3021	4,343
$\nu_1+\nu_3$	M	2.2865	4,372
$\nu_2+\nu_6$	MS	2.2291	4,485
$\nu_1+\nu_3+\nu_5$	VVW	1.7880	5,591
$2\nu_2+\nu_6$	VW	1.7553	5,695
$2\nu_2+\nu_1$	VW	1.7169	5,823
$2\nu_1$	M	1.7005	5,879
$\nu_1+\nu_6$	W	1.6818	5,944
$2\nu_6$	MS	1.6572	6,032

[a] Raman value.

is the only second harmonic band observed in the spectrum when the 5.0-cm cell was used and indicates that ν_7 is very intense. The first harmonic band of ν_2 is fairly intense in the infrared spectrum, and this increase in intensity is brought out by resonance with ν_1 at 2,993 cm^{-1}. In the spectrum of dichloromethane $2\nu_2$ is weak, as the conditions of resonance are not so favorable.

The resolution of some of the bands in the regions of 1.6 and 2.4μ into their rotational structures makes it possible to determine one of the moments of inertia for the molecule. The separation of the rotational lines varies slightly from one band to another. The average spacing of the lines is about 2.4 cm^{-1} in the 1.7005μ band. A study of the rotational structure of this molecule and that of dichloromethane and difluoromethane is being made and will be the subject of another report.

The spectrum of chlorofluoromethane supports the assignments of the fundamental bands made on the spectrum of dichloromethane. Further experimental work will be necessary to have sufficient data for determining the CClF angle in this molecule.

WASHINGTON, April 14, 1950.

Journal of Research of the National Bureau of Standards Vol. 45, No. 3, September 1950 Research Paper 2126

Resin Bonding of Hardwood Fibers in Offset Papers

By Bourdon W. Scribner, Merle B. Shaw, Martin J. O'Leary, and Joshua K. Missimer

A further investigation was made of the application of resin bonding to the development of strength in offset papers made principally of short hardwood fibers that develop little strength by the conventional beating. Melamine-formaldehyde resin was used. The papers were made from hardwood pulps produced at the U. S. Forest Products Laboratory in experimental study of the pulping of aspen, black gum, paper birch, and beech. The pulps were prepared by the mechanical, sulfate, soda, sulfite, and neutral sulfite processes. By the use of the melamine resin, papers having good strength and resistance to pick, combined with low expansion and curl, were produced with very little beating. The pulps that gave the best results comprised aspen sulfate, aspen soda, aspen sulfite, birch sulfite, and black gum sulfate. Resin-bonded papers containing 75 percent of these pulps compared favorably with papers made in the conventional way with the usual 50 percent of commercial hardwood fibers. An appreciable increase in the proportion of hardwood fibers used in offset papers would greatly extend pulpwood resources.

I. Introduction

Effective utilization of large quantities of hardwoods is an outstanding pulpwood problem. The pulp and paper industry has had an amazing growth during this century, but the supply of the more generally used pulp woods is steadily decreasing. Wood is the most important source of paper-making material. Pulp produced from coniferous or needle-leaved trees (softwoods), such as spruce, fir, and pine, is used to a much greater extent than that produced from the hardwood or broad-leaved trees, such as the various "poplars", birch, beech, gum, etc., commonly used for pulping. The use of hardwoods for pulping is good forestry practice, and in regions having a large volume of hardwood species or inferior trees unsuited for lumber or similar products is an economic necessity.

In comparison with spruce and other softwoods, however, the use of hardwoods has been limited by the characteristics of the hardwood fibers. The characteristics that affect the manufacture of paper vary in kind and quantity with different woods. One differentiation is the length of fiber, which is approximately from 1 to 1.5 mm for hardwoods and from 2.5 to 4.5 mm for coniferous wood. The fiber of the hardwood trees also has a structure that is different from that of the conifers. Its soft and absorbent texture renders it useful for bulky papers such as certain classes of printing paper, but it is not as strong as the softwood fiber.

The strength of paper depends on the strength of its fibers and on the adhesive bond between them. Cellulose is a colloid. It gelatinizes ("hydrates") on beating it in water and thus causes gel-like bonds to be formed between the fibers of the finished sheet.

Because of the large increase in external surface (fibrillation) produced by beating, the number of contacts and subsequent bonds is greatly increased, thereby increasing the strength of the paper. The hardwoods do not develop good bonding quality to the extent that conifers do.

The development of strength by beating the fibers tends to affect adversely some properties needed for good printing quality. Chief among these are high opacity, good oil absorption, high permeability to air, low expansivity, and low curl. Low expansion and contraction are particularly important in lithographic offset papers for good register of successive color prints, as in printing maps that may be run through the press as many as 15 times. Hardwood pulps have all the properties needed for good offset printing paper except strength.

An investigation at the Bureau during World War II resulted in the development of offset lithographic paper for war maps having great strength imparted by melamine-formaldehyde resin bonding and excellent printing quality.[1] A subsequent investigation of melamine-formaldehyde resin in papers made from various mixtures of a commercial softwood pulp and two commercial hardwood pulps showed that the proportion of the latter could be largely increased without impairment of the strength of the papers, and with improvement of their printing quality, thus permitting increased use of hardwood fibers.[2]

The investigation reported herein is an extension of such study of hardwood pulp to pulps produced experimentally from different species of woods at the U. S. Forest Products Laboratory, in a study of application of the various commercial pulping processes to hardwoods.

II. Experimental Paper-Making Equipment

The paper-making equipment at the Bureau is semicommercial in size and is adapted to the experimental manufacture of papers under conditions that simulate those of typical industrial plants. Detailed descriptions are contained in previous publications.[3 4 5]

The equipment used in this particular work consisted essentially of a 50-lb. beater with copper-lined tub and manganese-bronze bars and plate; a jordan refiner with bars of bronze and steel alloy; a fourplate, flat screen; a 29-in. fourdrinier paper-making machine with a wire 33 ft. in length, two presses, nine 15-inch dryers, a calender stack of seven rolls, and a reel; and a five-roll supercalender.

III. Fibrous Raw Materials

Two commercial pulps, bleached sulfite (coniferous) and bleached soda (deciduous), were used in various mixtures with the hardwood pulps prepared by the Forest Products Laboratory.

Bleached sulfite, made by cooking eastern spruce wood in a solution of calcium bisulfite, is a standard quality of pulp widely used in offset papers. It is composed of relatively long, strong fibers that hydrate rather readily with beating.

Soda pulp is a short-fibered filler-type pulp made by cooking hardwood in a solution of caustic soda. The fibers are characteristically soft and bulky and do not hydrate readily. The pulp had excellent strength for a pulp of this kind.

The hardwood pulps supplied by the Forest Products Laboratory were prepared from the following deciduous woods: Aspen, black gum (tupelo), paper birch, and beech. Also included was a coniferous pulp made from Douglas fir. The pulps were prepared by the mechanical (groundwood), sulfate, soda, sulfite, and neutral sulfite (semichemical) processes. The identification number assigned to each pulp by the Forest Products Laboratory, and their description of it follow.

Quaking Aspen Pulps

a. Unbleached free [6] groundwood pulp (item 1).—This pulp is characterized by its relatively short fiber length, low strength, and high freeness. It was prepared at a high rate of production and with low energy consumption. The energy requirement was about 40 percent that of the slower pulp described below (c).

b. Peroxide-bleached free groundwood pulp (item 2).—This pulp was bleached at a high density by a conventional single-stage sodium peroxide process to give a bright, free, low-strength, short-fibered pulp.

c. Unbleached book-grade groundwood pulp, slow (item 14).—This pulp is characterized by its low freeness, short fiber length, and fair strength. The production rate was low and the energy requirement high.

d. Bleached sulfate pulp (item 7).—A fully bleached sulfate pulp, conventionally cooked, and bleached by a three-stage, chlorination—alkali extraction—hypochlorite, bleaching process. This pulp is typical of short-fibered pulps having good strength and softness.

e. Bleached soda pulp (item 15).—This pulp was produced by the conventional soda process and bleached by a three-stage, chlorination—caustic extraction—hypochlorite, bleaching process. This short-fibered pulp was slow hydrating and relatively weak, as is typical for this kind of pulp, but was soft and bulky.

f. Bleached sulfite pulp (item 16).—This was a commercial pulp prepared by the calcium-bisulfite process and bleached by the conventional single-stage hypochlorite process. It is a weak, short-fibered pulp, typical of aspen sulfite.

g. Bleached neutral sulfite (semichemical) pulp (item 5).—The cooking process consisted of partially digesting the aspen chips with a solution of sodium sulfite and sodium bicarbonate and then

[1] J. Research NBS **37**, 325 (1946) RP1751.
[2] J. Research NBS **40**, 427 (1948) RP1887.
[3] Tech. Paper BS **21**, 338 (1927) T340.
[4] BS J. Research **3**, 904 (1929) RP121.
[5] Paper Trade J. **88**, No. 19, 60 (1929).

[6] "Free" is a term applied to fibers from which water drains rapidly because of the low hydration of the fibers. The converse term is "slow."

defibering the softened chips in an attrition mill. The pulp was bleached by a conventional multistage process including chlorination, alkali extraction, and hypochlorite treatment. A high yield of fully bleached pulp was obtained. It is characterized by fairly high strength, rapid hydration, and considerable hardness.

h. Mixed aspen and spruce bleached sulfate pulps (item 3).—Sulfate pulp was made by a conventional pulping procedure from a mixture of quaking aspen (67%) and spruce (33%) and bleached by a multistage treatment consisting of chlorination, alkali extraction, two-stage hypochlorite bleaching, and a sulfur dioxide wash. This pulp had a much lower bursting strength and a somewhat lower tearing strength than would be expected if less drastic bleaching conditions had been used. The mixture of long and short fibers in this pulp had a higher tearing resistance than the pulp made from the hardwood alone.

Black Gum (Tupelo) Pulp

Bleached sulfate pulp (item 6).—A bleachable sulfate pulp was made by a conventional sulfate pulping procedure and the pulp bleached by a multistage process involving chlorination, alkali extraction, and two-stage hypochlorite bleaching. A bright, fairly strong, and fairly soft short-fibered pulp was obtained. The bursting strength of the pulp was perhaps lower than would normally result from less drastic treatment.

Paper Birch Pulps

a. Peroxide-bleached groundwood pulp (item 8).—This pulp is very short fibered and has a correspondingly low strength. It was bleached to high brightness by a high-density single-stage peroxide process.

b. Bleached sulfite pulp (item 10).—The pulp was produced by the conventional sulfite process using calcium-base liquor. The pulp was bleached by a conventional two-stage chlorine-hypochlorite process. It is a fairly strong short-fibered pulp.

c. Bleached neutral sulfite (semichemical) pulp (item 9).—The wood was partially pulped with a sodium sulfite and sodium bicarbonate liquor, and the softened chips were then defibered in an attrition mill. The semichemical pulp was bleached by a multistage, chlorination—alkali extraction—hypochlorite, bleaching process. The fully bleached pulp was characterized by high yield, high strength, rapid hydration, and considerable hardness.

Beech Pulp

Bleached sulfate pulp (item 12).—The wood was pulped by a conventional sulfate pulping procedure. The pulp was bleached by a multistage process comprising chlorination, alkali extraction, and two-stage hypochlorite bleaching. This pulp was somewhat underbleached to give a fair brightness. The pulp is short-fibered and of fair strength.

Douglas Fir Pulp

Bleached neutral sulfite (semichemical) pulp (item 13).—A fully bleached pulp was made from Douglas fir (coniferous) by partial cooking with a sodium sulfite and sodium bicarbonate liquor followed by defibering the softened chips in an attrition mill. A fairly high yield of unbleached pulp was obtained. It was bleached by a conventional, chlorination—alkali extraction—hypochlorite, bleaching process. The pulp is characterized by its high strength, especially tearing resistance, and long fibers.

IV. Manufacturing Procedure

A series of papers was made from the pulps with and without the resin bonding. The manufacturing factors were kept as nearly constant as possible. The pulps were beaten for 1½ hr, which was considered the minimum time for satisfactory results.

Fifty pounds of pulp and 1 percent (based on weight of fiber) of resin size were used for each machine run. The beaten stock was dropped directly to a chest from which it was pumped in a continuous stream through the stuff box and the jordan refiner to the paper machine. The stuff box was of the regulating type with constant head over an adjustable orifice. The jordan was used as a mixer only, with the same setting for all papers.

The melamine-formaldehyde resin was added in the form of a colloidal solution made by dissolving the powdered resin in warm water acidified with hydrochloric acid. The solution was added continuously at uniform rate to the paper-making stock just before it entered the head box of the paper machine. The temperature of the stock at the head box was maintained at 90° ±2° F.

Melamine is a triamino derivative of symmetrical triazine consisting of a six-membered ring of alternate carbon and nitrogen atoms. It was discovered by Von Liebig in 1834 who, thinking it was the amine of melam, called it melamine. The particles of the colloidal resin have a positive charge and, since cellulose is negatively charged, they are therefore quickly adsorbed on the cellulose fiber. The heat of the paper-machine drying cylinders completes the polymerization of the resin particles, forming a water-insoluble bond between the fibers.

The finish imparted by the small paper machine calender was relatively low, therefore the papers were given light supercalendering to obtain a smoothness comparable to commercial "machine finish".

V. Sampling and Testing

The method of sampling paper from a machine run in the paper mill was as follows: The paper wound on the reel of the paper machine was slit across the web, thereby being converted into a stack of sheets. The stack was then cut so as to give an entire cross section of the sheets for sampling. The resultant stack was divided into seven parts. From the first part, 13 sheets were laid out as the first

sheets of 13 packs to be built up. From the second part, 13 sheets were likewise distributed as the second sheets of the packs. From each of the seven parts respectively a sheet was added to each pack. The procedure was then repeated until all the paper had been distributed into the 13 packs. The odd-numbered (1–3–5–7–9–11–13) packs were then assembled, one above the other, to make one bundle of paper, and similarly the even-numbered packs to make another. From these bundles sheets were taken for the test samples.

All tests of the papers were made according to the Standard Methods of the Technical Association of the Pulp and Paper Industry,[7] except the air permeability test by the Carson method. This was determined with a Carson Precision Permeability Tester,[8] which measures the rate of air flow through the paper per unit of area with a pressure difference of 1 g/cm².

VI. Discussion of Papers and Data

The complete test data for the papers are given in table 1. Table 2 shows the consistent improvement in strength obtained with melamine resin irrespective of the kind of experimental pulping processes used. Table 3 shows that for a given pulping process, the improvement in strength by use of melamine resin was uniformly good for different species of wood.

[7] Available from the Association at 122 East 42nd Street, New York 17, N. Y. The methods specify the number of specimens for each test, as well as the other details of testing.

[8] BS J. Research **12**, 567 (1934) RP681.

Figures 1 and 2 give a comparison of papers containing 75-percent experimental hardwood pulps and melamine resin, with papers made without melamine resin having the usual content of 50-percent commercial hardwood pulp. The other figures also show graphically the beneficial effects obtained with the use of the resin with various pulps. The word "blank" in the figures means that no melamine resin was added; an "M" is an abbreviation of melamine resin. Following is a discussion of the effects of melamine resin on the properties of the papers as shown by the data.

Unbleached aspen groundwood, free (item 1).—The fiber furnish for the three runs, 1492–4, was 75 percent of aspen groundwood. The tests on the papers show that the bursting strength, folding endurance, and tensile strength were all improved by the addition of melamine, the improvement being more pronounced with the greater amount of resin. The bonding resin improved also the resistance of the surface to picking, as measured by the wax test, without excessive increase in expansion of the papers or tendency to curl (fig. 3).

Malamine resin was not used in run 1498, and an equal amount of bleached aspen neutral sulfite pulp (item 5) was substituted for the sulfite (coniferous) pulp. The aspen pulp was characterized by fairly high strength, rapid hydration, and considerable hardness. The paper showed only fair bursting strength and low folding endurance, tensile strength, tearing strength and resistance to pick, although the

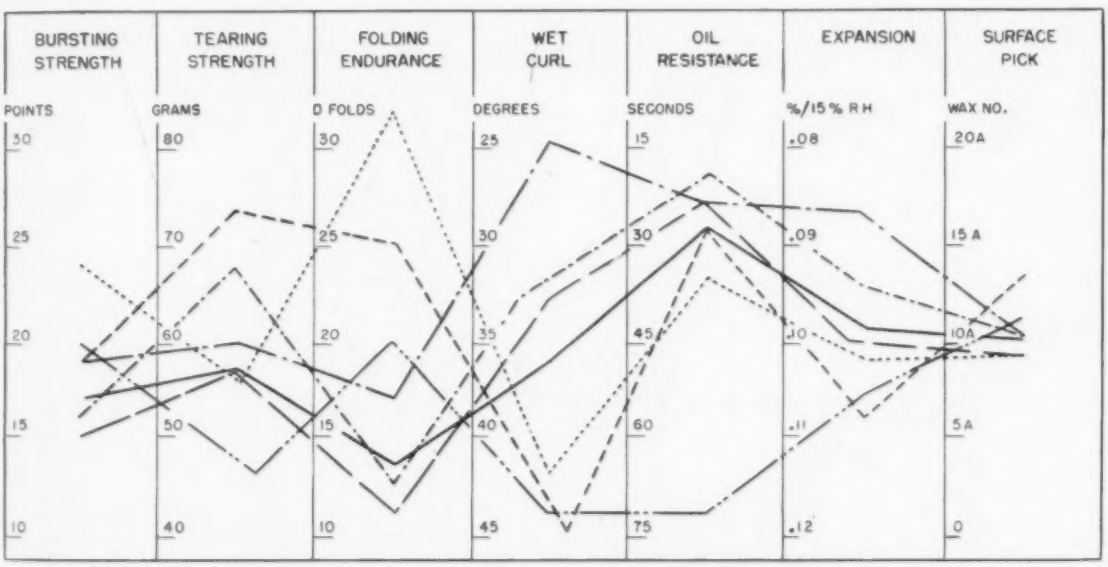

FIGURE 1. *For papers containing 1 percent of melamine resin, the physical properties of experimental papers composed of 75-percent hardwood fibers and 25-percent sulfite softwood fibers are as good as, and in some instances better than, papers composed of 50-percent commercial soda hardwood fibers and 50-percent commercial sulfite softwood fibers.*

——— 1560, 50% strong soda pulp, 50% eastern sulfite (commercial); —— —— 1538, 75% bleached aspen sulfate, 25% eastern sulfite (commercial); —— · —— 1558, 75% bleached aspen soda, 25% eastern sulfite (commercial); —— · · —— 1542, 75% bleached aspen sulfite, 25% eastern sulfite (commercial); - - - - 1516, 75% bleached black gum sulfate, 25% eastern sulfite (commercial); — · — · — 1534, 75% bleached paper birch sulfite, 25% eastern sulfite (commercial); · · · · · 1502, 40% strong soda pulp, 60% bleached sulfate (67% aspen, 33% spruce).
(All the above with 1% melamine resin.)

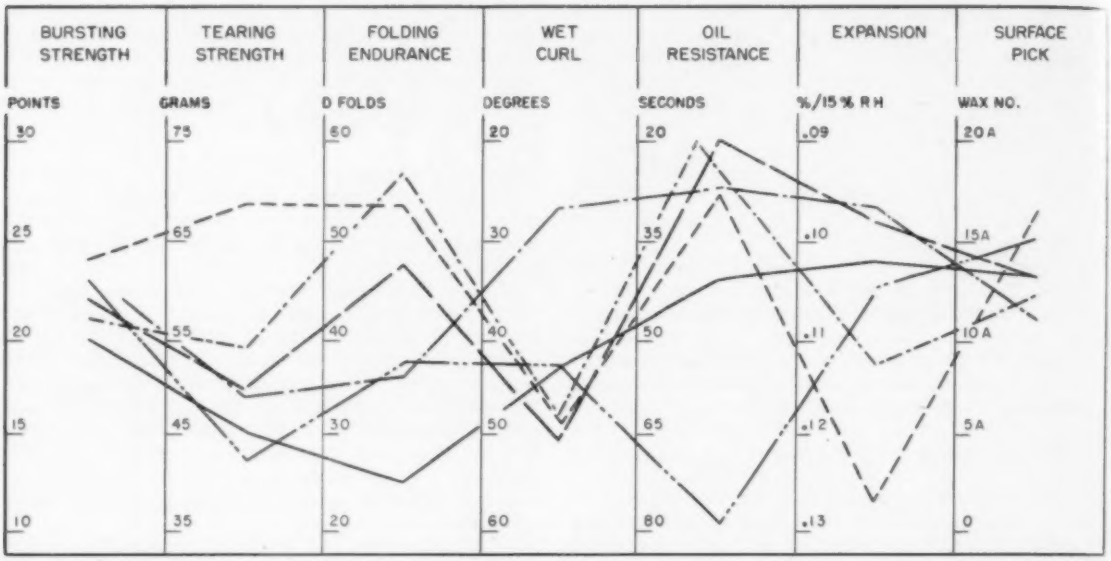

FIGURE 2. *For papers containing 3 per.ent of melamine resin, the physical properties of experimental papers composed of 75-percent hardwood fibers and 25-percent sulfite softwood fibers are better in most instances than the papers composed of 50-percent commercial soda hardwood fibers and 50-percent commercial sulfite softwood fibers.*

——— 1561, 50% strong soda pulp, 50% eastern sulfite (commercial); —— —— 1539, 75% bleached aspen sulfate, 25% eastern sulfite (commercial); —— · —— 1559, 75% bleached aspen soda, 25% eastern sulfite (commercial); — · · — 1543, 75% bleached aspen sulfite, 25% eastern sulfite (commercial); - - - - 1517, 75% black gum sulfate, 25% eastern sulfite (commercial); — · — · — 1535, 75% bleached paper birch sulfite, 25% eastern sulfite (commercial).
(All the above with 3% melamine resin.)

TABLE 1. *Comparative data on offset papers made from hardwood fibers bonded with melamine-formaldehyde resin*

Run No.	Pulp	Forest Products item No.	Melamine-formaldehyde resin added	Weight 1 25 by 40 in., 500 sheets	Thickness	Bursting strength	Folding endurance (double folds) MIT (tension 1 kg) Machine direction	Folding endurance (double folds) MIT (tension 1 kg) Cross direction	Tensile strength Machine direction	Tensile strength Cross direction	Tearing resistance Machine direction	Tearing resistance Cross direction	Expansivity (15% change in relative humidity) Machine direction	Expansivity (15% change in relative humidity) Cross direction	Opacity (contrast ratio)	Smoothness (Bekk)	Surface pick (wax No.)	Oil penetration	Air permeability	Sizing value (dry indicator)	Curl
			Pct.	*lb.*	*Inch*	*Pts.*			*kg*	*kg*	*g*	*g*	*Pct.*	*Pct.*	*Pct.*	*Sec.*		*Sec.*	*cm³/sec/ m²g/cm²*	*Sec.*	*Deg*
1492	75% unbleached aspen groundwood	1		56.3	0.0051	11	3	2	3.6	2.3	41	44	0.053	0.135	97.0	23	2A	60	402	77	25
1494	25% bleached "Eastern" sulfite		1	53.9	.0052	14	4	3	4.0	2.8	39	42	.065	.147	95.4	21	5A	71	337	79	31
1493			3	55.0	.0053	18	8	7	5.5	3.4	35	39	.061	.166	94.9	18	9A	76	239	86	32
1498	75% unbleached aspen groundwood	1		55.9	.0042	11	3	2	3.6	2.6	31	34	.070	.164	94.6	56	4A	77	183	81	32
	25% bleached aspen neutral sulfite (semi-chemical).	5																			
1544	75% peroxide-bleached aspen groundwood	2		54.4	.0042	13	7	4	9.1	6.0	28	41	.061	.153	91.0	57	6A	112	167	90	36
1545	25% bleached "Eastern" sulfite		1	53.1	.0039	13	10	7	9.7	7.2	34	34	.073	.146	90.5	53	10A	134	145	102	28
1546			3	55.4	.0042	17	16	11	11.8	8.2	35	37	.070	.187	91.0	46	10A	131	101	113	29
1523	75% unbleached aspen groundwood (slow)	14		52.8	.0038	13	7	8	4.0	3.1	32	32	.075	.157	97.0	109	9A	271	31	81	36
1524	25% bleached "Eastern" sulfite		1	55.2	.0039	15	9	13	4.5	3.6	32	32	.080	.174	97.0	97	11A	332	26	82	45
1525			3	55.0	.0038	18	24	26	5.7	4.1	29	30	.083	.199	97.0	85	14A	503	14	88	51
1526	100% unbleached aspen groundwood (slow)	14	3	54.7	.0037	14	1	1	5.5	3.7	21	22	.091	.202	98.0	97	13A	649	9	86	50
1537				55.4	.0040	8	2	2	2.7	2.0	58	56	.056	.116	86.0	47	2A	25	1163	68	27
1538	75% bleached aspen sulfate	7	1	55.2	.0039	15	11	11	4.8	3.6	57	57	.060	.140	85.0	51	9A	24	898	68	33
1539	25% bleached "Eastern" sulfite		3	54.6	.0037	22	52	43	5.8	4.2	50	50	.062	.135	84.0	58	13A	26	724	62	51
[2]1572				56.8	.0039	15	7	6	4.8	3.3	57	58	.061	.152	86.0	66	6A	31	419	63	39
1557				55.5	.0037	9	3	3	3.3	2.1	51	61	.058	.116	86.0	84	2A	22	900	41	27
1558	75% bleached aspen soda	15	1	56.5	.0037	19	20	14	5.4	3.7	60	60	.048	.126	87.0	75	10A	24	719	57	25
1559	25% bleached "Eastern" sulfite		3	55.0	.0034	22	42	30	6.3	4.4	51	48	.051	.143	85.0	89	11A	27	584	57	27
[2]1573				54.7	.0038	14	8	5	4.9	3.2	47	54	.050	.148	86.0	66	5A	30	422	63	37

See footnotes at end of table.

TABLE 1. *Comparative data on offset papers made from hardwood fibers bonded with melamine-formaldehyde resin*—Continued

Run No.	Pulp	Forest Products item No.	Melamine-formaldehyde resin added	Weight [1] 25 by 40 in., 500 sheets	Thickness	Bursting strength	Folding endurance (double folds): MIT (tension 1 kg)		Tensile strength		Tearing resistance		Expansivity (1% change in relative humidity)		Opacity (contrast ratio)	Smoothness (Bekk)	Surface pick (wax No.)	Oil penetration	Air permeability	Sizing value (dry indicator)	Curl
							Machine direction	Cross direction	Machine direction	Cross direction	Machine direction	Cross direction	Machine direction	Cross direction							
			Pct.	*lb.*	*Inch*	*Pts.*			*kg*	*kg*	*g*	*g*	*Pct.*	*Pct.*	*Pct.*	*Sec.*		*Sec.*	*cm³/sec/ m²g/cm²*	*Sec.*	*Deg*
1541	75% bleached aspen sulfite	16		56.6	.0036	14	9	6	11.2	6.9	50	51	.055	.151	86.0	73	5A	67	198	102	40
1542	25% bleached "Eastern" sulfite		1	56.4	.0036	20	27	13	14.6	9.1	44	48	.057	.159	85.0	69	11A	72	149	104	44
1543			3	56.3	.0034	23	44	31	16.9	10.9	43	42	.056	.154	84.0	68	15A	79	130	126	43
1495	75% bleached aspen neutral sulfite (semi-chemical)	5		56.3	.0038	23	84	49	7.5	4.3	53	56	.086	.282	79.1	27	12A	81	114	69	120
	25% bleached strong soda																				
1496	50% bleached aspen neutral sulfite (semi-chemical)	5		56.0	.0037	20	26	16	6.3	4.0	48	53	.078	.219	83.8	55	10A	56	189	73	70
	50% bleached strong soda																				
1497	25% bleached aspen neutral sulfite (semi-chemical)	5		56.1	.0039	14	8	6	4.6	3.2	45	52	.071	.184	88.0	58	5A	31	364	67	50
	75% bleached strong soda																				
1499	67% bl. aspen, 33% bl. spruce sulfate	3		56.4	.0039	20	32	13	6.5	3.4	73	78	.053	.173	85.2	53	6A	37	405	73	41
1500			1	56.3	.0037	29	97	54	7.6	4.6	60	64	.066	.164	85.9	48	10A	40	318	78	44
1501	40% bl. aspen, 20% bl. spruce sulfate	3		55.0	.0040	16	11	7	5.1	3.1	58	63	.057	.135	88.2	61	5A	32	434	77	37
1502	40% bl. strong soda		1	55.5	.0040	24	46	17	6.9	4.4	53	59	.058	.146	87.0	63	9A	36	373	77	42
1503	75% bl. black gum (tupelo) sulfate	6		54.4	.0042	11	4	3	3.0	2.1	66	75	.071	.160	83.0	36	3A	15	1675	50	35
1516	25% bl. "Eastern" sulfite		1	55.2	.0037	19	27	23	5.0	3.5	71	75	.070	.146	84.0	92	13A	28	834	58	45
1517			3	53.1	.0038	24	57	49	5.6	4.1	71	65	.073	.181	83.0	50	16A	26	975	60	49
1518	100% bl. black gum (tupelo) sulfate	6	3	54.2	.0039	24	57	50	5.6	4.1	69	71	.079	.175	82.0	40	16A	20	1537	55	46
1519	75% peroxide-bl. paper birch groundwood	8		52.8	.0039	9	2	2	1.4	1.1	30	32	.061	.141	94.0	88	2A	79	156	54	31
1520	25% bl. "Eastern" sulfite		1	52.6	.0038	11	3	3	3.9	2.6	27	29	.064	.162	93.0	113	6A	87	131	25	31
1521			3	52.3	.0037	14	4	4	4.5	2.9	24	28	.063	.181	93.0	113	10A	123	77	33	37
1533	75% bl. paper birch sulfite	10		54.2	.0036	9	4	2	3.0	1.8	64	70	.052	.137	84.0	68	2A	25	1638	66	33
1534	25% bl. "Eastern" sulfite		1	54.6	.0036	16	16	9	4.3	2.7	67	68	.049	.140	83.0	54	10A	20	1359	73	33
1535			3	52.4	.0034	23	79	35	5.6	3.6	54	55	.056	.169	80.0	53	12A	20	1178	72	48
1508	75% bl. paper-birch neutral sulfite (semi-chemical)	9		53.1	.0034	38	382	169	9.6	5.6	51	59	.098	.303	76.0	47	18A	224	43	57	144
	25% bl. strong soda																				
1509	50% bl. paper-birch neutral sulfite (semi-chemical)	9		54.6	.0035	28	103	41	7.7	4.7	48	54	.091	.252	83.0	66	13A	99	112	59	92
	50% bl. strong soda																				
1510	25 bl. paper-birch neutral sulfite (semi-chemical)	9		55.7	.0037	20	19	13	6.1	3.9	48	53	.082	.195	88.0	115	10A	59	235	56	58
	75% bl. strong soda																				
1568				53.3	.0037	9	3	2	2.7	1.8	53	53	.059	.133	88.0	66	2A	16	1397	51	38
1569	75% bl. beech sulfate	12	1	54.9	.0039	13	4	6	3.4	2.4	52	50	.050	.133	89.6	47	6A	15	1227	60	35
1570	25% bl. "Eastern" sulfite		3	52.9	.0040	17	10	10	4.7	3.6	50	47	.055	.150	88.0	45	11A	17	1102	57	36
[2]1571				53.1	.0039	14	6	6	4.4	3.0	46	44	.060	.174	86.0	52	10A	27	565	55	42
1529	75% bl. Douglas fir neutral sulfite (semi-chemical)	13		52.9	.0036	21	163	53	5.5	3.4	112	128	.061	.165	79.0	66	11A	62	302	50	48
	25% bl. strong soda																				
1530	50% bl. Douglas fir neutral sulfite (semi-chemical)	13		54.1	.0035	19	79	28	5.1	3.2	98	112	.061	.164	85.0	62	10A	61	326	56	47
	50% bl. strong soda																				
1531	25% bl. Douglas fir neutral sulfite (semi-chemical)	13		54.0	.0036	15	14	9	4.2	2.8	79	87	.048	.133	88.0	70	7A	52	425	61	36
	75% bl. strong soda																				
1562	75% bl. strong soda			53.2	.0034	9	4	4	3.3	2.5	47	49	.049	.123	91.0	148	3A	36	416	53	32
1563	25% bl. "Eastern" sulfite		1	54.0	.0033	16	10	8	4.8	3.5	46	47	.056	.132	90.0	147	7A	36	359	69	33
1564			3	54.3	.0033	19	18	16	5.4	4.0	46	44	.054	.136	89.0	151	11A	38	327	67	36
1540	50% bl. strong soda			54.8	.0040	12	6	4	3.7	2.6	61	63	.049	.126	88.0	64	3A	34	556	93	31
1560	50% bl. "Eastern" sulfite		1	54.4	.0036	17	15	12	4.7	3.3	57	58	.056	.142	87.0	79	10A	28	309	45	36
1561			3	53.6	.0031	20	29	21	5.9	3.8	46	44	.058	.146	87.0	166	13A	41	295	69	43

[1] All physical tests made under conditions of 50-percent relative humidity and 73° F, by the standard methods of the Technical Association of the Pulp and Paper Industry, except Carson air permeability.

[2] Stock was given more drastic beating in an attempt to obtain greater strength without the use of a bonding resin.

TABLE 2. *Effect of melamine resin on tensile breaking strength of papers [1] containing aspen pulp produced by various pulping processes*

Amount of melamine	Groundwood process		Sulfate process		Sulfite process		Soda process	
	Machine direction	Cross direction	Machine direction	Cross direction	Machine direction	Cross direction	Machine direction	Cross direction
Percent	*kg/15 mm*	*kg/15 mm*	*kg/15 mm*	*kg/15 mm*	*kg/15 mm*	*kg/15 mm*	*kg/15 mm*	*kg/15 mm*
	9.1	6.0	2.7	2.0	11.2	6.9	3.3	2.1
1	9.7	7.2	4.8	3.6	14.6	9.1	5.4	3.7
3	11.8	8.2	5.8	4.2	16.9	10.9	6.3	4.4

[1] 75% aspen (hardwood) pulp, 25% sulfite softwood pulp.

TABLE 3. *Effect of melamine resin on tensile breaking strength of papers [1] containing hardwood pulps produced from various species of wood by the sulfate pulping process*

Amount of melamine	Aspen		Black gum		Beech	
	Machine direction	Cross direction	Machine direction	Cross direction	Machine direction	Cross direction
Percent	*kg/15 mm*	*kg/15 mm*	*kg/15 mm*	*kg/15 mm*	*kg/15 mm*	*kg/15 mm*
	2.7	2.0	3.0	2.1	2.7	1.8
1	4.8	3.6	5.0	3.5	3.4	2.4
3	5.8	4.2	5.6	4.1	4.7	3.6

[1] 75% hardwood pulp, 25% sulfite softwood pulp.

expansivity of the sheet was nearly as much as when 3 percent of bonding resin was used (run 1493) and the air permeability less. The aspen neutral sulfite pulp was not a good substitute for the resin bonding in developing desirable properties in the finished paper (fig. 3).

Peroxide-bleached aspen groundwood, slow (item 2).—The papers of runs 1544–6 showed improvement in strength properties as a result of bleaching the pulp, but the expansivity was somewhat high when the percentage of bonding resin was increased. Except for improvement in color, whether the effect on other qualities would warrant the extra cost of the bleaching operations is doubtful (fig. 4).

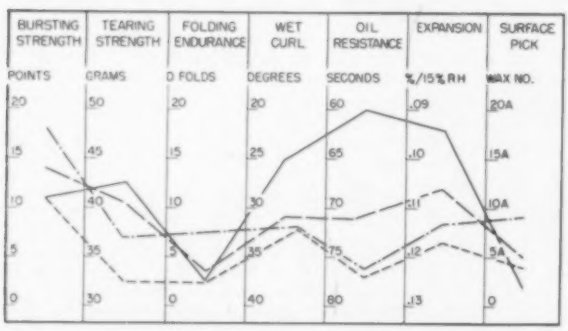

FIGURE 3. *Effect of melamine resin in papers containing unbleached aspen groundwood pulp (FPL item 1).*

——— 1492, blank, 75% unbleached aspen groundwood, 25% bleached eastern sulfite; — — — 1494, 1% M, 75% unbleached aspen groundwood, 25% bleached eastern sulfite; —·—·— 1493, 3% M, 75% unbleached aspen groundwood, 25% bleached eastern sulfite; - - - - 1498, blank, 75% unbleached aspen groundwood, 25% aspen neutral sulfite.

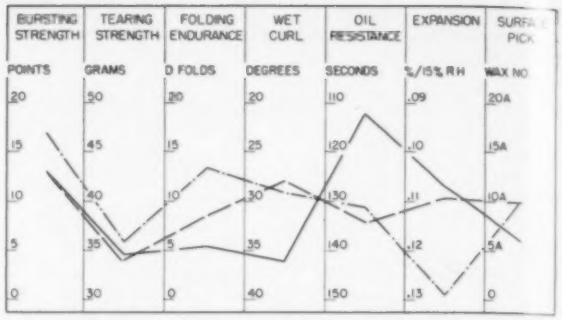

FIGURE 4. *Effect of melamine resin in papers containing peroxide-bleached aspen groundwood pulp (FPL item 2).*

——— 1544, blank, 75% peroxide-bleached aspen groundwood, 25% eastern sulfite; — — — 1545, 1% M, 75% peroxide-bleached aspen groundwood, 25% eastern sulfite; ———·— — 1546, 3% M, 75% peroxide-bleached aspen groundwood, 25% eastern sulfite.

Unbleached aspen book-grade groundwood pulp, slow (item 14).—The strength properties of papers made of this pulp (runs 1523–6) were better in general than for the papers made from the free unbleached aspen groundwood (item 1), but the expansivity was too high and the air permeability of the sheet very low. The folding endurance for paper (run 1526) made from 100-percent book-grade groundwood pulp and 3 percent of bonding resin was almost negligible.

Aspen sulfate pulp (item 7).—Papers (runs 1537–9) with good strength and resistance to surface pick, combined with low expansion, were made from a mixture of this pulp with only 25 percent of sulfite pulp (coniferous) and having 1 and 3 percent, respectively, of melamine-formaldehyde resin added for bonding (fig. 5).

Run 1572 was made to try to develop strength in the paper as a result of beating instead of with melamine resin. The beating did not develop sufficient strength however, whereas bonding with 3 percent of melamine-formaldehyde resin produced

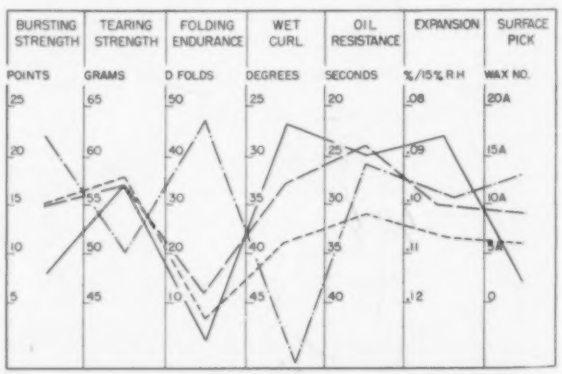

FIGURE 5. *Effect of melamine resin in papers containing aspen sulfate pulp (FPL item 7).*

——— 1537, blank, 75% bleached aspen sulfate; 25% eastern sulfite; ——— 1538, 1% M, 75% bleached aspen sulfate, 25% eastern sulfite; ——·—— 1539, 3% M, 75% bleached aspen sulfite, 25% eastern sulfate; - - - - 1572, blank, 75% bleached aspen sulfate, 25% eastern sulfite, long beating time.

good strength properties without appreciable beating. The more drastic beating increased the expansivity above that produced by the bonding resin (fig. 5).

Aspen soda pulp (item 15).—Generally satisfactory papers (runs 1557–9) were obtained with this pulp when either 1 or 3 percent of bonding resin was used. Drastic beating (run 1573) did not develop the necessary strength in the paper to the extent that 3 percent of melamine-formaldehyde resin did, and it increased expansivity and greatly reduced air permeability (fig. 6).

Aspen sulfite pulp (item 16).—This is another pulp from which papers (runs 1541–3) with good strength and resistance to surface pick, combined with low expansivity, were produced when bonding resin was used (fig. 7).

Aspen neutral sulfite pulp (item 5).—Papers (runs 1495–7) made from this pulp mixed with varying percentages—25, 50, and 75, respectively—

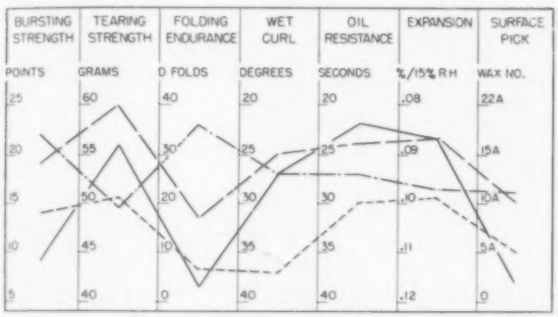

FIGURE 6. *Effect of melamine resin in papers containing aspen soda pulp (FPL item 15).*

—— 1557, blank, 75% bleached aspen soda, 25% bleached eastern sulfite; ———— 1558, 1 M, 75% bleached aspen soda, 25% bleached eastern sulfite; ——. —— 1559, 3 M, 75% bleached aspen soda, 25% bleached eastern sulfite; - - - - 1573, blank, longer beating time.

of soda pulp (hardwood), with no bonding resin added, were unsatisfactory because of very high expansivity and curl.

Mixed aspen and spruce sulfate pulp (item 3).—The papers (runs 1499 and 1500) from 100-percent sulfate pulp (67 percent of aspen and 33 percent of spruce), without and with 1 percent of bonding resin, had satisfactory strength properties but with expansivity nearing the border line (fig. 8).

In order to get a softer sheet with the bleached sulfate, and less expansivity, it was decided to make two more runs (1501–2) duplicating runs 1499 and 1500 except in the pulp furnish, which included a strong hardwood soda pulp. The pulp furnish for the runs (1501–2) was 40 percent of sulfate, aspen; 20 percent of sulfate, spruce; and 40 percent of soda, hardwood. The strength properties of the papers were fairly good and the expansivity satisfactory, but the resistance to surface picking was somewhat less. However, it is believed that aspen sulfate pulp prepared alone and then mixed with coniferous sulfite in 75- to 25-percent proportion respectively, and having 3 percent of melamine-formaldehyde resin

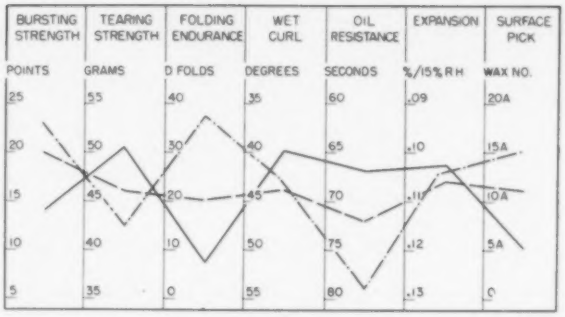

FIGURE 7. *Effect of melamine resin in papers containing aspen sulfite pulp (FPL item 16).*

—— 1541, blank, 75% bleached aspen sulfite, 25% bleached eastern sulfite; —— —— 1542, 1% M, 75% bleached aspen sulfite, 25% bleached eastern sulfite; ——. —— 1543, 3% M, 75% bleached aspen sulfite, 25% bleached eastern sulfite.

added, would give paper equally as good, if not better, for offset printing (fig. 8).

Black gum (tupelo) sulfate pulp (item 6).—When this pulp was used in combination with 25 percent of sulfite (coniferous) and had 1 or 3 percent of bonding resin added, the papers made (runs 1503–16–17) were of good strength and had very high resistance to surface pick, but the expansivity was too high. The expansivity of paper from run 1518, 100 percent of black gum sulfate pulp with 3 percent of bonding resin, was also too high (fig. 9).

Since black gum sulfate pulp looks so promising in strength development and resistance to surface pick, it seems likely that if the pulp were combined with another hardwood pulp, instead of a coniferous, a very satisfactory paper could be obtained if 1 to 3 percent of bonding resin were used.

Peroxide-bleached paper-birch groundwood (item 8).—On the whole, in these papers (runs 1519–21) the melamine resin had little beneficial effect.

Paper-birch sulfite pulp (item 10).—Papers (runs 1533–5) with good strength and resistance to surface pick, combined with low expansion, were made from this pulp in combination with only 25 percent of sul-

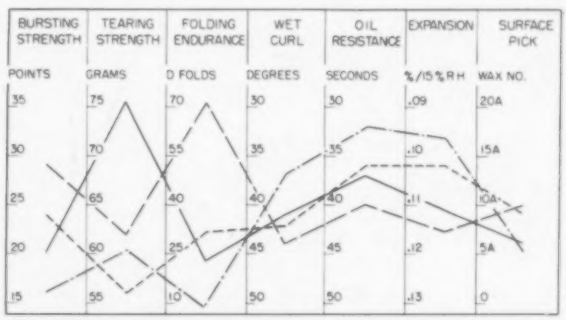

FIGURE 8. *Effect of melamine resin in papers containing aspen and spruce sulfate pulp (FPL item 3).*

—— 1499, blank, 100% bleached sulfate, 67% aspen, 33% spruce; —— —— 1500, 1% M, 100% bleached sulfate, 67% aspen, 33% spruce; ——. —— 1501, blank, 60% bleached sulfate (67% aspen, 33% spruce), 40% strong soda; - - - - 1502, 1% M, 60% bleached sulfate (67% aspen, 33% spruce), 40% strong soda.

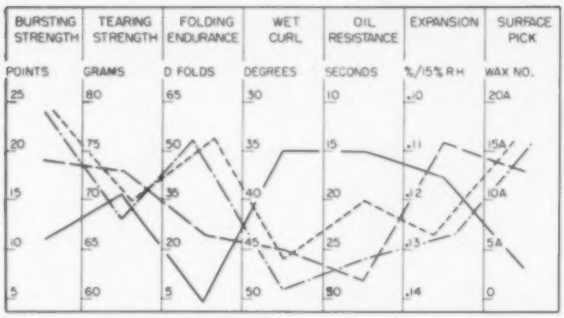

FIGURE 9. *Effect of melamine resin in papers containing black gum sulfate pulp.(FPL item 6).*

——— 1503, blank, 75% bleached black gum (tupelo) sulfate, 25% eastern sulfite; — — — 1516, 1% M, 75% bleached black gum (tupelo) sulfate, 25% eastern sulfite; — . — 1517, 3% M, 75% bleached black gum (tupelo) sulfate, 25% eastern sulfite; - - - - 1518, 3% M, 100% bleached black gum (tupelo) sulfate.

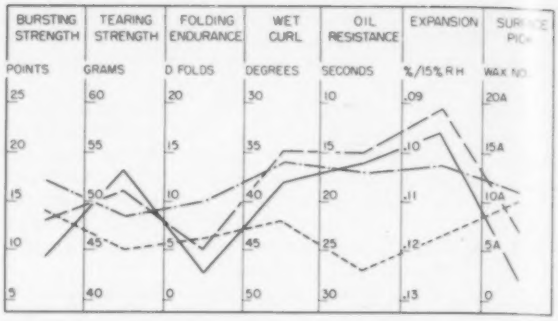

FIGURE 11. *Effect of melamine resin in papers containing beech sulfate pulp (FPL item 12).*

——— 1568, blank, 75% bleached beech sulfate, 25% bleached eastern sulfite; — — — 1569, 1% M, 75% bleached beech sulfate, 25% bleached eastern sulfite; — . — 1570, 3% M, 75% bleached beech sulfate, 25% bleached eastern sulfite; - - - - 1571, blank, longer beating time.

fite pulp (coniferous) and having 1 or 3 percent of bonding resin added (fig. 10).

Paper-birch neutral sulfite pulp (item 9).—As shown in the table the papers (runs 1508–10) made from this pulp and varying percentages—25, 50, and 75, respectively—of soda pulp (hardwood) without bonding resin added were unsatisfactory because of very high expansivity and curl.

Beech sulfate pulp (item 12).—Beech sulfate was another pulp from which papers (runs 1568–70) were produced with satisfactory strength and resistance to surface pick, combined with low expansivity when 1 or 3 percent of melamine-formaldehyde resin was added. Drastic beating alone did not develop the necessary strength in the paper (run 1571). Moreover, it increased the expansivity above that of the paper in which bonding resin was used and reduced tearing strength and air permeability (fig. 11.)

Douglas-fir neutral sulfite pulp (item 13).—This is a coniferous wood pulp, whereas the other pulps supplied by Forest Products Laboratory were wholly or predominately hardwood. The papers (1529–31) made from the Douglas-fir pulp mixed with soda pulp (hardwood)—25, 50, and 75 percent, respectively—without bonding resin, were fairly satisfactory, but the expansivity was approximately the maximum allowable.

Since a long-fibered pulp characterized by high strength, especially tearing resistance, was produced from Douglas fir by the neutral sulfite, semichemical process, it seems that the wood might better be cooked by one of the other pulping processes. It would thereby make available long-fibered, softer pulp, which would doubtless be satisfactory for use with such hardwood pulps as have been used in these experiments, and release the spruce sulfite pulp (coniferous) for other types of papers. Douglas fir appears to show great promise as a wood for paper-making.

Other hardwood-coniferous pulp mixtures.—To afford comparisons, two series of papers were made from a furnish of commercial bleached soda pulp (hardwood) and commercial sulfite pulp (coniferous), without and with melamine resin. For one series (runs 1562–4) 75 percent and 25 percent of the pulps, respectively, were used (fig. 12); for the other series (1540–60–61) 50 percent of each was used (fig. 13).

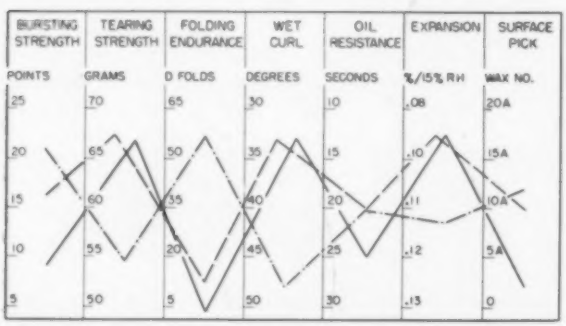

FIGURE 10. *Effect of melamine resin in papers containing paper-birch sulfite pulp (FPL item 10).*

——— 1533, blank, 75% bleached paper-birch sulfite, 25% bleached eastern sulfite; — — — 1534, 1% M, 75% bleached paper-birch sulfite, 25% bleached eastern sulfite; — . — 1535, 3% M, 75% bleached paper-birch sulfite, 25% bleached eastern sulfite.

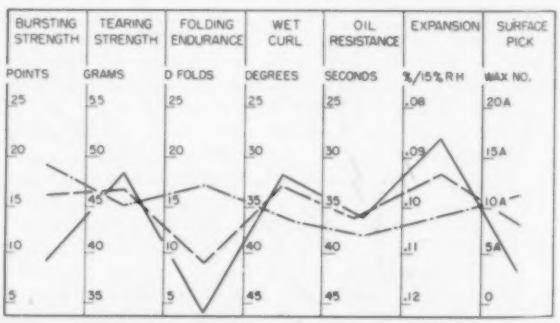

FIGURE 12. *Effect of melamine resin in papers containing Douglas-fir neutral sulfite pulp (FPL item 13).*

——— 1562, blank, 75% strong soda, 25% eastern sulfite; — — — 1563, 1% M, 75% strong soda, 25% eastern sulfite; — . — 1564, 3% M, 75% strong soda, 25% eastern sulfite.

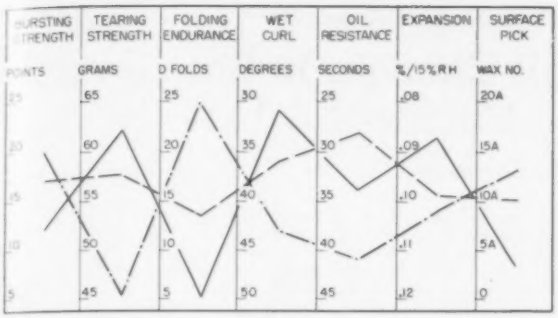

FIGURE 13. *Effect of melamine resin in papers containing commercial hardwood soda pulp and coniferous sulfite pulp.*

—— 1540, blank, 50% bleached strong soda, 50% bleached eastern sulfite;
— — 1560, 1% M, 50% bleached strong soda, 50% bleached eastern sulfite;
—·— 1561, 3% M, 50% bleached strong soda, 50% bleached eastern sulfite.

VII. Summary

Promising results were obtained with the hardwood pulps alone and mixed in the production of lithographic-type papers. Papers with good strength and resistance to surface pick, combined with low expansion and curl, were made from the hardwood pulps with melamine-formaldehyde resin added for bonding. By use of the resin (1 or 3 percent, based on dry fiber) the paper could be made from a less hydrated stock, the strength being developed mainly by bonding the fibers with the resin instead of by the conventional beating. The pulps giving particularly promising results comprised aspen sulfate, aspen soda, aspen sulfite, birch sulfite, and black gum sulfate. The qualities of the papers made from these pulps are as good as, and in some respects better than, those of paper made from 50-percent commercial hardwood pulp and 50-percent commercial sulfite softwood pulp.

Although not a hardwood, Douglas fir was also included in the study to evaluate its paper-making characteristics. Only neutral sulfite (semichemical) pulp was used, but since the fibers were long and seemed to have high strength, especially tearing resistance, it is believed that if the pulp were prepared by any of the other chemical processes an excellent paper-making material could be produced. In general, papers made from the pulps prepared from any of the woods by the neutral sulfite (semichemical) process were not entirely satisfactory. The pulps tended to hydrate too quickly and to develop considerable hardness, and the papers made from them had high expansivity and curl.

An example of the possibilities of resin bonding used to develop strength in papers made from hardwood pulps is shown by the measurements obtained on the papers made from 75-percent bleached aspen sulfate and 25-percent commercial sulfite pulp. With all other factors constant, the addition of 3-percent melamine-formaldehyde resin to this fiber increased the bursting strength fro . 8 to 22 points, the folding endurance from 2 to 46 double folds, and the resistance to surface pick from wax 2A to 13A, yet the expansivity remained low. These results were obtained without beating the fibers to any considerable extent.

Judged by the laboratory test data, the results appear very satisfactory. The performance of the experimental papers in the printing operations, however, will be the determining factor in their satisfactoriness for lithographic use.

Printing tests of them are being made in the experimental printing plant of the Lithographic Technical Foundation, and the results will be published by the Foundation. If they are satisfactory, the development of strength through the use of synthetic resins in offset papers may greatly increase the use of hardwood fibers.

The cooperation of George M. Hunt, Director, and G. H. Chidester, Chief, Division of Pulp and Paper, U. S. Forest Products Laboratory, in furnishing the pulps for this investigation is gratefully acknowledged. This investigation and the previous investigations dealing with offset papers were conducted with the counsel of an advisory committee of technicians of the paper-making and printing industries, under the Chairmanship of R. F. Reed, Research Consultant, Lithographic Technical Foundation. The investigation was made under the direction of Charles G. Weber, deceased.

WASHINGTON, May 18, 1950.

Journal of Research of the National Bureau of Standards Vol. 45, No. 3, September 1950 Research Paper 2137

Determination of Very Small Changes in Rate Over Intervals of Several Days in Mechanical Timepieces

By Horace A. Bowman

A device for automatically plotting the isochronism of a clock or watch is described. It was developed to assist in precision tests on marine chronometers and watches, but it may be altered without difficulty to plot the curves for any timepiece. Its accuracy is 0.01 second, which is sufficient for ordinary timepieces, but by a few simple changes this accuracy may be increased. Some of the curves plotted by this instrument are shown. The sensitivity of this instrument, as well as its graphic scale, may be varied depending upon the quality of the timepiece being tested.

I. Introduction

The balance assembly of a watch is a mechanical oscillator, and like most oscillators, its resonant frequency changes with variations in the amplitude of oscillations. The amount of frequency variation that the balance assembly experiences as the watch runs down is known as isochronism. A curve in which the integrated time error of this oscillator is plotted as a function of the interval from winding is called the isochronism curve, or dial error, curve. As long ago as 1861 Phillips [1] stated the geometric conditions for the formation of a hairspring that would show no change in frequency of oscillation when the amplitude of oscillation is changed. These conditions are:

1. that the center of gravity of the terminal must fall on the radius that completes the first quadrant of the spring through which the curve passes, and

2. that it must be distant from the center of the spring by an amount that equals R^2/L: where R is the connecting radius and L the length of the theoretical terminal.

These conditions, while quite simple to state, are difficult to obtain in mass-production practice.

However, the theoretically isochronous hairspring terminal (sometimes called the "overcoil" because it is a coil of the hairspring that is carried above the main body of the spring from the outer edge and terminates on a nonoscillating part of the watch) is quite closely approached in the very fine watches manufactured today. The isochronous error is also reduced by increasing the power delivered by the mainspring, so that there is little change in the amplitude of oscillation of the balance wheel in the 24 hours that the watch is designed to keep good time. As a result, the isochronism error frequently drifts less than two or three hundredths of a second per hour. Plotting a curve by observing the watch once or twice per hour with the assistance of a chronograph and a standard of time will not show up these tiny drifts of rate. As timepieces improve, methods of testing must improve in order that the test may continue, to have meaning.

The Bureau's Time Section has developed an instrument that observes the watch every 0.4 second and plots the integrated time error to an accuracy of 1/100 of a second.

[1] M. Phillips, Memoire sur le spiral reglant des chronometers et des montres (1861).

II. Design of the Instrument

This instrument is essentially a relay-type servo system, which, by means of advancing or retarding the phase of a very accurate quartz-crystal-controlled frequency, keeps this standard frequency in phase with the frequency of the balance assembly of the watch being tested. The phase and frequency of the oscillator itself are unchanged by the action of this system. By plotting the amount of phase shift that is thus introduced into the standard frequency and choosing graphic coordinates referring to time rather than degrees of phase shift, a plot of the dial error is generated.

The standard frequency, accurate to 1 part in 50,000,000 [2] at a magnitude of 60 c/s and at low impedance, is passed through a continuous phase shifter [3] constructed from a Bendix two-phase self-synchronous motor. (See fig. 1.) Clockwise rotation of the shaft of the motor results in advancing the phase of the output frequency, and counterclockwise rotation causes a retardation of the phase. One complete rotation of the shaft introduces a phase shift of 360°. This output frequency is passed through an amplifier and used to drive a 150-rpm synchronous motor. A galvanometer mirror is attached to the shaft of this motor. This mirror, rotating in a beam of light, causes light to fall alternately upon two vacuum photocells. The optical system is so arranged (see fig. 2) that the interval between the illumination of photocell V_1 and the illumination of photocell V_2 is 0.3 second, and the interval between the illumination of V_2 and the illumination of V_1 is 0.1 second.

The pulse formed by V_1 is passed through a triode connected as a cathode follower, and used to trigger a 2050 Thyratron, V_3. The audible tick of the watch is amplified and used to trigger a second Thyratron, V_4. The coils of two double-throw relays are inserted in the plate circuits of both V_3 and V_4, and the two relay coils terminate on one side of a condenser inserted in the $B+$ lead (see fig. 3).

[2] J. M. Shaull, Adjustment of high-precision frequency and time standards, Proc. IRE **38**, 6 (1950).

[3] Invented by M. G. Pawley, Electronics and Ordnance Division, National Bureau of Standards.

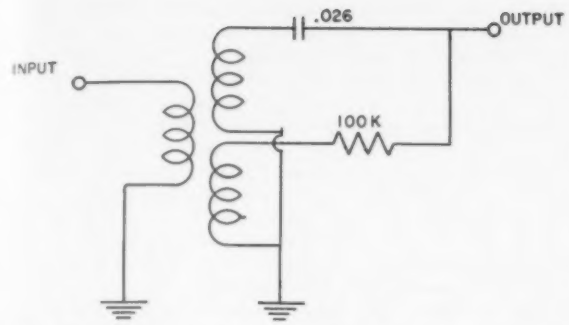

FIGURE 1. *Phase shift circuit used with the isochronism recorder.*

The condenser is chosen so that its capacitative reactance will equal the resistance at the input frequency. The values illustrated are for 60-cycle operation.

When a pulse from V_1 ionizes V_3, relay 1 closes (it is normally open) and remains closed as long as V_3 conduits. However, when the lower plate of C_1 is saturated with electrons, there being no other electron path available, V_3 deionizes and relay 1 opens. Now a pulse on the control grid of V_4 will not cause V_4 to ionize because a completely charged C_1 blocks the electron path. It is obvious that had the pulse on V_4 arrived before the pulse on V_3, V_4 would have ionized, closing relay 2, and V_3 would have remained deionized. In other words, V_3 and V_4 act as a pulse selection circuit, closing either relay 1 or relay 2 depending on whether the pulse from the watch tick arrived before or after the pulse from the motor-mirror driven by the standard frequency (watch fast or watch slow).

With C_1 charged, additional pulses on V_3 and V_4 will cause no action; hence it becomes necessary to insert a mechanism to bleed the electrons from the lower plate of C_1. This is done by V_5, a 2050 Thyratron, which is triggered by the pulse from V_2 through a cathode follower. Relay 3, with its points in series with its coil, is inserted in the plate circuit of V_5. This relay is normally closed and opens only when V_3 conducts. Its armature is heavily weighted to increase armature inertia. Hence when V_3 becomes ionized there is a sluggishness in the opening of relay 3. This permits the electrons on the lower plate of C_1 to escape completely to $+B$ through V_3 before the relay opens and destroys the electron path to $+B$. Likewise, the sluggishness of the armature of relay 3 permits V_5 to become completely deionized before it again closes the path to $+B$. This protects V_4 and V_5 from becoming permanently ionized by a burst of noise on V_4 at the same instant that V_5 is ionized.

Remembering that the pulse from V_2 is 0.3 second later than that from V_1, and realizing that only 0.2 second elapses, between the "tick" and the "tock" of a watch, if the tick of the watch triggered V_4, the tock, arriving 0.2 second later, would cause no action because C_1 would be still charged. In other words,

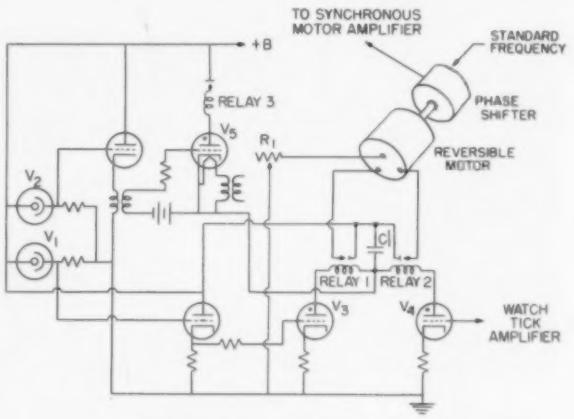

FIGURE 3. *Simplified diagram of the isochronism recorder.*

Due to cathode-filament potential separation limitations a separate bias and filament supply is required for V_5. The connections between the points of relays 1 and 2 and the reversible motor are drawn in simplified form. The true connections are shown in figure 5. The input to the phase shifter is the standard frequency, and the output goes to the 150-rpm synchronous motor shown in figure 2.

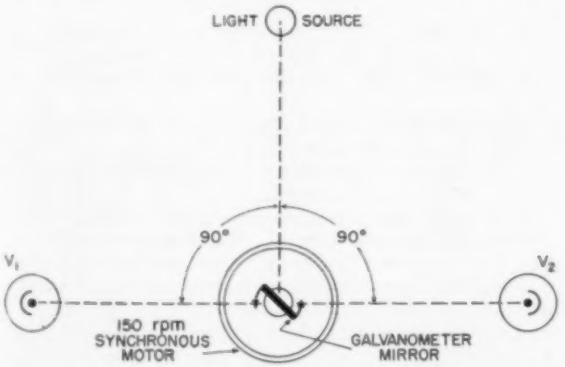

FIGURE 2. *Diagramatic outline of the optical system used for the alternate illumination of V_1 and V_2.*

At a motor-mirror speed of 150 rpm, the interval between the illumination of V_1 and V_2 is 0.3 second, while the interval from the illumination of V_2 to the illumination of V_1 is 0.1 second.

this instrument will accept for comparison only the ticks or only the tocks. This condition was chosen because even watches in the best of condition have an interval from the tick to the tock different from the interval from the tock to the tick. Either the ticks or the tocks are suitable for comparison purposes, but if they were both accepted the instrument would register alternately "fast" and "slow", a condition that obviously does not exist within the watch.

A small, reversible motor is so connected that when relay 1 closes it rotates in a clockwise direction, and when relay 2 closes it rotates in a counterclockwise direction; thus a slow watch causes the motor to run clockwise, and vice versa.

The servo loop is completed by a mechanical coupling between the armature of the reversible motor and the armature of the phase shifter. Thus, the motor introduces motion into the phase shifter in such a manner that the order of pulses received by

UNIVERSITY OF MICHIGAN LIBRARIES

FIGURE 4. *Isochronism recorder.*

A, Relays 1, 2, and 3 are at the front of the chassis and mounted on sponge rubber to minimize noise. The gear train performs two functions: first, it limits the amount of motion transmitted from the reversible motor to the phase shifter; and second, it controls the motion transmitted to the recording section via a self-synchronous motor.

B, Recording section of the isochronism recorder. The self-synchronous motor at the left is controlled by a similar one just behind the gear train in *A*.

the comparison circuit, V_3-V_4, tends to be reversed. A gear train (see fig. 4, *A*) reduces the amount of motion transmitted to the phase shifter by the motor.

The motion of the phase shifter is transmitted via a self-synchronous motor system to a remote recorder (see fig. 4, B) where one complete revolution of thep hase shifter is plotted as $\frac{1}{10}$ of a second. Rheostat R_1 (fig. 3) varies the voltage dropping across the reversible motor and thereby acts as a sensitivity control, governing the amount of motion performed by the motor for each impulse received.

Relays 1 and 2 are connected as indicated in figure 5. This type of connection is used to prevent both a clockwise and a counterclockwise impulse being applied to the motor at the same instant. Condenser C_1 (fig. 3) is chosen so that it will store enough energy at the plate voltage used to keep relays 1 and 2 closed 0.005 second. This means that if the pulse arrival from the photocell differs by less than 0.005 second from the pulse arrival from the watch tick amplifier, both relays will partially act because there will be enough positive charge on the lower plate of C_1 to permit both V_3 and V_4 to ionize. This is the factor that limits the sensitivity of the instrument, as the comparator cannot distinguish between pulses separated by less than 0.005 second. If greater sensitivity is required, a smaller condenser should be used in place of C_1. The value of 0.2 μf (the actual value of C_1 in this instrument) is not a limiting value. In the development of this instrument values as low as 0.05 μf were used, with correspondingly smaller relays and a more sensitive motor, with quite satisfactory results; however, it was felt that the larger, more rugged motor and relays were desirable for a constantly working laboratory instrument.

Considering the other errors in the instrument, such as the lag in the self-synchronous-motor system that transmits the information to the recorder, the stylus friction in the recorder, et cetera, the instrument has an accuracy of ±0.01 second at any time. As stated previously, this accuracy could be considerably increased by certain mechanical changes, but since watches do not repeat observations with great precision, no effort is contemplated to increase this value.

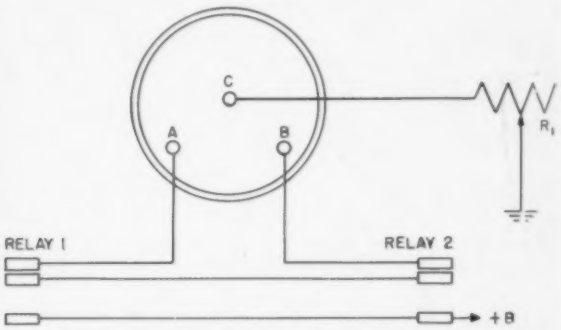

FIGURE 5. *Motor-control relay connections.*

Details of the connections between the reversible motor and the double-throw relays 1 and 2, which control its direction of motion. When a pulse is applied between *A* and *C* on the motor, the armature rotates counterclockwise while the pulse is being applied. When a pulse is applied between *B* and *C*, the motion is clockwise. By making the connections as illustrated, the motor is protected against having both a clockwise and counterclockwise impulse applied at the same instant. The relay points are shown in their normal position. R_1 is the sensitivity control that governs the amount of motion executed by the motor for any one impulse.

Upon examination of figure 3, several simplifying devices become apparent. The elimination of relays 1 and 2 can be accomplished and the pulse actuating them can be applied directly to the reversible motor, the only change necessitated thereby being the enlargement of condenser C_1. The photoelectric system performs two functions: First, it eliminates alternate ticks, and second, it controls the drain of electrons from the lower plate of C_1. The separation of ticks from tocks could be accomplished by a flip-flop and the discharge of C_1 by a bleeder resistor. The more complicated arrangement was used because this instrument will be called upon in future problems to control electric motors too large for convenient Thyratron drive.

III. Use of the Instrument

This instrument is used in plotting the isochronism curves that accompany class A watch tests performed by the Bureau. The 150-rpm motor may be changed to a 120-rpm motor, thereby making it possible to plot the isochronism curve of a marine chronometer. Provisions have been made on the instrument to make this change quickly and conveniently. For that matter, it is possible to make a plot of the isochronism of any timepiece as long as the revolutions per minute of the motor just equal the nominal value of the balance frequency (remembering that in most watches the "beat" of a watch equals twice the balance frequency).

To use the instrument, a watch is wound and placed on the vibration pick-up provided. The instrument will take about one minute in "hunting" for the watch tick or tock. The noise that occurs during the first coincidence in the comparator circuit is thereafter held in synchronization whether it is the tick or the tock. Thereafter the servo loop keeps the standard frequency in phase with this particular noise.

In each tick or tock there are several important noises to consider (see fig. 6) that are caused by the action of the balance assembly.

The loudest noise is the dropping of the escape wheel tooth onto the locking face of the pallet stone. This noise depends upon the mainspring force for both its amplitude and position on the time axis, so it is not a particularly good noise on which to operate.

Since we are primarily concerned with the frequency of the balance wheel, it is best to use a noise that always occurs at the same angular position of the balance wheel. This noise, the first, although not a loud noise, is caused by the roller jewel (attached to the balance wheel) striking the fork slot. The position of the loudest noise on the time axis becomes quite erratic in the minutes preceding the complete run-down of the mainspring. In order to assure sufficient amplification to receive the first noise, a pentode and a triode are connected together in a two-stage microphone amplifier.

Two neon indicators show when the instrument has accomplished synchronization. One of them is connected across relay 1, with sufficient series resistance to prevent burnout, and the other across relay 2. When both lights flash, the instrument is holding the standard frequency in phase with the watch.

This isochronism plotter may be used as an ordinary watch rate recorder to give the instantaneous rate of the watch if desired. Inasmuch as the plot generated by the recorder is the integrated time error, the slope of this curve is the instantaneous rate. In this respect it gives a clearer picture of the instantaneous rate than a regular rate recorder, because in watches in which the train friction varies widely, the operator may draw a smooth curve through the true irregular curve and determine a "better" instantaneous rate.

Figure 7 illustrates four isochronism curves plotted by this instrument. They are for the same watch in the same position (dial up). The irregularities in these curves of less than 0.1 second would have escaped notice had these curves been plotted by a chronograph, even with the assistance of a high-precision standard of time. On a 24-hour basis this watch was running at a rate constant to 1.8[illegible] sec/day.

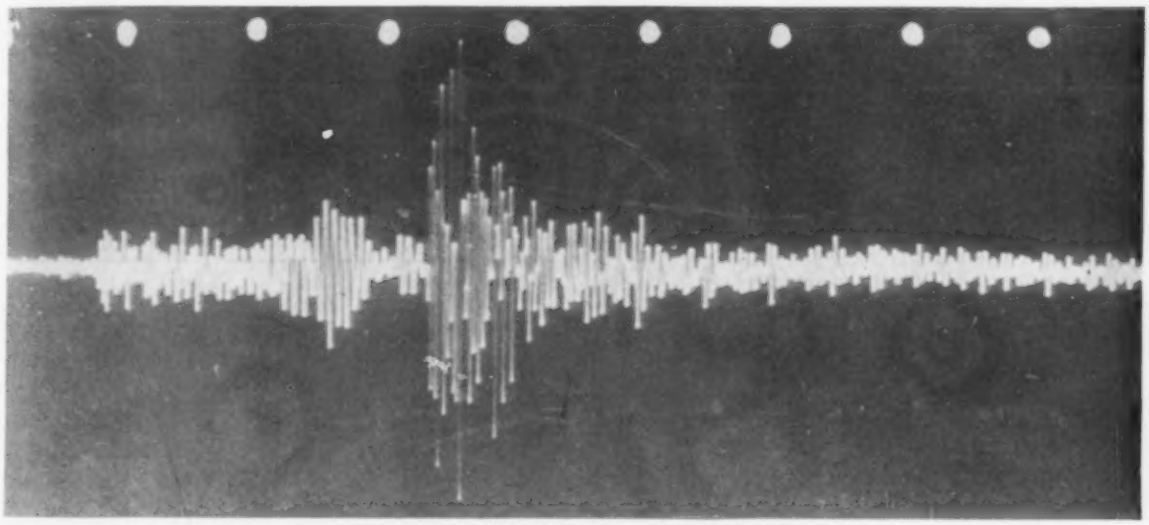

FIGURE 6. *Oscillogram of a watch tick*

Photograph of an oscilloscope trace of a watch tick as picked up by a microphone. It has been estimated that there are 140 sources of sound in a single tick. The first sound, although not the loudest, is the one most suitable to use in the operation of the isochronism recorder because its position on the time axis is a function of the angular position of the balance wheel. The white dots above the trace are approximately 4 1/2 msec apart.

UNIVERSITY OF MICHIGAN LIBRARIES

The adjustment of a watch is intended to eliminate the differences in the rate when it is operated in various positions. Figure 8 shows the actual differences in rate of a newly cleaned and overhauled 19-jewel, size 12, pocket watch. If the watch had been in "perfect" adjustment and contained a "perfectly" isochronous hairspring, the six curves would have been superimposed one upon the other. The variations are caused by frictional changes and gravitational effects that deform the hairspring from its truly isochronal configuration. It might be pointed out here that isochronism tests are usually performed with the watch in either the dial up or dial down position.

In addition to the routine testing for which this instrument was designed, it is being used in researches currently being conducted upon the effects of friction in the train, balance lubrication, and variations in amplitude. It plots curves that are sufficiently accurate to permit differentiation and interpretation. It has eliminated the necessity of a long vigil with a watch, reading it at regular intervals and recording the observation on a chronograph in order to obtain the information necessary to plot an isochronism

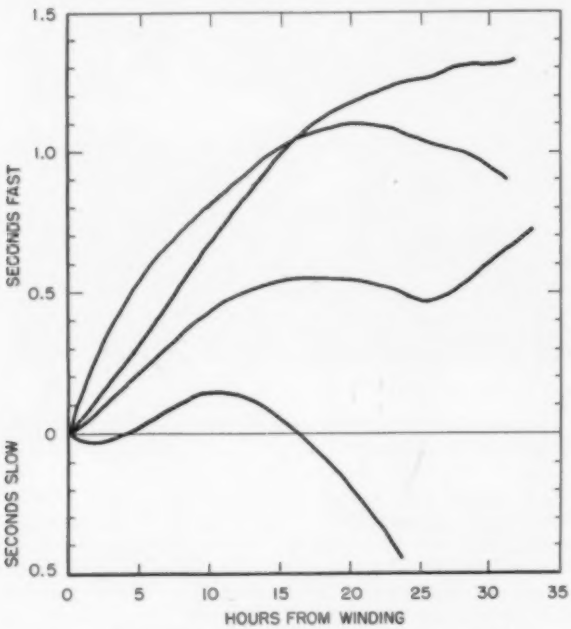

FIGURE 7. *Four successive isochronism curves on the same watch.*

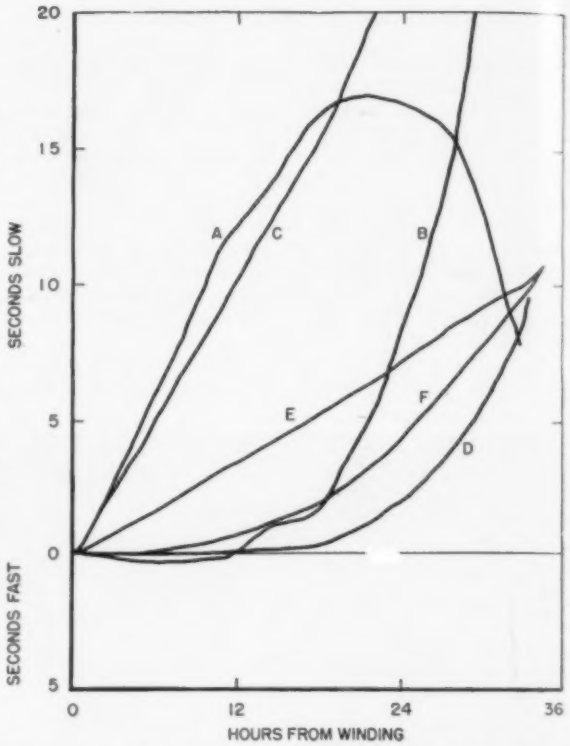

FIGURE 8. *"Run-down" curves plotted for a newly cleaned and overhauled size 12, 19-jewel pocket watch.*

This watch is poorly adjusted since placing it in various positions for test results in widely diverging isochronism curves. Ordinarily the isochronism curve is drawn for the "dial up" and "dial down" positions only.

A, Pendant right; *B*, pendant left; *C*, pendant down; *D*, pendant up; *E*, dial up; *F*, dial down.

curve. Under the previously used procedure the factors of human fatigue limited the accuracy of any observation to ± 0.2 second, and since the watch was seldom observed more frequently than once each hour, the curve finally arrived at was comparatively crude. The benefit of an observation every 0.4 second, accurate to ± 0.01 second, permits the plotting of a curve upon which the most exacting analysis may be conveniently performed.

The criticisms, comments, and assistance given by C. N. Challacombe, Research Physicist, Elgin National Watch Co., are gratefully acknowledged.

WASHINGTON, April 11, 1950.

Journal of Research of the National Bureau of Standards Vol. 45, No. 3, September 1950 Research Paper 2128

A Sulfate Susceptibility Test for Portland Cements

By W. C. Taylor[1] and R. H. Bogue[2]

A procedure has been developed by means of which portland cements may be given ratings indicative of their resistivity to chemical attack by sulfate-containing solutions. The test, which may be performed in about a day, reveals the intrinsic resistivity to such attack by the cement itself as contrasted with the usual performance tests on mortar or concrete specimens, which require periods of weeks or months. The method involves the measurement of the amount of dissolved SO_3 rendered insoluble when cement is shaken with limewater for a stated period. The test has been examined critically and extensive correlations made with performance tests on laboratory and commercial portland cements.

I. Introduction

It has long been recognized [3] [3] that the resistivity of concrete structures to attack by sulfate waters is a function of both chemical and physical factors. Thus the cement paste may contain materials that are reactive with sulfate solutions, but the life of the concrete structure exposed to such solutions will be affected by other factors than the composition of the paste. It will be prolonged by any device that will give greater impermeability or greater constancy of volume to the hydrating member and shortened by the use of lean mixes and the presence of volume-expansive constituents.

The principal chemical cause of the disintegration of concrete in sulfate waters has been shown [2, 5, 13, 15] to be associated with a reaction between the sulfate ions of the solution, in the presence of calcium hydroxide, and the alumina-containing phases of the cement that dissolve in the solution. It has been observed [4] that crystalline tricalcium aluminate is less resistant to attack in sulfate solutions than is the same composition in the glassy state, whereas crystalline tetracalcium alumino ferrite (or the iron-phase solid solution) is more resistant to such attack than its glassy counterpart. Also it has been noted that alumina in the form of the tricalcium aluminate is less resistant to attack in sulfate solutions than it is when in the form of the tetracalcium alumino ferrite. No reason has been advanced for the apparently anomalous behavior of the tricalcium aluminate.

Calcium sulfate and tricalcium aluminate, in the presence of calcium hydroxide (always present in cement pastes owing to the hydrolysis of tricalcium silicate) react to form calcium sulfoaluminate [11]. Under the conditions of the test, the high-sulfate form is produced according to the equation:

$$3CaSO_4+3CaO.Al_2O_3+31H_2O=3CaO.Al_2O_3.3CaSO_4.31H_2O.$$

If we assume a constant SO_3 concentration in the solution, the rate and extent of the above reaction will increase with the amount of alumina that enters the solution in any given period of time. Since, however, this amount varies with the state of the tricalcium aluminate and is also affected by the presence of crystalline or glassy iron-alumina solid solutions, the reaction cannot be defined by a mere proportionality factor applied to the Al_2O_3 or $3CaO.Al_2O_3$ present.

The usual method for evaluating the resistivity of cements to sulfate attack has been to note the behavior (change in length, strength, sonic modulus, appearance, etc.) of mortar or concrete specimens when placed for extended periods in natural or synthetic sulfate solutions. The time element, however, militates against such tests for specification purposes. Furthermore, these tests measure the total capacity of the *specimen* to withstand attack rather than the inherent resistivity of the *cement*. For these reasons they are not ideally designed for the purpose of indicating the sulfate resistivity of cements.

An investigation initiated in this laboratory in 1941 has resulted in a method by which the progress of the above reaction may be noted. In principle, it consists of a measurement of the amount of dissolved SO_3 rendered insoluble by reaction with aluminates when cement is shaken with limewater for a stated period of time. In the treatment that follows, the adopted procedure will first be given, followed by a discussion of critical aspects of the test and correlations obtained between the test and other methods of evaluating sulfate resistivity.

II. Test Procedure

The SO_3 content of the cement to be tested is first determined by any acceptable procedure [1].

About 30 g of standard Ottawa sand, or some similar silica sand, is placed in a dry 100-ml graduated cylinder, so designed that it can be fitted with a stopper. (A blank determination should be made with each lot of sand employed.) A sample of cement is weighed out equal in grams to 5.4 divided by the percentage of SO_3 in the cement. This sample is placed in the cylinder containing the sand. One hundred milliliters of saturated limewater is measured in a 100-ml pipette and added rapidly to the cylinder by inverting the pipette. A clean rub-

[1] Research Associate at the National Bureau of Standards, representing the Portland Cement Association; Mr. Taylor is now chief chemist with the Owens-Illinois Glass Co.

[2] Director of the Portland Cement Association Fellowship at the National Bureau of Standards.

[3] Figures in brackets indicate the literature references at the end of this paper.

UNIVERSITY OF MICHIGAN LIBRARIES

ber stopper is inserted and the mixture at once shaken vigorously by hand. The cylinder is then fastened to a rotary shaker that is operated at a rate of 60 rpm for 6 hr from the time of the addition of the limewater. (The rack should be so designed that no cylinder is more than 6 in. from the hub.) In order to obtain consistent results within a laboratory or between different laboratories, it is essential that the test be performed at a constant temperature.

Just before the end of the 6-hr reaction period, a 9-cm No. 42 filter paper (or a comparable paper) is inserted in a Buchner funnel and moistened with distilled water. Suction is applied, and the contents of the cylinder are poured into the funnel. The cylinder is washed with 50 to 60 ml of distilled water and the washings poured onto the funnel. This step is repeated once.

The filtrate is transferred to a 600-ml beaker. The filter flask is twice washed with 50 to 60 ml of distilled water and the washings added to the filtrate. The volume is then made up to about 350 ml, 5 ml of concentrated HCl added, and the weight of SO_3 determined by precipitation with $BaCl_2$ solution in accordance with standard procedure [1].

After the amount of SO_3 remaining in the solution is determined, that value is subtracted from the amount of SO_3 that was present in the sample of the cement taken. This difference is assumed to be the quantity of SO_3 that has reacted to form calcium sulfoaluminate during the period of the test. This is calculated as percentage of the SO_3 originally present in the cement and is designated as the "sulfate reaction value". These values are reported to the nearest whole number.

III. Critical Aspects of the Test

1. Source of Sulfate

There would seem to be an advantage if an excess of SO_3 could be provided for interaction with the aluminates, but no satisfactory means for accomplishing that has been found.

An attempt to use sodium sulfate for this purpose gave erratic results, and the differentiation between resistant and nonresistant cements was not satisfactory. This is believed to have been due to a reaction between the sodium sulfate and calcium hydroxide by which gypsum was precipitated. In such case, the change in SO_3 concentration of the solution would not be a measure solely of the interaction of SO_3 with the aluminates.

If gypsum is to be the source of the SO_3, it is obvious that the amount present must be such that it will dissolve completely in the solution used. For, if gypsum were present in excess of that amount, then, as SO_3 was removed from the solution by the reaction with the aluminates, more SO_3 would enter the solution from the gypsum, and the progress of the reaction would not be measured by the SO_3 concentration of the resulting solution. An amount of cement must therefore be taken such that its content of gypsum (or other form of calcium sulfate) will be completely dissolved. And, since a cement paste is quickly saturated with $Ca(OH)_2$ due to the hydrolysis of $3CaO.SiO_2$, it appears proper that the solvent be saturated limewater.

2. Solubility of Calcium Sulfate and Sulfoaluminate

According to Cameron and Bell [6], $Ca(OH)_2$ and $CaSO_4.2H_2O$ can coexist as solid phases in equilibrium with a solution containing 1.588 g of $CaSO_4$ and 1.222 g of CaO per liter at 25° C. This means that 0.0934 g of SO_3 from gypsum (equivalent to 0.2008 g of $CaSO_4.2H_2O$ or 0.1588 g of $CaSO_4$) may be dissolved in 100 ml of saturated limewater at 25° C. In a more recent report by Hansen and Pressler [8], it was found that 0.0123 mole/liter of SO_3 can dissolve from gypsum in a saturated solution of $Ca(OH)_2$ at 25° C. This means that 0.0985 g of SO_3 from gypsum (equivalent to 0.2118 g of $CaSO_4.2H_2O$ or 0.1674 g of $CaSO_4$) may be dissolved in 100 ml of saturated limewater at 25° C. Hansen and Pressler show also that the solubility of the gypsum in the saturated limewater increases rapidly with increasing amounts of KOH or NaOH in the solution.

The solubility of the calcium sulfoaluminate in saturated limewater is so small as to be practically insignificant in the test; i. e. about 0.005 percent [10].

3. The SO_3 Limit

From these data it appeared that the method would rest on safe ground by fixing the upper limit of SO_3 allowed to be present at 0.09 g /100 ml, equivalent to a gypsum limit of 0.19 g/100 ml of saturated lime solution. Assuming the use of 3 g of cement with 100 ml of solution, the 0.09 g of SO_3 limit would be equivalent to an SO_3 concentration in the cement of 3 percent, which is sufficiently high to provide for any cement passing present ASTM specifications.

It is necessary, however, to consider the effect on the sulfate reaction value of a variation in the SO_3 content of cements. An examination of more than a hundred commercial cements analyzed in 1945 shows a range in SO_3 from 1.1 to 2.2 percent. Seventy-five percent of these cements fall within the range of 1.6 to 1.9 percent of SO_3. The 106 cements reported by Miller and Manson [13] in 1940 show a range (excepting one clinker) of 1.3 to 2.6 percent of SO_3, of which 74 percent fall between 1.6 and 1.9 percent of SO_3.

Two ways of providing a constant SO_3 content in the test samples were considered. The more direct method would be to add gypsum in such amount as to provide the upper limit allowable (in order to include all cements). That would be equivalent to 3.0 percent of SO_3. It has been observed, however, that the sulfate resistivity of a cement may be improved by certain increases in its SO_3 content [5]. Hence this arbitrary addition might change the sulfate resistivity and so give fictitious values. The other method would be to take an amount of sample such that the SO_3 content would be equal to that in 3 g of a cement containing 1.8 percent of SO_3 (an

average value). In other words, the weight in grams of cement to be taken should equal 5.4 divided by the percentage of SO_3 in the cement.

4. Availability of Calcium Sulfate

Since anhydrite ($CaSO_4$) and plaster of Paris ($CaSO_4.\frac{1}{2}H_2O$) are sometimes present with the gypsum ($CaSO_4.2H_2O$) added to control the setting time of cements, it was necessary to examine their relative solubilities in saturated limewater. Pure specimens of natural anhydrite and gypsum, and hemihydrate prepared from the gypsum, were ground to three size fractions. Samples containing 0.09 g of SO_3 were shaken in 100-ml portions of limewater for different periods of time at about 70° F, and the percentage of the SO_3 in solution was then determined. The results are shown below.

It is seen that gypsum and hemihydrate dissolved completely in 1 hr, but the anhydrite was much more slowly soluble. In 6 hr the finest fraction was only two-thirds dissolved.

In order to ascertain if this relatively slow solubility of anhydrite might affect the usefulness of the test, a series of cements was examined. A number of commercial clinkers were ground to two orders of specific surface (about 1,800 and 2,550 cm^2/g) in one case with pure gypsum and in another with gypsum in which 10 percent of its SO_3 content had been replaced with natural anhydrite. The total SO_3 was fixed at 1.7 percent in all cases.

The sulfate reaction values are shown in table 1, together with the ages of disintegration of 1 by 1 by 6 in. 1:3 mortar bars that had been stored in 10 percent of Na_2SO_4 solution after 1 day in the molds and 6 days in water. The amount of the difference in sulfate reaction value due to the presence of the anhydrite is seen to be small in all cases, and usually would be altogether insignificant in establishing the sulfate resistivity of the cement.

Time of shaking	Percentage solubility for the screen-size fraction indicated								
	Gypsum			Hemihydrate			Anhydrite		
	100 to 200	200 to 325	Minus 325	100 to 200	200 to 325	Minus 325	100 to 200	200 to 325	Minus 325
hr	%	%	%	%	%	%	%	%	%
1	100	100	100	100	100	100	6.1	7.9	45.0
3	100	100	100	100	100	100	11.2	14.2	55.0
6	100	100	100	100	100	100	24.2	26.1	66.3

TABLE 1. *Effect of fineness and anhydrite on sulfate reaction values and life of mortar specimens stored in 10-percent* Na_2SO_4 *solution*

The cements, prepared from commercial clinkers, contained 1.7-percent total SO_3

No.	Calculated $3CaO.Al_2O_3$	Gypsum replaced by natural anhydrite	Specific surface	Sulfate reaction value	Age at disintegration of 1 by 1 by 6 in. 1:3 mortar bars in 10% Na_2SO_4
	%	%	cm^2/g		*Weeks*
419 A	2	0	1,850	22	Good at 1 yr
B	2	0	2,530	28	Do.
C	2	10	1,795	25	Do.
D	2	10	2,540	29	Do.
418 A	4	0	1,800	24	Do.
B	4	0	2,480	36	Do.
C	4	10	1,800	26	Do.
D	4	10	2,540	40	Do.
417 A	10	0	1,840	49	24
B	10	0	2,510	73	16
C	10	10	1,830	53	24
D	10	10	2,550	65	16
420 A	9	0	1,785	57	19
B	9	0	2,550	83	14
C	9	10	1,795	55	19
D	9	10	2,500	82	17
421 A	12	0	1,845	84	17
B	12	0	2,550	100	12
C	12	10	1,790	82	16
D	12	10	2,570	99	12
416 A	15	0	1,830	100	12
B	15	0	2,490	99	8
C	15	10	1,830	99	8
D	15	10	2,475	100	8

5. Effect of Specific Surface of Cement

It will be noted also from table 1 that an increase in the fineness of the cements, of a given composition and anhydrite content, resulted in an increase in the sulfate reaction value. That is, the finer the cement the less resistant it is indicated to be by this test. This indication was confirmed by the relative life of mortar bars of these cements stored in 10-percent solutions of sodium sulfate. Because the correlation is excellent, it can be postulated that the effect of surface area of the cement in the test is reflected in the performance of exposed specimens.

6. Effect of Temperature and Agitation of Reacting Solutions

It is to be expected that the rate of the reaction of calcium sulfoaluminate formation will be affected by temperature. The correctness of this supposition is indicated by the following results obtained by Hansen [9] on cements at three temperatures:

° F	Sulfate reaction values at temperature indicated		
	Cement No. 13	Cement No. 14	Cement No. 12
79	61	94	94
84	66	97	97
97	86	97	98

898894—50——3

UNIVERSITY OF MICHIGAN LIBRARIES

The increase in activity with rise in temperature points to the necessity, for comparable results, of carrying out the reactions involved in the test at a constant temperature.

Runs performed with different periods of agitation of the reacting solution showed that the amount of SO_3 removed from the solution increased with time of shaking. The SO_3 was removed rapidly during the first hour, but after 4 hr the rate of decrease in SO_3 concentration of the solution was slow and nearly constant over prolonged periods. It appears, therefore, that the selection of a 6-hr period serves the purpose of the test.

Changes in the speed of rotation and in the distance of the sample from the axis of rotation, were found also to affect slightly the rate of the reaction, and hence to necessitate the arbitrary fixing of these items in the procedure.

7. Solubility of Tricalcium Aluminate

The amount of SO_3 in a cement is usually inadequate to react with all of the aluminates that are in the cement. Thus the SO_3 in a given quantity of cement containing 1.8 percent of SO_3 can react with only 2.02 percent of $3CaO.Al_2O_3$. It has been found, however, that the $3CaO.Al_2O_3$ goes into solution slowly, the amount entering solution in a given period of time increasing with the concentration of the compound in the cement [10]. Hence it may be observed in the experiments throughout this series that only when the $3CaO.Al_2O_3$ is present in amounts many times greater than 2 percent, will the 1.8 percent of SO_3 be consumed completely in the period allowed for the test.

The range of differentiation in the test has been so adjusted that positive distinction may be had in the sulfate reaction value from an unreactive cement, at zero on the percentage scale, to a highly reactive cement, at 95 to 100 on the percentage scale.

8. Reproducibility of Results

A large number of sulfate resistivity tests have been made on identical cements by different operators in this and other laboratories. An anlysis of the data reveals that it is reasonable to expect an operator to obtain reaction values for a given cement that agree within three points. Similar agreement is obtained between different operators, provided the temperature and procedure are rigorously identical.

Although the technique of the test is simple, care must be used throughout because of the small amounts of SO_3 involved. A 3-g sample of cement having an SO_3 content of 1.8 percent contains 0.0540 g of SO_3. A difference of 1 mg in the amount of SO_3 determined in the filtrate will be responsible for a difference of about two points in the reaction value.

IV. Correlation of the Sulfate Susceptibility Test With Performance Records

1. Selected Clinkers

The 24 cements specially prepared from six commercial clinkers (table 1) showed an excellent correlation between the results obtained with the new test and the durability of 1 by 1 by 6 in. 1:3 mortar bars stored in 10-percent sodium sulfate solution. None of the cements that remained sound at 1 yr gave a sulfate-reaction value above 40, but every cement that distintegrated within that period gave sulfate-reaction values ranging from 49 to 100.

2. Laboratory Cements

A more extensive examination was made with the use of a series of 68 cements prepared in a laboratory kiln from commercial raw materials. Four clinkers were prepared from each of 17 different raw mixtures by varying the heat treatment, indicated as follows:

S_1=single-burned clinker slowly cooled,
S_2=double-burned clinker slowly cooled,
Q_1=single-burned clinker quickly cooled,
Q_2=double-burned clinker quickly cooled.

The compositions were designed to give a large variation in the potential $3CaO.Al_2O_3$ content, and also to give two groups of cements with respect to magnesia content; one group having about 1 percent of MgO and the other about 5 percent. The resulting clinkers were ground to approximately the same specific surface (about 1,700 cm^2/g) with gypsum to give 1.8 percent of SO_3 in the cements. From these cements 1 by 1 by 6 in. 1:2 mortar bars were moulded and duplicate specimens stored in 2-percent solutions of $MgSO_4$ and Na_2SO_4 following 1 day of damp curing and 6 days in water. The length of the bars was measured at stated periods. Sulfate reaction values were determined on all cements.

The linear expansions of the bars at 3 yr and various other data are shown in table 2, in which the cements are arranged in six groups in order of increasing sulfate reaction value.

An examination of this table will show that the division between definitely resistant and definitely nonresistant cements is clearly marked by the sulfate reaction values. It will be noted further that no specimen in group 1, having sulfate reaction values (*SR*) of 16 to 19, had a linear expansion greater than 0.200 percent at 3 yr. In group 2, *SR* 21 to 34, the 3-yr expansions with one exception were under 0.300 percent. In group 3, *SR* 35 to 50, the expansions reached as high as 1.026 at 3 yr, but in no case had any specimens disintegrated. Three cements fell between *SR* 52 and 54, one of which

TABLE 2. *Correlation of sulfate reaction values of laboratory cements with length change of 1 by 1 by 6-inch 1:2 mortar bars stored in 2-percent solutions of Na_2SO_4 and $MgSO_4$*

Arranged in order of increasing sulfate reaction values

Group	K–5 No.	Potential $3CaO.Al_2O_3$	MgO	Sulfate reaction value	2% $MgSO_4$ solution				2% Na_2SO_4 solution			
					Age at disintegration		Percentage expansion at 3 years		Age at disintegration		Percentage expansion at 3 years	
					Low MgO	High MgO	Low MgO	High MgO	Low MgO	High MgO	Low MgO	High MgO
		%	%		*Months*	*Months*	%	%	*Months*	*Months*	%	%
	$24Q_2$	2.6	1.2	16			0.040				0.029	
	$25S_1$	2.3	6.1	17				0.111				0.062
	$25S_2$	2.3	6.1	18				.114				.178
1	$25Q_2$	2.3	6.1	18				.178				.107
	$24S_1$	2.6	1.2	18			.128				.026	
	$25Q_1$	2.3	6.1	19				.200				.123
	$24S_2$	2.6	1.2	19			.039				.029	
	Average						0.096	0.151			0.028	0.118
	$24Q_1$	2.5	1.2	21			.140				.087	
	$1Q_2$	5.1	1.6	21			.247				.043	
	$3S_1$	4.7	5.2	24				.219				.063
	$1S_1$	5.6	1.4	26			.156				.096	
	$1Q_1$	5.8	1.4	26			.287				.043	
	$27Q_2$	5.8	4.8	27				.730				.229
2	$26S_2$	4.5	0.8	30			.074				.020	
	$3S_2$	4.7	5.2	31				.268				.032
	$26Q_2$	4.5	0.8	31			.125				.028	
	$3Q_2$	4.7	5.2	32				.287				.036
	$26Q_1$	4.5	0.8	33			.176				.052	
	$21Q_2$	6.7	1.4	33			.109				.065	
	$27S_1$	5.8	4.8	34				.296				.164
	Average						0.164	0.360			0.043	0.105
	$31Q_1$	6.9	5.2	35				.703				.170
	$26S_1$	4.5	0.8	35			.115				.018	
	$22Q_2$	7.1	1.5	35			.675				.016	
	$22S_2$	5.6	1.5	37			.370				.058	
	$23Q_2$	7.3	5.2	40				.956				.358
	$22S_1$	7.1	1.5	40			.410				.020	
	$27Q_1$	5.8	4.8	41				.632				.178
	$23S_2$	7.3	5.2	41				.641				.228
	$23Q_1$	7.3	5.2	42				1.026				.200
3	$27S_1$	5.7	4.8	43				.274				.139
	$21Q_1$	6.6	1.4	43			.177				.065	
	$23S_1$	7.3	5.2	44				.427				.138
	$31Q_2$	6.9	5.2	44				.850				.100
	$31S_2$	6.9	5.2	44				.334				.100
	$22S_2$	7.1	1.5	47			.350				.019	
	$31S_1$	6.9	5.2	48				.314				.075
	$3Q_1$	4.7	5.1	48				.681				.078
	$21S_1$	6.7	1.4	49			.104				.096	
	$22Q_1$	7.1	1.5	49			.797				.062	
	$30Q_2$	9.5	0.9	50			.425				.033	
	Average						0.380	0.622			0.033	0.160
	$17Q_2$	15.0	5.0	52		36				21		
4	$21S_2$	6.7	1.4	54			.104				.023	
	$30Q_1$	9.5	0.9	54			.525				.066	
	$17Q_1$	15.0	5.0	70		18				18		
5	$15Q_2$	14.5	1.4	73	24						.035	
	$30S_1$	9.5	0.9	76	36						.065	
	$30S_2$	9.5	.9	80	36						.058	
	$15Q_1$	14.5	.8	82	18						.362	
	$29Q_2$	15.3	4.6	84		9				9		
	$15S_2$	14.5	0.8	88	18				21			
	$28Q_1$	15.7	.9	91	12				9			
	$28Q_2$	15.7	.9	93	12				9			
	$29Q_1$	15.3	4.6	94		9				6		
	$33Q_2$	23.6	4.9	96		9				6		
	$32Q_2$	22.5	0.9	97	9				9			
	$33Q_1$	23.6	4.9	97		6				6		
6	$17S_1$	15.0	5.0	97		18				9		
	$15S_1$	14.5	0.8	97	18				18			
	$17S_2$	15.0	5.0	97		18				9		
	$32Q_1$	22.5	0.9	97	12				18			
	$29S_1$	15.2	4.6	98		6				1		
	$29S_2$	15.3	4.6	98		6				3		
	$28S_2$	15.7	0.9	98	9				6			
	$33S_2$	23.6	4.9	98		6				3		
	$32S_1$	22.5	0.9	99	6				6			
	$28S_1$	15.7	.9	99	6				3			
	$33S_1$	23.6	4.9	100		5				3		
	$32S_2$	22.5	0.9	100	6				2			
	Average				12	9			10	5		

UNIVERSITY OF MICHIGAN LIBRARIES

disintegrated in both sulfate solutions in less than 3 yr. All cements above *SR* 70 had disintegrated in the $MgSO_4$ solution by the end of the 3-yr period.

On the other hand, there may be noted several types of departure from concordance of results within the several groups. The expansion of specimens in the $MgSO_4$ solution was consistently higher than duplicate specimens in the Na_2SO_4 solution. This is because the Mg ion is converted to difficultly soluble $Mg(OH)_2$, which induces an additional expansion not directly related to that brought about by the SO_4 ion [5]. Also, the expansion of the specimens prepared from the high-MgO cements was consistently higher than that of specimens prepared from the low-MgO cements. This illustrates the physical contribution in the sulfate disintegration of mortar specimens due to an agent (periclase) that causes expansion in water alone [5, 16]. But, as revealed by these tests, the same material has no effect upon the inherent resistivity of the cement to sulfate attack. The total expansion in such cases is a function of the two superimposed effects (1) expansion in water and (2) the chemical interaction with sulfate solutions.

It will be noted further that the specimens within a given group, immersed in the same sulfate solution and prepared from cements of equivalent MgO content, show a spread in percentage expansions that bears no relation to the sulfate reaction values. Some of these can be explained by compositional differences; others cannot. This would be disturbing to our supposition that such a relation should exist, provided the specimen test were known to produce consistent results. A long experience with that test, however, has shown that uncontrollable factors in the preparation, storage, and measurement of specimens are of such a character that, in every series of tests, unpredictable variations of considerable magnitude may occur. Our difficulty lies in the necessity of using, as a criterion for the adequacy of a new test, an empirical test of admitted inadequacy. The best that can be done in such a case is to observe the high-level relationships and ignore the relatively insignificant low-level discrepancies. And, as already noted, the agreement between the two tests in the separation of resistant from nonresistant cements is excellent.

3. Commercial Cements

The sulfate susceptibility test was applied to the 106 portland cements that were selected by Miller and Manson [13] for comparative studies on sulfate resistivity by various methods. A vast number of data were accumulated by these investigators in collaboration with other laboratories [12], and additional tests on the same cements have been reported by Gause [7].

The sulfate-reaction values of these cements are given in table 3, together with the calculated potential tricalcium aluminate content and the results of a critical test reported by Miller and Manson [13]. This test shows the percentage of the 5-yr strength of 2 by 4-in. concrete cylinders stored in tap water that was attained by companion specimens stored for a similar period in Medicine Lake, S. Dak.[4]

TABLE 3. *Sulfate reaction values of the Miller and Manson cements* [13], *together with calculated potential* $3CaO.Al_2O_3$ *contents, and the percentage of normal strength (water storage) retained by 2- by 4-inch concrete cylinders after 5 years in Medicine Lake*

(Arranged in order of increasing sulfate-reaction value)

Cement No.	Sulfate reaction value	Potential $3CaO.Al_2O_3$	Percentage of normal strength of 2- by 4-in. cylinders after 5 yrs. in Medicine Lake
		Percent	*Percent*
631	22	3	92
507	28	2	77
582	31	5	83
405	32	5	79
513	33	1	70
628	38	0	83
611	40	5	85
543	44	4	67
531	45	4	88
387	48	6	81
561	49	6	61
393	49	4	63
591	49	4	80
576	49	4	74
426	50	4	69
441	51	7	30
605	52	5	76
540	52	7	27
564	53	6	32
399	53	9	13
486	54	9	60
432	54	7	42
381	55	4	86
462	55	9	17
438	56	9	0
396	55	5	39
489	55	5	66
608	55	6	62
528	55	7	52
384	55	10	30
510	56	9	25
516	57	10	70
414	58	10	16
435	58	10	35
402	58	9	0
390	58	5	86
453	58	7	16
378	60	9	35
624	61	8	29
621	62	3	63
596	62	7	68
474	63	10	44
534	64	7	54
619	64	10	0
546	65	9	27
408	66	6	38
570	66	10	41
549	67	9	0
602	67	10	0
444	67	7	24
465	67	10	0
644	67	10	0
558	68	10	17
663	68	10	0
650	68	11	0
450	68	6	0
525	68	10	49
447	68	8	0
579	68	12	0
620	69	11	0
504	69	10	0
645	69	9	0
537	70	10	0
656	70	11	0
459	70	7	0

[4] This lake contained an average of 12 percent of salt, of which two-thirds was $MgSO_4$, one-fourth Na_2SO_4, and the remainder a mixture of other salts.

TABLE 3. *Sulfate reaction values of the Miller and Manson cements* [13], *together with calculated potential* $3CaO.Al_2O_3$ *contents, and the percentage of normal strength (water storage) retained by 2- by 4-inch concrete cylinders after 5 years in Medicine Lake*—Continued

Cement No.	Sulfate reaction value	Potential $3CaO.Al_2O_3$	Percentage of normal strength of 2- by 4-in. cylinders after 5 yrs. in Medicine Lake
		Percent	*Percent*
423	70	9	0
552	71	8	0
519	72	8	48
471	74	5	53
594	75	13	0
555	75	11	0
477	76	12	0
669	76	12	0
375	76	11	0
495	77	10	0
641	78	10	0
501	78	11	0
590	78	10	33
614	78	9	8
417	79	11	0
573	79	11	15
567	79	11	7
629	80	12	0
618	81	14	0
498	81	9	26
411	82	12	0
492	84	10	0
420	85	11	0
595	88	13	0
372	89	13	0
468	90	12	0
627	90	9	0
668	91	10	0
480	92	13	0
662	94	14	0
429	95	13	0
680	95	14	0
630	96	11	0
685	98	10	0
632	98	11	0
483	98	12	0
456	98	7	0
615	99	14	0
522	99	12	0
593	99	14	0
599	100	6	0

In figure 1, the sulfate-reaction values are plotted against the percentages of normal strength for these 106 cements. For purposes of differentiation, a specimen was regarded as satisfactory when its percentage of normal strength was 55 or above, and as unsatisfactory when that value fell below 55. The horizontal line at 55-percent normal strength indicates that separation. It may then be noted that every cement having a sulfate-reaction value below 50 (to the left of the vertical line at 50) has a satisfactory performance record, whereas every cement having a sulfate-reaction value above 63 (to the right of the vertical line at 63) has an unsatisfactory performance record. Of the cements having sulfate-reaction values between 50 and 63, a few have shown a satisfactory performance (above 55 percent of normal strength), and a larger number have not.

It will be noted that, if a curve were to be drawn through the mean positions of the individual values, it would be relatively horizontal in the upper left and lower right sections. In the central area it would be steep. This means that the durability changes slowly with inherent sulfate resistivity when the latter is either high or low, but changes rapidly at intermediate values of sulfate resistivity. It is not to be expected that the correlation will be as good where the rate of change is large.

This relationship may be explained and generalized as follows: As long as the inherent sulfate resistivity of a cement is good, the speciment made from it will have a good durability in sulfate solutions. When that resistivity is poor, the specimens will have a low life expectancy in sulfate solutions. There will, however, be an intermediate range in the sulfate resistivity of a cement (indicated by sulfate reaction values between about 50 and 65) wherein the durability of specimens in sulfate solutions will be governed in large measure by other factors. The physical character of the specimen, the care used in its fabrication, or the presence of constituents that

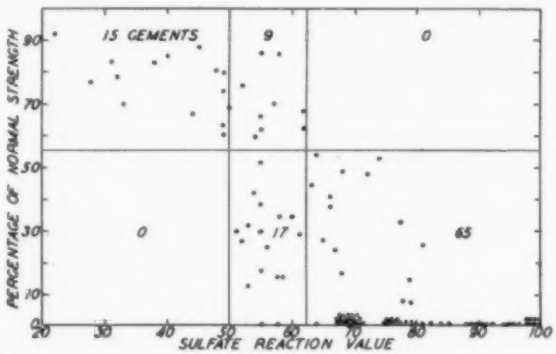

FIGURE 1. *Relation between the sulfate reaction values and the percentage of normal strength (2- by 4-in. concrete cylinders stored in tap water for 5 years) attained by specimens (similar to above at same age) stored in Medicine Lake.*

produce changes in structure or composition will be particularly effective within this range.

The comparison was supplemented by a study of the relationships found between the sulfate reaction values and 17 additional tests that have been reported on this series of cements.

These tests were as follows:

1. 2- by 4-in. concrete cylinders having 70 percent or more of "normal" strength after 5 yr in Medicine Lake [Miller 13].
2. Same having 25 percent or more of normal strength after 5 yr in Medicine Lake [13].
3. Same having less than 0.01-in. expansion after 5 yr in Medicine Lake [13].
4. Same having less than 0.01-in. expansion after 5 yr in 1-percent Na_2SO_4 solution [13].
5. 1:5 mortar bars having less than 1.0-percent expansion after 5 yr in 10-percent Na_2SO_4 solution following 3 days' damp curing [Gause 7].
6. Same having less than 1.0-percent expansion after 1 yr in 10-percent Na_2SO_4 solution following 3 days' damp curing [7].

UNIVERSITY OF MICHIGAN LIBRARIES

7. Same having less than 1.0-percent expansion after 5 yr in 10-percent Na_2SO_4 solution following 7 days' damp curing [7].

8. Same having less than 1.0-percent expansion after 1 yr in 10-percent Na_2SO_4 solution following 7 days' damp curing [7].

9. 1:5 mortar bars having less than 0.1-percent expansion after 21 days in 0.78 *M* Na_2SO_4 solution [Nat. Bur. Standards 12].

10. Same having less than 1.0-percent expansion after 21 days in 0.78 *M* Na_2SO_4 solution [12].

11. 1:5 mortar bars having less than 0.1-percent expansion after 28 days in 0.50 *M* Na_2SO_4 solution [University Farm 12].

12. Same having less than 1.0-percent expansion after 28 days in 0.50 *M* Na_2SO_4 solution [12].

13. 1:6 mortar bars having less than 0.1-percent expansion after 28 days in 0.15 *M* Na_2SO_4 solution [California Portland Cement Company 12].

14. Same having less than 1.0-percent expansion after 28 days in 0.15 *M* Na_2SO_4 solution [12].

15. 1:6 mortar bars having less than 0.1-percent expansion after 28 days in 0.15 *M* Na_2SO_4 solution [Portland Cement Association 12].

16. Same having less than 1.0-percent expansion after 28 days in 0.15 *M* Na_2SO_4 solution [12].

17. Same having sonic change greater than +1 after 28 days in 0.15 *M* Na_2SO_4 solution [12].

Cements that passed all of these tests were given ratings of 17; those that passed none of them received ratings of 0; the ratings given to other cements were the number of tests that they passed. Such a classification is arbitrary but has the advantage of cancelling discrepancies that are due to the various anomalous effects as described earlier.

For purposes of comparison, a cement having a rating of 14 or above is considered as having excellent sulfate resistance, one having a rating between 13 and 8 as fair, and one having a rating of 7 or less as poor. When the results of this composite test were plotted against sulfate reaction value, the diagram shown in figure 2 was obtained. It will be observed that 15 cements have reaction values of 50 or less, all but one of which are rated as excellent. Sixty-one cements have reaction values of 65 or more, only two of which attain a fair rating. Between the reaction values of 50 and 65, the spread is wide. This confirms the results already presented that a sulfate reaction value up to 50 indicates a sulfate-resistant cement; above 65 a nonsulfate-resistant cement; and that cements having sulfate reaction values between 50 and 65 are in a critical position where other factors of composition, fabrication, etc., may greatly affect the durability of specimens or structures in sulfate exposures.

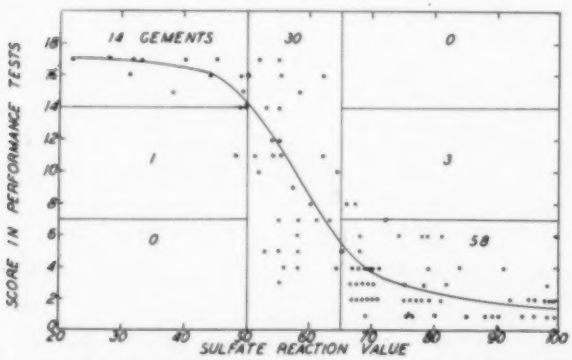

FIGURE 2. *Comparison of reaction values with ratings of the Miller cements based on 17 performance requirements.*

It may be pointed out that the establishment of sulfate resistivity from computed tricalcium aluminate content is subject to certain inherent errors. Statistically the relationship is good but lacks assurance of accuracy. The reasons are: 1, that the calculation of potential tricalcium aluminate gives no indication of the relative amounts of that material or of the alumina-iron solid solution that are in the crystalline and the glassy states (for, as pointed out earlier, the sulfate resistivity of the cement differs with the state of those materials) and, 2, recent investigations by Swayze [14] have indicated that the usual bases for the computation of tricalcium aluminate are subject to correction due to the iron-phase solid solution.

V. Conclusions

From a consideration of the correlations as above reported, it appears that the sulfate susceptibility test may be useful as an index of the inherent resistivity of cements to attack by sulfate solutions. Since this chemical attack is very largely associated with the formation of calcium sulfoaluminate by interaction between the sulfate and aluminate in saturated limewater, a measurement of that reaction may be expected to reveal the intrinsic sulfate reactivity of the cement.

It should be emphasized that this test does not indicate the resistivity that may be induced in a concrete or mortar specimen by any physical means, such as change in density, permeability, air entrainment, etc. Nor does it indicate the life of specimens in sulfate solutions, insofar as that life is affected by the presence of constituents in the cement (as periclase) or in the aggregate (as reactive siliceous materials) that may interact expansively quite irrespective of the sulfate reaction.

By correlations made with performance tests, it is concluded that:

1. A cement having a sulfate reaction value up to 50 may be considered as relatively resistant to sulfate attack; the lower that value, the greater the resistivity of the cement. Concrete or mortar structures made with such a cement may be expected to have a satisfactory durability when exposed to sulfate waters, except as factors other than sulfate reaction may be involved in disintegrative forces.

2. A cement having a sulfate reaction value between 50 and 65 should be regarded with apprehension insofar as its sulfate resistivity is concerned. Concrete or mortar structures made with such a cement may be durable, in sulfate exposures, if they

are dense and impermeable, and are free of other disintegrative agents. In this range of cements, air-entrainment would undoubtedly be beneficial, and good workmanship would be absolutely necessary.

3. A cement having a sulfate reaction value of over 65 should be considered as relatively nonresistant to sulfate attack; the higher that value, the lower the resistivity of the cement. Concrete or mortar structures made with such a cement may be expected to have a relatively short life when exposed to sulfate waters, regardless of the quality of the workmanship or the presence of beneficial agents.

The authors take pleasure in acknowledging the contribution of I. C. Bechtold in the development of the sulfate susceptibility test, and the assistance of A. C. Bonanno, E. G. Siggers, and C. Pinkerton in numerous analyses and tests.

VI. References

[1] Am. Soc. Testing Materials, Standard methods of chemical analysis of portland cement, C 114–47.
[2] P. H. Bates, A. J. Phillips, and R. J. Wig, Tech. Pap. BS **2,** 7 (1912) T12.
[3] R. H. Bogue, Chemistry of portland cement, pp. 508 to 520 (Reinhold Pub. Co., New York, N. Y., 1947).
[4] R. H. Bogue, Studies on the volume stability of portland cement pastes, privately printed by the Portland Cement Association Fellowship, PCAF Paper 55 (1949).
[5] R. H. Bogue, Wm. Lerch, and W. C. Taylor, Ind. Eng. Chem. **26,** 1049 (1934); PCAF Paper 28.
[6] F. K. Cameron and J. W. Bell, U. S. Dept. Agr. Bul. **23,** 47 (1906).
[7] G R. Gause, Am. Soc. Testing Materials Bul. **112,** 17 (1941).
[8] W. C. Hansen and E. E. Pressler, Ind. Eng. Chem. **39,** 1280 (1947).
[9] W. C. Hansen, personal communication.
[10] Wm. Lerch, Proc. Am. Soc. Testing Materials **46,** 1252 (1946).
[11] Wm. Lerch, F. W. Ashton, and R. H. Bogue, BS J. Research **2,** 715 (1929) RP54; PCAF Paper 19.
[12] D. G. Miller, Report of Working Committee on Sulfate Resistance, Com. C–1, ASTM (July 1943).
[13] D. G. Miller and P. W. Manson, U. S. Dept. Agr. Bul. 358; Proc. Am. Soc. Testing Materials **40,** 988 (1940).
[14] M. A. Swayze, Am. J. Sci. **244,** 1, 65 (1946).
[15] T. Thorvaldson, R. H. Harris, and D. Wolochow, Ind. Eng. Chem. **17,** 467 (1925).
[16] A. H. White and H. S. Kemp, Concrete **51,** 105 (1943).

Washington, June 17, 1949.

Journal of Research of the National Bureau of Standards Vol. 45, No. 3, September 1950 Research Paper 2129

Cascade-Connected Attenuators

By Robert W. Beatty

A method is presented for evaluating the error obtained when the attenuation of a number of cascade-connected attenuators is determined by adding the attenuation of each unit. The error is caused by mismatches at the attenuator junctions and is expressed in terms of reflection coefficients measured at the junctions. The analysis is pertinent to the case in which individual calibrated attenuators are available, but it is not feasible or possible to calibrate the combination of two or more attenuators. A nomogram is drawn that shows the limits of error (for two cascaded attenuators) in terms of voltage standing-wave ratios. Inspection of the nomogram shows that the error for typical UHF and microwave attenuators is generally of the same order of magnitude as the calibration errors.

I. Introduction

In order to obtain a desired attenuation, it is often necessary to connect two or more calibrated attenuators in series (cascade). Cascade-connected attenuators are used as "gage blocks" to extend the range of power meters without appreciable loss of accuracy.[1] Fixed and variable attenuators are cascade-connected in order to obtain increased range.

The attenuation of such combinations could be obtained by accurate measurement (calibration), but this is not feasible or possible in many cases because attenuator calibration equipment is not widely available.

The total attenuation of cascade-connected attenuators is usually obtained by adding the attenuation of each unit. If mismatch exists at the attenuator junctions, the attenuation obtained by this method is incorrect. The resulting error is a function of the amount of mismatch and may be evaluated in terms of the reflection coefficients measured at the attenuator junctions.

[1] C. G. Montgomery, Technique of microwave measurements, p. 835 (McGraw-Hill Book, Co., Inc., New York, N. Y., 1947).

II. Analysis

In the following analysis, UHF or microwave attenuators are considered. It is assumed that the individual attenuators have been calibrated in a transmission-line system having the same characteristic impedance (Z_0) and critical dimensions as the system in which the attenuators are to be used. A further requirement is that the attenuators are passive linear four-terminal networks having terminals that permit connection to the transmission-line system without discontinuity.

UNIVERSITY OF MICHIGAN LIBRARIES

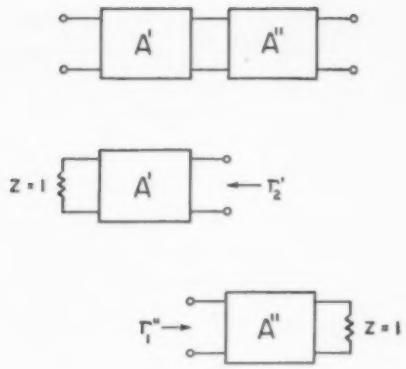

FIGURE 1. *Two cascaded networks.*

For convenience, wave matrices [2] are used and the following symbols are defined:

Γ_1 = Voltage reflection coefficient measured at the input terminals of an attenuator when the output terminals are connected to an impedance Z_0.

Γ_2 = Voltage reflection coefficient measured at the output terminals of an attenuator when the input terminals are connected to an impedance Z_0.

Z = Voltage transmission coefficient of an attenuator terminated in an impedance Z_0.

The elements of the wave matrix designated as the A-matrix are:

$$\left.\begin{aligned} A_{11}&=\frac{1}{T} & A_{12}&=-\frac{\Gamma_2}{T}\\ A_{21}&=\frac{\Gamma_1}{T} & A_{22}&=T-\frac{\Gamma_1\Gamma_2}{T}\end{aligned}\right\} \tag{1}$$

The attenuation of two cascaded attenuators is considered first. This is followed by the case of three attenuators and finally, the attenuation of any number of attenuators is obtained.

1. Two Attenuators

The cascade connection of two attenuators is shown in figure 1. The A-matrix of the combination is:

$$A=\begin{bmatrix}A_{11} & A_{12}\\ A_{21} & A_{22}\end{bmatrix}=\begin{bmatrix}A'_{11} & A'_{12}\\ A'_{21} & A'_{22}\end{bmatrix}\times\begin{bmatrix}A''_{11} & A''_{12}\\ A''_{21} & A''_{22}\end{bmatrix} \tag{2}$$

[2] George L. Ragan, Microwave transmission circuits, p. 551 to 554 (McGraw-Hill Book Co., Inc., New York, N. Y., 1948).

This is equivalent to,

$$A=\begin{bmatrix}A'_{11}A''_{11}+A'_{12}A''_{21} & A'_{11}A''_{12}+A'_{12}A''_{22}\\ A'_{21}A''_{11}+A'_{22}A''_{21} & A'_{21}A''_{12}+A'_{22}A''_{22}\end{bmatrix} \tag{3}$$

From inspection of eq 2 and 3,

$$A_{11}=A'_{11}A''_{11}+A'_{12}A''_{21} \tag{4}$$

Substituting eq 1 in eq 4

$$\frac{1}{T}=\frac{1}{T'T''}(1-\Gamma'_2\Gamma''_1). \tag{5}$$

The attenuation (in decibels) of the combination is:

$$A_T=20\log_{10}\left|\frac{1}{T}\right|. \tag{6}$$

The attenuation of a network [3] [4] is defined as its insertion loss when placed in a matched system. From eq 5 and 6 it follows that

$$A_T=20\log_{10}\left|\frac{1}{T'}\right|+20\log_{10}\left|\frac{1}{T''}\right|+20\log_{10}|1-\Gamma'_2\Gamma''_1|. \tag{7}$$

$$A_T=A'_T+A''_T+20\log_{10}|1-\Gamma'_2\Gamma''_1|. \tag{8}$$

The last term in eq 8 represents the error (ϵ_2). This term must be added to the sum of the attenuations of the individual units to obtain the correct attenuation for the combination.

It may be expedient in some cases to measure only the voltage standing-wave ratios σ'_2 and σ''_1 corresponding to Γ'_2 and Γ''_1. In this event only the magnitudes of Γ'_2 and Γ''_1 are obtained, and the actual value of ϵ_2 lies between the limits

$$20\log_{10}\left(1+\frac{\sigma'_2-1}{\sigma'_2+1}\cdot\frac{\sigma''_1-1}{\sigma''_1+1}\right)>\epsilon_2>$$

$$20\log_{10}\left(1-\frac{\sigma'_2-1}{\sigma'_2+1}\cdot\frac{\sigma''_1-1}{\sigma''_1+1}\right). \tag{9}$$

From the measured values of σ'_2 and σ''_1, the limits of error ϵ_2 may be readily determined by use of the nomogram of figure 4.

2. Three Attenuators

The cascade connections of three attenuators are shown in figures 2 and 3. The A-matrix of the combination is:

[3] See footnote 2, pp. 550 to 552.

[4] See footnote 1, pp. 679 to 682.

$$A=\begin{bmatrix} A_{11} & A_{12} \\ A_{21} & A_{22} \end{bmatrix}=\begin{bmatrix} A'_{11} & A'_{12} \\ A'_{21} & A'_{22} \end{bmatrix}\times\begin{bmatrix} A''_{11} & A''_{12} \\ A''_{21} & A''_{22} \end{bmatrix}\times\begin{bmatrix} A'''_{11} & A'''_{12} \\ A'''_{21} & A'''_{22} \end{bmatrix}. \tag{10}$$

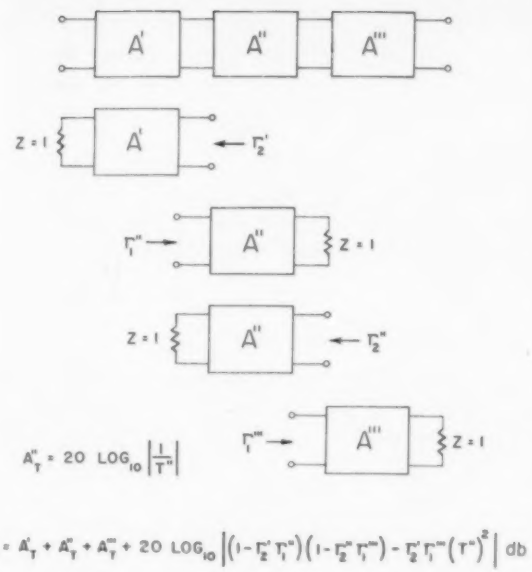

FIGURE 2. *Three cascaded networks (each network considered a unit).*

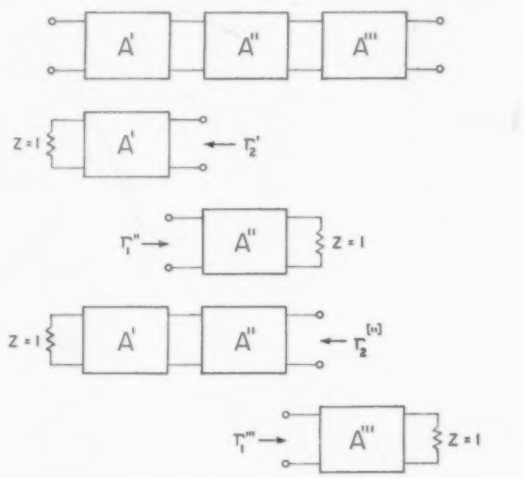

FIGURE 3. *Three cascaded networks (two input networks considered one unit).*

Only A_{11} need be considered:

$$A_{11}=A''''_{11}(A'_{11}A''_{11}+A'_{12}A''_{21})+A''''_{21}(A''_{11}A''_{12}+A'_{12}A''_{22}). \tag{11}$$

This is equivalent to:

$$\frac{1}{T}=\frac{1}{T'T''T'''}\,[(1-\Gamma'_2\Gamma''_1)(1-\Gamma''_2\Gamma'''_1)-\Gamma'_2\Gamma'''_1(T'')^2]. \tag{12}$$

The attenuation of the combination is:

$$A_T=A'_T+A''_T+A'''_T+ 20\log_{10}|(1-\Gamma'_2\Gamma''_1)(1-\Gamma''_2\Gamma'''_1)-\Gamma'_2\Gamma'''_1(T'')^2|. \tag{13}$$

The last term in eq 13 represents the error ϵ_3. It is apparent that ϵ_3 depends not only upon the reflection coefficients at the junctions but also upon the transmission coefficient T'' of the central attenuator. From eq 6 it can be seen that $|T''|$ is a function of A''_T. When the attenuation of the central unit is large, $|T''|$ is small and the following approximation is made:

$$\epsilon_3\approx 20\log_{10}|1-\Gamma'_2\Gamma''_1|+20\log_{10}|1-\Gamma''_2\Gamma'''_1|. \tag{14}$$

The two components of ϵ_3 can readily be obtained from the measured values of Γ'_2, Γ''_2, Γ''_1, and Γ'''_1, using the nomogram of figure 4. The limits of ϵ_3 are obtained in this case by adding the individual limits.

If the reflection coefficients are measured in a different way, it is possible to obtain the attenuation A_T without considering T''. This procedure is described in the following discussion.

3. Any Number (n) of Attenuators

The attenuation of any number (n) of cascade-connected attenuators is:

$$A_T=\sum_{K=1}^{n} A_T^K+\epsilon_n. \tag{15}$$

In the above equation the symbol K is a superscript designating the position of the attenuator, numbering from the input of the cascade-connection.

In determination of ϵ_n, it is unnecessary to consider complex transmission coefficients if the following procedure (illustrated in fig. 3) is used. First, the attenuation of the combination of the two units at the input end is determined by the method illustrated in figure 1. The two attenuators are now considered as a single unit whose attenuation is known. The attenuation of the combination of this

UNIVERSITY OF MICHIGAN LIBRARIES

$$20 \log_{10}\left(1+\frac{\sigma_2'-1}{\sigma_2'+1}\cdot\frac{\sigma_1''-1}{\sigma_1''+1}\right) > \varepsilon_2 > 20 \log_{10}\left(1-\frac{\sigma_2'-1}{\sigma_2'+1}\cdot\frac{\sigma_1''-1}{\sigma_1''+1}\right)$$

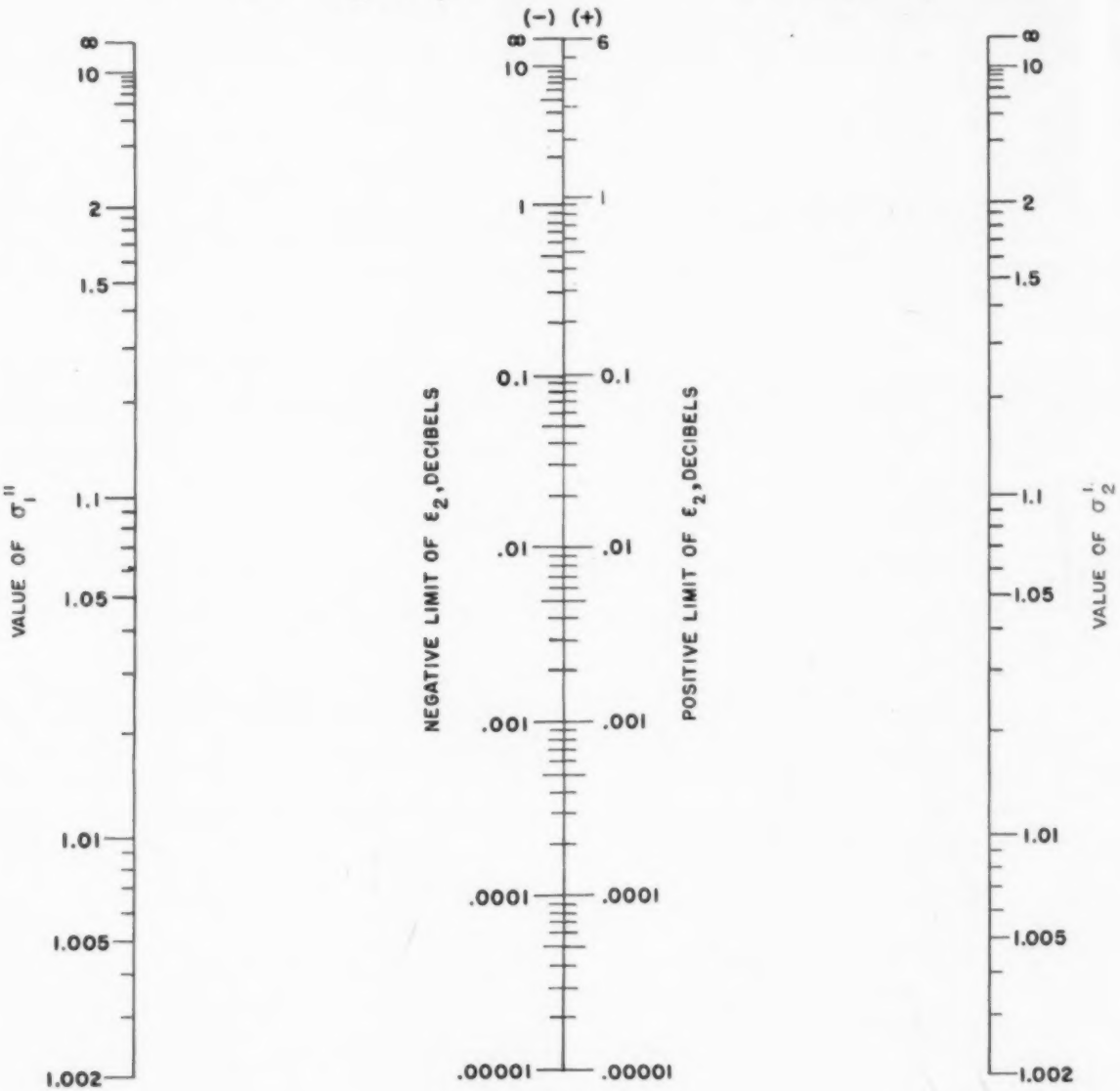

FIGURE 4.—*Limits of error.*

unit with the third is also determined by the method illustrated in figure 1.

It is apparent that a continuation of this process will yield the correct attenuation of the combination of any number of attenuators.

An extension of the process illustrated in figure 3 yields:

$$A_T = \sum_{K=1}^{n} A_T^K + \sum_{l=2}^{n} 20 \log_{10} |1 - \Gamma_2^{l-1} \Gamma_1^l| \qquad (16)$$

where,

A_T^K = attenuation of K^{th} network.

Γ_1^l = reflection coefficient measured at the input terminals of the l^{th} attenuator with its output terminals connected to an impedance Z_0.

Γ_2^{l-1} = reflection coefficient measured at the output terminals of the $[l-1]^{th}$ attenuator with the input terminals of attenuator no. 1 connected to an impedance Z_0.

These results may be applied to attenuators that are not used in a transmission-line system if expressions of the form $\left(\frac{Z-Z_0}{Z+Z_0}\right)$ are substituted for the appropriate reflection coefficients and the same reference impedance (Z_0) is used throughout.

WASHINGTON, May 23, 1950.

Journal of Research of the National Bureau of Standards Vol. 45, No. 3, September 1950 Research Paper 2130

Total Ionization of Hydrocarbons From Mass Spectral Data

By Fred L. Mohler, Laura Williamson, and Helen M. Dean

The total ionization is computed by adding all the mass peaks in the spectrum and multiplying by the sensitivity (current per unit pressure) for the maximum peak. This is divided by the corresponding product for *n*-butane to obtain a relative value independent of the units used. Data are taken from the API Catalog of Mass Spectral Data using revised values of sensitivity obtained by measuring pressure with a micromanometer. Total ionizations of all the isomers of a compound are nearly equal with only a few values differing greatly from the mean value. This is true in all cases where data are available for many isomers. With some exceptions total ionization increases with increasing number of carbon atoms in each series C_nH_{2n+2}, C_nH_{2n}, etc. Total ionization tends to decrease in compounds with the same number of carbon atoms and decreasing number of hydrogen atoms but there are many exceptions. Tables summarize data for 198 hydrocarbons.

Values of total ionization of isomers will in some cases permit computing all isomers as a group in chemical analysis without identifying the compounds.

I. Introduction

Tables of mass spectra [1] [1] commonly give the intensity of mass peaks relative to the maximum peak taken as 100 and the sensitivity (current per unit pressure in the gas reservoir) for the maximum peak in arbitrary units. The tables also give the sensitivity for the maximum peak of *n*-butane at mass 43 in the same units. The ratio of the sensitivity of any compound to that of *n*-butane is a number that is independent of the arbitrary units of current and rate of leak from the gas reservoir to the ionization chamber. The sum of all the mass peaks times the sensitivity for the maximum peak is a number proportional to the total ionization for the compound, and the ratio of this to the total ionization of *n*-butane is again a number independent of the arbitrary units. These relative values will depend to some extent on instrumental selectivity and will differ somewhat for different types of instruments. In the Consolidated mass spectrometer the spectrum is covered by varying the ion accelerating voltage with constant magnetic field, and heavy ions are collected with less efficiency than light ions. This introduces a small but unknown uncertainty in deriving total ionization by adding the mass peaks.

A greater source of error in published data comes from the determination of the sensitivity or current per unit pressure in the gas reservoirs. The common procedure for measuring this pressure has been to admit the gas into a volume of about 2 cubic centimeters and measure the pressure of 10 to 40 millimeters on a mercury manometer. Then the gas is expanded a thousandfold to give a pressure of 10 to 40 microns in the reservoir. The gas pipet method leads to very large errors when the vapor pressure is nearly equal to the manometer pressure and the estimated pressure will be much too high. Dibeler, Cordero, and Greenough [2, 3] have developed a micromanometer suitable for measuring directly the pressure in the gas reservoir. The pressure-sensitive element is a thin metal diaphragm and the motion of the diaphragm is measured electrically by the change in mutual induction between two coils close to the diaphragm.

Comparative measurements with the gas pipet and with the micromanometer show that use of the gas pipet leads to large experimental errors for all hydrocarbons with eight or more carbon atoms. For this reason all tables of mass spectra published by

[1] Figures in brackets indicate the literature references at the end of this paper.

VALUE OF σ_2^1

UNIVERSITY OF MICHIGAN LIBRARIES

this Bureau in the API catalog since February 1949 give sensitivities based on micromanometer readings, and sensitivities have been redetermined for nearly all the heavier hydrocarbon spectra published before this date. A table of revised values relative to *n*-butane has been published in the API Catalog of Mass Spectral Data [1].

When the total ionization is recomputed on the basis of the corrected values of the sensitivity relative to *n*-butane, some regularities are found that were previously concealed by experimental errors in estimating the pressure. This paper gives a summary of results.

II. Computation of Total Ionization

In nearly all cases we have used the data at 50 volts ionizing voltage published in the API catalog. All the mass peaks are added and multiplied by the sensitivity for the base peak, and this product is divided by the similar product for *n*-butane. As noted above there is some error introduced because the Consolidated mass spectrometer is slightly less sensitive to heavy ions than to light ions. This is partly compensated for by the fact that larger magnetic fields are used to cover the spectra of heavier compounds. Thus, hydrocarbons with less than six carbon atoms including *n*-butane are measured with a magnetic field requiring 865 volts ion accelerating voltage to focus ions of mass 43. Hydrocarbons with six to eight carbon atoms are measured with a field requiring 1,130 volts for mass 43, and the sensitivity is increased by a factor 1.06. For hydrocarbons with nine or more carbon atoms the field is 1,700 volts for mass 43 and the sensitivity 1.08 times that at 865 volts. This effect could easily be corrected, but it compensates at least in part for the fact that the average mass of the ions of a heavy hydrocarbon is in general greater than the average mass of *n*-butane ions. The tables give values relative to *n*-butane measured with 865 volts ion accelerating voltage for mass 43.

Results of independent measurements of sensitivity relative to *n*-butane are reproducible to within about 2 percent. Larger errors seem to arise over long periods of time or when ionization chambers are changed. Possibly this is because the efficiency of collecting ions depends rather critically on focusing fields and slit widths and on the initial kinetic energy of the ions.

III. Results

Table 1 gives the sum of the mass peaks, the sensitivity, and the total ionization relative to *n*-butane for the eighteen C_8H_{18} isomers. A previous publication of this laboratory [4] gives a similar table but with sensitivity measured by the gas pipet. Values of the sensitivity derived in reference [4] are much higher than those given in table 1 by factors ranging from 1.7 to 1.07. This gives a serious error in the total ionization reported in [4] and completely conceals a regularity shown in table 1. Whereas the sum of the mass peaks and sensitivities cover a

TABLE 1. *Sensitivity and total ionization relative to n-butane for octane mass spectra*

Compound	Maximum peak	Sum of mass peaks	Sensitivity relative to n-butane	Total ionization relative to n-butane
n-Octane	43	397	1.44	1.83
2-Methylheptane	43	422	1.30	1.75
3-Methylheptane	43	472	1.21	1.83
4-Methylheptane	43	363	1.67	1.94
2,2-Dimethylhexane	57	242	2.41	1.87
2,3-Dimethylhexane	43	370	1.52	1.80
2,4-Dimethylhexane	43	455	1.29	1.88
2,5-Dimethylhexane	43	416	1.35	1.80
3,3-Dimethylhexane	43	390	1.43	1.78
3,4-Dimethylhexane	56	488	1.14	1.78
3-Ethylhexane	43	309	1.89	1.87
2,2,3-Trimethylpentane	57	292	1.86	1.74
2,2,4-Trimethylpentane	57	249	2.33	1.86
2,3,3-Trimethylpentane	43	374	1.41	1.69
2,3,4-Trimethylpentane	43	337	1.56	1.68
2-Methyl-3-ethylpentane	43	348	1.61	1.79
3-Methyl-3-ethylpentane	43	326	1.68	1.75
2,2,3,3-Tetramethylbutane	57	237	2.12	1.61
Mean				1.79±0.06

nearly two-fold range of values, the total ionization relative to *n*-butane is nearly constant. Most of the octanes give values of total ionization that are equal within experimental error, but four or five values differ from the mean by more than the expected error. This variation cannot be ascribed to instrumental selectivity for ions that differ in mass, since four of the compounds that have nearly identical spectra give total ionizations that differ considerably. These are 2,2-dimethyl-hexane; 2,2,3-trimethylpentane; 2,2,4-trimethylpentane; and 2,2,3,3-tetramethylbutane. For these compounds the total ionization ranges from 1.87 to 1.61.

Table 2 summarizes values of total ionization for a large number of compounds. Column 1 gives the empirical chemical formula, column 2 gives the number of isomers measured, and column 3 gives the mean value of the total ionization relative to *n*-butane and the mean deviation from the mean value. In every case where a large number of isomers has been measured one can make the same generalization as was made for the 18 octanes. The values of the total ionization are nearly equal and most, but not all, of the values are equal within the expected experimental errors.

Compounds in table 2 have been grouped according to the empirical formulae, and the first twelve compounds are the paraffins of formula C_nH_{2n+2}. Total ionization for all isomers has been computed for compounds with less than ten carbon atoms and only the normal compounds are given for compounds with 10, 11, and 12 carbon atoms. For compounds with six or less carbon atoms the sensitivity was measured with the gas pipet, and a few check measurements indicate that there is no serious error. Heptanes give appreciably higher values of sensitivity by this method. Data for the 35 nonanes corresponding to table 1 have been published in a paper on "Mass spectra of the nonanes" [5]. These values have been computed from data for 70 volts ionizing voltage. The total ionization at 70 volts is slightly greater than at 50 volts in all compounds, but there seems to be

TABLE 2. *Total ionization relative to n-butane*

Formula	Number of isomers	Total ionization	Formula	Number of isomers	Total ionization
CH_4	1	0.46			
C_2H_6	1	.70	C_2H_4	1	0.56
C_3H_8	1	.87	C_3H_6	2	.75 ±0.06
C_4H_{10}	2	.98 ±0.02	C_4H_8	5	.86 ±0.02
C_5H_{12}	3	1.09 ±0.07	C_5H_{10}	7	1.03 ±0.03
C_6H_{14}	5	1.54 ±0.06	C_6H_{12}	20	1.42 ±0.06
C_7H_{16}	9	1.69 ±0.05			
C_8H_{18}	18	1.79 ±0.06	C_8H_{16}	22	1.58 ±0.07
C_9H_{20}	35	1.94 ±0.13	C_9H_{18}	6	1.91 ±0.09
n−$C_{10}H_{22}$	1	1.80	n−1−$C_{10}H_{20}$	1	2.27
n−$C_{11}H_{24}$	1	1.98	n−1−$C_{11}H_{22}$	1	2.06
n−$C_{12}H_{26}$	1	1.94			
C_2H_2	1	0.55			
C_3H_4	1	.87			
C_4H_6	4	.87 ±0.07	C_6H_4	1	0.43
C_5H_8	11	1.03 ±0.04			
C_6H_{10}	7	1.26 ±0.09	C_6H_8	1	1.06
C_8H_{16}	2	1.67 ±0.04	C_8H_{12}	1	1.34
$C_{10}H_{18}$	2	1.64 ±0.22	$C_{10}H_{16}$	2	1.61 ±0.01
C_4H_2	1	0.69			
C_6H_6	2	1.10 ±0.04			
C_7H_8	1	1.13			
C_8H_{10}	4	1.15 ±0.06	C_8H_8	1	1.18
C_9H_{12}	8	1.27 ±0.07			
$C_{10}H_{14}$	4	1.17 ±0.05			
$C_{10}H_8$	1	1.45			

little if any difference in the value of the ratio to *n*-butane. The mean error and the extreme departures from the mean are somewhat greater than for the octanes. Eight nonanes with nearly identical spectra show nearly the full range of values for total ionization, so again there is no evidence that variation in total ionization is caused by instrumental selectivity. Experimental errors may be somewhat greater here as the spectra were measured over a long period of time. Values of total ionization increase progressively with increasing number of carbon atoms up to $C_{10}H_{22}$.

Values for total ionization of compounds of formula C_nH_{2n} are given in the same row as the paraffins with the same value of n. These compounds include olefins and cycloparaffins. C_3H_6 includes propene, 0.69, and cyclopropane, 0.80. C_4H_8 includes four butenes of mean total ionization, 0.87, and cyclobutane, 0.83. The C_5 compounds are six pentenes, 1.02, and cyclopentane, 1.07. C_6H_{12} includes 16 hexenes and six cycloparaffins with mean values of 1.43 and 1.40, respectively. C_7H_{14} isomers have been omitted as most of the sensitivity values have not been based on micromanometer pressure measurements and data are considered inaccurate. C_8H_{16} includes four olefins and 18 cycloparaffins giving values of 1.63 and 1.57. Mean values for six C_9 cycloparaffins and for 1-decene and 1-undecene are given. In general, differences between cyclics and olefins are no greater than the differences found among isomers of the same chemical class. Except for the two heaviest compounds, C_nH_{2n} compounds give values of total ionization slightly less than the corresponding paraffins.

The C_nH_{2n-2} compounds include a variety of chemical classes. C_2H_2 is acetylene, C_3H_4 methylacetylene, and C_4H_6 includes butadienes and butynes. The eleven C_5H_8 isomers include a variety of chemical compounds that differ strikingly in their spectra and the equality of the total ionization is very significant [6]. There is more variation in total ionization among the C_6H_{10} isomers. C_8H_{14} includes 1-octyne and 2,5-dimethyl-1,5-hexadiene. The two $C_{10}H_{18}$ compounds are *cis*- and *trans*-decahydronaphthalene. The total ionization values are 1.42 and 1.85, respectively, which is an exceptionally large difference for two isomers. Values for total ionization of C_nH_{2n-2} compounds are sometimes greater and sometimes less than the C_nH_{2n} compounds with the same value of n.

Only five examples of C_nH_{2n-4} compounds have been studied. C_4H_4 is 1-buten-3-yne from a spectrum published by Humble Oil and Refining Co. [7], C_6H_8 is cyclohexadiene, and C_8H_{12} is vinylcyclohexene. Two terpenes, $C_{10}H_{16}$, are alpha pinene and tricyclene, and the total ionization of these is identical within experimental error. These chemically different compounds are in this respect in marked contrast to the two decahydronaphthalenes ($C_{10}H_{18}$), which are structurally similar although they show a large difference in total ionization.

C_nH_{2n-6} compounds are alkylbenzenes with two exceptions. C_4H_2 is butadiyne computed from data published by Union Oil Co. [8]. The C_6H_6 isomers include benzene and 2,4-hexadiyne. The two compounds are chemically very different but the mass spectra and the total ionization are similar. The C_nH_{2n-6} compounds give less total ionization than compounds with more hydrogen atoms with one or two exceptions.

There is only one measurement for a compound C_nH_{2n-8}, namely styrene. The total ionization falls in the same range of values as found for the C_8 alkylbenzenes.

Naphthalene is an example of a compound of formula C_nH_{2n-12}. The total ionization is greater than that of C_{10} alkylbenzenes and comparable with the decahydronaphthalenes of formula C_nH_{2n-2}.

The only striking generalization concerning total ionization is that the total ionization of isomers is nearly equal. Wherever there are many isomers this relation is shown conclusively, but individual compounds occasionally differ from the mean value by much more than the experimental error. The total ionization tends to increase with increasing number of carbon atoms within the same series up to C_{10}. It tends to decrease with decreasing number of hydrogen atoms and equal number of C atoms but there are many exceptions.

It is of interest to consider structurally related compounds instead of all the isomers, and table 3 gives values for the normal paraffins, the normal olefins with a double bond in the first position, and some normal acetylenes with a triple bond in the first position. The values for the normal compounds do not differ systematically from the average for all isomers, and the trend of values with increasing number of carbon atoms and decreasing number of H atoms shows the same type of irregularities that were noted for average values. It was noted above that cyclics and olefins of the same molecular weight show no systematic difference in total ionization.

UNIVERSITY OF MICHIGAN LIBRARIES

The irregularities are not of a type to be explained by instrumental selectivity arising from the fact that heavy ions are collected with somewhat less efficiency than light ions.

TABLE 3. *Total ionization relative to n-butane*

Normal paraffins	Total ionization	Normal 1-olefines	Total ionization	Normal 1-acetylenes	Total ionization
CH_4	0.46				
C_2H_6	.70	C_2H_4	0.56	C_2H_2	0.55
C_3H_8	.87	C_3H_6	.69	C_3H_4	.87
C_4H_{10}	1.00	C_4H_8	.87	C_4H_6	.83
C_5H_{12}	1.17	C_5H_{10}	1.05	C_5H_8	1.06
C_6H_{14}	1.55	C_6H_{12}	1.49	C_6H_{10}	1.29
C_7H_{16}	1.64				
C_8H_{18}	1.83	C_8H_{16}	1.79	C_8H_{14}	1.64
C_9H_{20}	1.98	C_9H_{18}	2.13		
$C_{10}H_{22}$	1.80	$C_{10}H_{20}$	2.27		
$C_{11}H_{24}$	1.98	$C_{11}H_{22}$	2.06		
$C_{12}H_{26}$	1.94				

The fact that isomers give nearly the same total ionization can be applied to analysis of complicated mixtures when it is impossible to determine the separate components. Thus, one could analyze for a trace of gasoline vapor in air on the basis of the sum of all the peaks and an estimate as to the average number of carbon atoms in the mixture. If, for instance, the spectrum indicated that heptanes were predominant, the sensitivity factor would be, from table 2, $1.69 \times 312 \times$ sensitivity of *n*-butane where 312 is the sum of the peaks in the *n*-butane spectrum. This is a better approximation than is obtained by using the sensitivity of any one compound in cases where one may reasonably expect that a mixture of compounds is present. We are indebted to S. Schuhmann of this Bureau for calling attention to the possibility of analyzing for all isomers as a group.

IV. References

[1] Catalog of Mass Spectral Data, American Petroleum Institute, Research Project 44.
[2] V. H. Dibeler and F. Cordero, J. Research NBS, publication pending.
[3] M. L. Greenough and W. F. Williams, J. Research NBS, publication pending.
[4] E. G. Bloom, F. L. Mohler, J. H. Lengel, and C. E. Wise, J. Research NBS 41, 129 (1948).
[5] F. L. Mohler, L. M. Williamson, C. E. Wise, E. J. Wells, H. M. Dean, and E. G. Bloom, J. Research NBS, in press.
[6] F. L. Mohler, E. G. Bloom, L. M. Williamson, C. E. Wise, and E. J. Wells, J. Research NBS 43, 533 (1949).
[7] API Catalog of Mass Spectral Data, Serial No. 423.
[8] API Catalog of Mass Spectral Data, Serial No. 74

WASHINGTON, May 18, 1950.

Journal of Research of the National Bureau of Standards Vol. 45, No. 3 September 1950 Research Paper 2131

Generalization of S. Bernstein's Polynomials to the Infinite Interval

By Otto Szasz

Let $P(u,x)=e^{-ux}\sum_{v=1}^{\infty}\frac{(ux)^v}{v!}f\left(\frac{v}{u}\right), u>0.$

The paper studies the convergence of $P(u,x)$ to $f(x)$ as $u\to\infty$. The results obtained are generalized analogs, for the interval $0\leq x\leq\infty$, of known properties of S. Bernstein's approximation polynomials in a finite interval.

1. With a function $f(t)$ in the closed interval [0,1], S. Bernstein in 1912 associated the polynomials

$$B_n(t)=\sum_{v=0}^{n}\binom{n}{v}t^v(1-t)^{n-v}f(v/n),\ n=1,2,3,\cdots \tag{1}$$

He proved that if $f(t)$ is continuous in the closed interval [0,1], then $B_n(t)\to f(t)$ uniformly, as $n\to\infty$. This yields a simple constructive proof of Weierstrass's approximation theorem.

More generally the following theorems hold:

Theorem A. If $f(t)$ is bounded in [0,1] and continuous at every point of $[a,b]$, where $0\leqq a<b\leqq 1$, then $B_n(t)\to f(t)$ uniformly in $[a,b]$. (See [6], p. 66)[1].

Theorem B. If $f(t)$ is bounded in [0,1] and continuous at a point τ, then $B_n(\tau)\to F(\tau)$. (See [3], p. 112).

Theorem C. If $f(t)$ satisfies a Lipschitz-Hölder condition

$$|f(t)-f(t')|<c|t-t'|^{\lambda}, 0<\lambda\leqq 1,$$

then $|f(t)-B_n(t)|<c_2n^{-\lambda/2}, c_1, c_2$ constants (see [7], p. 53;4). $B_n(t)$ is a linear transform of the function $f(t)$; for the infinite interval $(0,\infty)$ we define an analogous transform:

$$P(u;f)=e^{-ux}\sum_{v=0}^{\infty}\frac{1}{v!}(ux)^v f(v/u),\ u>0.[2] \tag{2}$$

We shall prove corresponding theorems of approximation for this transform; $u\to\infty$ corresponds to $n\to\infty$ in eq 1. We also sharpen theorem B to *uniform* convergence *at* the point τ.

Definition: A set of continuous functions $P(u,x)$ is said to converge uniformly to the value S at a point $x=\zeta$, as $u\to\infty$ if $P(u_n,x_n)\to S$, whenever $x_n\to\zeta$ and $u_n\to\infty$, as $n\to\infty$. An equivalent formulation is: to any $\epsilon>0$ there exists a $\delta(\epsilon)$ and an $\eta(\delta,\epsilon)$ so that $|P(u,x)-S|<\epsilon$ for $|x-\zeta|<\delta$ and $u>\eta$.

2. In this section we introduce some lemmas for later application.

Lemma 1. For $\lambda>0$, $u>0$,

$$\sum_{|v-u|\geqq\lambda}\frac{u^v}{v!}<\lambda^{-2}ue^u. \tag{3}$$

The following identity is easily verified:

$$\sum_{v=0}^{\infty}(v-u)^2\frac{u^v}{v!}=ue^u; \tag{4}$$

it follows that

$$\lambda^2\sum_{|v-u|\geqq\lambda}\frac{u^v}{v!}>\sum_{v=0}^{\infty}(v-u)^2\frac{u^v}{v!}=ue^u.$$

This proves lemma 1.

Lemma 2. For $u\geqq 0$

$$\sum_{0}^{\infty}|v-u|\frac{u^v}{v!}\leq\sqrt{ue^u}. \tag{5}$$

[1] Figures in brackets indicate the literature references at the end of this paper.

[2] M. Kac also considered the transform (2) independently, from a similiar point of view.

UNIVERSITY OF MICHIGAN LIBRARIES

By Schwarz's inequality and by eq 4

$$\left(\sum_0^\infty |v-u|\,\frac{u^v}{v!}\right)^2 \leqq \left\{\sum_0^\infty (v-u)^2\,\frac{u^v}{v!}\right\}\left(\sum_0^\infty \frac{u^v}{v!}\right)=ue^{2u};$$

this proves lemma 2.
Observe that

$$\sum_{v=0}^\infty (v-u)\,\frac{u^v}{v!}=0, \tag{6}$$

thus, if u is a positive integer

$$\sum_0^\infty |v-u|\,\frac{u^v}{v!}=\sum_{v\leqq u}(u-v)\,\frac{u^v}{v!}+\sum_{v\geq u}(v-u)\,\frac{u^v}{v!}=$$

$$2\sum_{v\leqq u}(u-v)\,\frac{u^v}{v!}=2u\sum_{v\leqq u}\frac{u^v}{v!}-2u\sum_{v\leqq u-1}\frac{u^v}{v!}=$$

$$2u\,\frac{u^u}{u!}\sim\frac{2\sqrt{u}}{\sqrt{2\pi}}\,e^u,$$

by Stirling's formula. Thus the estimate (5) is the sharpest possible, except for a constant factor.

3. *Theorem 1.* Suppose that $f(x)$ is bounded in every finite interval; if $f(x)=0(x^k)$ for some $k>0$ as $x\to\infty$ and if $f(x)$ is continuous at a point ζ, then $P(u;f)$ converges uniformly to $f(x)$ at $x=\zeta$.
Consider

$$e^{ux}\{P(u;f)-f(x)\}=\sum_{v=0}^\infty \{f(v/u)-f(x)\}(ux)^v\,\frac{1}{v!}=$$

$$\sum_{|v/u-x|\leqq\delta}+\sum_{|v/u-x|>\delta}=S_1+S_2, \text{ say}$$

and assume that $|x-\zeta|<\delta$.
Let

$$\max|f(x)-f(\xi)|=m(\delta,\xi)=m(\delta),$$

for

$$|x-\xi|\leq\delta,$$

then $m(\delta)\to 0$ as $\delta\to 0$. Now

$$f(v/u)-f(x)=f(v/u)-f(\zeta)+f(\zeta)-f(x),$$

and

$$\frac{v}{u}-\zeta=\frac{v}{u}-x+x-\zeta. \tag{7}$$

In S_1 $\left|\frac{v}{u}-x\right|\leqq\delta$,

hence, from eq 7

$$|v/u-\zeta|\leqq 2\delta$$

and

$$|f(v/u)-f(x)|\leqq m(2\delta)+m(\delta)\leqq 2m(2\delta).$$

Hence

$$|S_1|<2m(2\delta)\sum_0^\infty\frac{(ux)^v}{v!}=2m(2\delta)e^{ux}.$$

Next write

$$S_2=\sum_{v<u(x-\delta)}+\sum_{v>u(x+\delta)}=S_3+S_4, \text{ say.}$$

Then

$$|S_3|<\sum_{v<u(x-\delta)}\frac{(ux)^v}{v!}\,|f(v/u)-f(x)|.$$

Let

$$\sup|f(x)|=U(\delta), \text{ for } x\leqq\delta.$$

Then

$$|S_3|<2U(\zeta+\delta)\sum_{ux-v>u\delta}\frac{(ux)^v}{v!}.$$

Applying lemma 1 with $\lambda=u\delta$, we get

$$|S_3|<2U(\zeta+\delta)\,\frac{uxe^{ux}}{u^2\delta^2}=2U(\zeta+\delta)\,\frac{xe^{ux}}{u\delta^2}.$$

Finally, assuming $u(x+\delta)>k$,

$$S_4=0\left(\sum_{v>u(x+\delta)}\frac{(ux)^v}{v!}\left(\frac{v}{u}\right)^k\right)=0\left(\sum_{v>u(x+\delta)}x^k\,\frac{(ux)^{v-k}}{(v-k)!}\right)$$

$$=0\left(\sum_{\mu>u(x+\delta)-k}x^k\,\frac{(ux)^\mu\rho}{\mu!}\right).$$

We apply again lemma 1, with $\lambda=u\delta-k>0$,

then

$$S_4=0\left(x^k\,\frac{uxe^{ux}}{(u\delta-k)^2}\right)=0\left(\frac{ue^{ux}}{(u\delta-k)^2}\right),\ u\to\infty.$$

Summarizing, we find

$$P(u;f(x))-f(x)=0\left\{m(2\delta)+\frac{1}{u\delta^2}+\frac{u}{(u\delta-k)^2}\right\}.$$

Letting $u\to\infty$ for a fixed δ,

$$\limsup|P(u;f(x))-f(x)|\leqq 0(m(2\delta)), u\to\infty, |x-\zeta|\leqq\delta,$$

from which our theorem follows.

It can be shown easily that uniform convergence at each point of a closed set D implies uniform convergence over the set D. A similar argument applies to the transform (1), thus sharpening the theorems A and B.

4. *Theorem 2.* If $f(x)$ satisfies the Lipschitz-type condition

$$|f(x_1)-f(x_2)|<\gamma\frac{|x_2-x_1|^\rho}{(x_1+x_2)^{\rho/2}},\ 0<x_1<x_2<\infty, \quad (8)$$

γ, ρ constants, $0<\rho\leqq 1$,

then

$$|P(u;f(x))-f(x)|\leqq\gamma u^{-\rho/2},$$

uniformly for $0<x<\infty$, as $u\to\infty$.

We have, for $\rho=1$

$$|P(u;f)-f(x)|\leqq e^{-ux}\sum_0^\infty (ux)^v\frac{1}{v!}|f(v/u)-f(x)|$$

$$<e^{-ux}\gamma\sum_0^\infty\frac{(ux)^v}{v!}\frac{|v/u-x|}{(v/u+x)^{\frac{1}{2}}}=\gamma\frac{e^{-ux}}{\sqrt{u}}\sum_0^\infty\frac{(ux)^v}{v!}\frac{|v-ux|}{(v+ux)^{\frac{1}{2}}}$$

$$<\frac{\gamma e^{-ux}}{u\sqrt{x}}\sum_0^\infty\frac{(ux)^v}{v!}|v-ux|\leqq\frac{\gamma}{\sqrt{u}},$$

by lemma 2. This proves theorem 2 for $\rho=1$. Now from Hölder's inequality, for $0<\rho<1$

$$e^{ux}|P(u;f)-f(x)|=\sum_0^\infty\frac{(ux)^{v(1-\rho)}}{(v!)^{1-\rho}}\frac{(ux)^{v\rho}}{(v!)^\rho}|f(v/u)-f(x)|$$

$$\leqq\left(\sum_0^\infty\frac{(ux)^v}{v!}\right)^{1-\rho}\left\{\sum\frac{(ux)^v}{v!}|f(v/u)-f(x)|^{1/\rho}\right\}^\rho.$$

Assume that

$$|f(x_1)-f(x_2)|<\gamma\frac{|x_2-x_1|^\rho}{(x_1+x_2)^{\rho/2}},$$

then

$$e^{ux}|P(u;f)-f(x)|<\exp\left((1-\rho)ux\right)\gamma\left(\sum\frac{(ux)^v}{v!}\cdot\frac{|v/u-x|}{(v/u+x)^{\frac{1}{2}}}\right)^\rho$$

$$<\gamma\exp\left((1-\rho)ux\right)\left(\frac{1}{u\sqrt{x}}\sqrt{uxe^{ux}}\right)^\rho=\gamma u^{-\rho/2}e^{ux}.$$

This completes the proof of theorem 2.

Let $\rho=1$, and $f(x)=c-x$, for $0\leqq x\leqq c$, c a positive constant; $f(x)=0$ for $x\geqq c$. Now the condition (8) is satisfied. Furthermore

$$P(u;f)-f(c)=P(u;f)=e^{-uc}\sum_{v\leqq uc}\frac{(uc)^v}{v!}(c-v/u)=\frac{1}{u}e^{-uc}\sum_{v\leqq uc}(uc-v)\frac{(uc)^v}{v!}.$$

Let $[uc]=k$, then

$$u^{\frac{1}{2}}P(u,c)>u^{-\frac{1}{2}}e^{-k-1}\sum_{v=0}^k(k-v)\frac{k^v}{v!},$$

and, from section 2

$$\sum_{v=0}^k(k-v)\frac{k^v}{v!}=\frac{k^{k+1}}{k!}\sim\left(\frac{k}{2\pi}\right)^{\frac{1}{2}}e^k.$$

Thus

$$\liminf_{u\to\infty}u^{\frac{1}{2}}P(u,c)>0.$$

This proves that for $\rho=1$ the order of the estimate in theorem 2 is the sharpest possible. We do not know of a similar example for $\rho<1$. For Bernstein's polynomials an exact result has been given by M. Kac [4].

5. Suppose that $f(x)$ is continuous in the infinite interval $(0,\infty)$.

Let

$$x=\log\frac{1}{t},\ 0\leqq t\leqq 1,$$

$f(x)=f(\log\ 1/t)=\phi(t)$ is continuous in $0\leqq t\leqq 1$. Given $\epsilon>0$, we can find a polynomial $\sum_0^n a_kt^k=p_n(t)$ so that $|\phi(t)-p_n(t)|<\epsilon$. It follows that

$$|f(x)-p_n(e^{-x})|<\epsilon,\ 0<x<\infty.$$

Now

$$P(u;f)=e^{-xu}\sum_0^\infty\frac{(ux)^v}{v!}f(v/u),$$

and for $p_n(e^{-x})$

$$P(u;p_n)=e^{-xu}\sum_0^\infty\frac{(ux)^v}{v!}\sum_0^n a_ke^{-kv/u}$$

$$=e^{-xu}\sum_0^n a_k\sum_0^\infty\frac{(ux\exp\ (-k/u))^v}{v!}$$

$$=e^{-xu}\sum_0^n a_k\exp\ (ux\exp\ (-k/u))$$

$$=\sum_0^n a_ke^{-ux(1-\exp -k/u)}.$$

Clearly for $u\to\infty$, $P(u;p_n)\to p_n(e^{-x})$ uniformly in $(0,\infty)$; furthermore

$$f(x)=p_n(e^{-x})+\epsilon_n(x),\ |\epsilon_n(x)|<\epsilon,$$

UNIVERSITY OF MICHIGAN LIBRARIES

and

$$P(u;f)=P(u,f-p_n)+P(u,p_n).$$

Here

$$|P(u;f-p_n)|<\epsilon,$$

hence

$$|P(u;f)-f(x)|<\epsilon+|P(u;p_n)-f(x)|\leqq\epsilon+$$
$$|P(u;p_n)-p_n(e^{-x})|+|p_n(e^{-x})-f(x)|.$$

Thus, the theorem:

Theorem 3. If $f(x)$ is continuous in $(0,\infty)$ then $P(u;f)\to f(x)$ uniformly in $(0,\infty)$.

6. *Theorem* 4. If $f(x)$ is r-times differentiable, $f^{(r)}(x)=0(x^k)$ as $x\to\infty$, for some $K>0$, and if $f^{(r)}(x)$ is continuous at a point ζ, then $P^{(r)}(u;f)$ converges uniformly to $f^{(r)}(x)$ at $x=\zeta$.

We write $1/u=h$, and introduce the notation

$$\Delta f(vh)=f(\overline{v+1}h)-f(vh).$$

$$\Delta^2 f(vh)=\Delta\Delta f(vh)=f(\overline{v+2}h)-2f(\overline{v+1}h)+f(vh).$$

$$\Delta^r f(vh)=\Delta\Delta^{r-1}f(vh)$$
$$=\sum_{k=0}^{r}(-1)^k\binom{r}{k}f(\overline{v+k}h),\ r\geqq 0.$$

$$P(1/h;f)=Q(h;f)=e^{-x/h}\sum_{v=0}^{\infty}1/v!\left(\frac{x}{h}\right)^v f(vh).$$

Lemma 3. We have

$$e^{x/h}\frac{d^r}{dx^r}Q(h;f)=\sum_0^\infty\Delta^r f(vh)\,1/v!\left(\frac{x}{h}\right)^v h^{-r}.$$

Differentiation gives

$$\frac{d}{dx}Q(h;f)=e^{-x/h}\sum_0^\infty\frac{1}{(v-1)!}\left(\frac{x}{h}\right)^{v-1}\frac{1}{h}f(vh)-$$
$$\frac{1}{h}e^{-x/h}\sum_0^\infty\frac{1}{v!}\left(\frac{x}{h}\right)^v f(vh)$$
$$=\frac{1}{h}e^{-x/h}\sum_0^\infty\frac{1}{v!}\left(\frac{x}{h}\right)^v\Delta f(vh).$$

The lemma now follows by induction.
It is known that

$$\frac{\Delta^r f(vh)}{h^r}=f^{(r)}(\eta),$$

where

$$vh<\eta<(v+r)h.$$

Now

$$D_rQ(h;f)-f^{(r)}(x)$$
$$=e^{-x/h}\sum_0^\infty\left\{\frac{h^{-r}\Delta^r f(vh)-f^{(r)}(x)}{v!}\right\}\left(\frac{x}{h}\right)^v$$
$$=e^{-x/h}\left\{\sum_{|vh-x|\leqq\delta}+\sum_{|vh-x|>\delta}\right\},$$

where we assume that $|x-\zeta|<\delta$. Using the same device as in the proof of theorem 1, we get theorem 4. For Bernstein's polynomials see G. Lorentz [5], and his reference to Wigert's work.

For $\rho=1$ theorem 2 and formula (6) suggest the following proposition:

Theorem 5. If $f(x)$ is bounded in every finite interval, if it is differentiable at a point $\zeta>0$, and if $f(x)=0(x^k)$ for some $k>0$, $x\to\infty$, then

$$u^{1/2}\{P(u;f(\zeta))-f(\zeta)\}\to 0,\ u\to\infty.$$

Let

$$\max\left|\frac{f(\zeta+h)-f(\zeta)}{h}-f'(\zeta)\right|=\mu(\delta,\zeta)=\mu(\delta),$$

then $\mu(\delta)\to 0$ as $\delta\to 0$. We may write

$$f(\zeta+h)-f(\zeta)=hf'(\zeta)+h\epsilon(\zeta,h),$$

where

$$|\epsilon(\zeta,h)|\leqq\mu(\delta)\text{ for }|h|\leqq\delta.$$

Now

$$P(u;f(\zeta))-f(\zeta)=e^{-u\zeta}\sum_0^\infty\frac{(u\zeta)^v}{v!}\left\{\left(\frac{v}{u}-\zeta\right)f'(\zeta)+\left(\frac{v}{u}-\zeta\right)\epsilon_v(u)\right\},$$

where

$$|\epsilon_v(u)|\leqq\mu(\delta)\text{ for }\left|\frac{v}{u}-\zeta\right|\leqq\delta.$$

Utilizing formula (6) we get

$$P(u;f)-f(\zeta)=\frac{1}{u}e^{-u\zeta}\sum_0^\infty\frac{(u\zeta)^v}{v!}(v-u\zeta)\epsilon_v(u)$$
$$=\frac{1}{u}e^{-u\zeta}\left\{\sum_{|v-u\zeta|\leqq\delta u}+\sum_{|v-u\zeta|>\delta u}\right\}.$$

Using the same device as in the proof of theorem 1, and employing lemma 2, we can complete the proof of theorem 3.

The result can be generalized to higher derivatives. We restrict ourselves here to the case that $f''(\zeta)$ exists. Thus,

$$f(\zeta+h)-f(\zeta)=hf'(\zeta)+\frac{1}{2}h^2\{f''(\zeta)+\epsilon(\zeta,h)\},$$

where

$$|\epsilon(\zeta, h)| \leqq \eta(\delta) \text{ for } |h| \leqq \delta, \text{ and } \eta(\delta) \to 0,\ \delta \to 0.$$

Now

$$P\{u; f(\zeta)\} - f(\zeta) = e^{-u\zeta} \sum_0^\infty \frac{(u\zeta)^v}{v!} \left\{ \left(\frac{v}{u} - \zeta \right) f'(\zeta) + \frac{1}{2} \left(\frac{v}{u} - \zeta \right)^2 f''(\zeta) \right\} + e^{-u\zeta} \sum_0^\infty \frac{(u\zeta)^v}{v!} \frac{1}{2} (v/u - \zeta)^2 \epsilon_v(u),$$

where

$$|\epsilon_v(u)| \leqq \eta(\delta) \text{ for } \left| \frac{v}{u} - \zeta \right| \leq \delta. \tag{9}$$

It follows from formulas 4 and 6 that

$$P(u; f(\zeta)) - f(\zeta) = \frac{\zeta}{2u} f''(\zeta) + \frac{e^{-u\zeta}}{2u^2} \sum_0^\infty \frac{(u\zeta)^v}{v!} (v - u\zeta)^2 \epsilon_v(u),$$

or

$$u\{P(u; f) - f(\zeta)\} = \frac{1}{2} \zeta f''(\zeta) + \frac{e^{-u\zeta}}{2u} \sum_0^\infty \frac{(u\zeta)^v}{v!} (v - u\zeta)^2 \epsilon_v(u).$$

We write

$$\sum_0^\infty \frac{(u\zeta)^v}{v!} (v - u\zeta)^2 \epsilon_v(u) = \sum_{|v - u\zeta| \leqq u\delta} + \sum_{|v - u\zeta| > u\delta} = T_1 + T_2, \text{ say.}$$

From (9) and (4),

$$|T_1| < \eta(\delta) u\zeta e^{u\zeta}. \tag{10}$$

Hence,

$$\frac{e^{-u\zeta}}{2u} |T_1| < \frac{1}{2} \eta(\delta) \zeta.$$

Next write

$$T_2 = \sum_{v < u(\zeta - \delta)} + \sum_{v > u(\zeta + \delta)} = T_3 + T_4, \text{ say,}$$

and note that

$$\frac{1}{2} \left(\frac{v}{u} - \zeta \right)^2 \epsilon_v(u) = f\left(\frac{v}{u} \right) - f(\zeta) - (v/u - \zeta) f'(\zeta) - \frac{1}{2} \left(\frac{v}{u} - \zeta \right)^2 f''(\zeta).$$

Let

$$\sup |f(x)| = M(\zeta), x \leqq \zeta$$

then

$$|T_3| < \left\{ 2M(\zeta) + \zeta |f'(\zeta)| + \frac{1}{2} \zeta^2 |f''(\zeta)| \right\} \sum_{u\zeta - v > u\delta} u^2 \xi^2 \frac{1}{v!} (u\zeta)^v,$$

We now employ the formula (see e. g. [2], p. 200)

$$\sum_{|v - u| > \delta u} e^{-u} \frac{u^v}{v!} = 0\left(\exp\left(-\frac{1}{3} \delta^2 u \right) \right), u \to \infty$$

It follows that

$$e^{-u\zeta} \sum_{u\zeta - v > u\delta} \frac{(u\zeta)^v}{v!} = 0\left(\exp\left(-\frac{1}{3} \frac{\delta^2}{\zeta} u \right) \right),$$

so that

$$\frac{e^{-u\zeta}}{u} T_3 = 0\left\{ u \exp\left(-\frac{1}{3} \frac{\delta^2}{\zeta} u \right) \right\}.$$

Finally, in view of $f(x) = 0(x^k)$, we have for $v > u\zeta$ and $k \geq 2$

$$(v - u\zeta)^2 \epsilon_v(u) = 0\left(u^2 \frac{v^k}{u^k} \right),$$

hence

$$T_4 = 0\left(\sum_{v - u\zeta > u\delta} \frac{(u\zeta)^v}{v!} \frac{v^k}{u^k} \right) = 0\left(\sum_{v - u\zeta > u\delta} u^2 \frac{(u\zeta)^{v-k}}{(v-k)!} \right)$$

$$= 0\left(\sum_{v - u\zeta > u\delta - k} u^2 \frac{(u\zeta)^v}{v!} \right) = 0\left\{ u^2 \exp\left(u\zeta - \frac{\delta^2}{3\zeta} u \right) \right\}.$$

Thus,

$$\frac{e^{-u\zeta}}{u} T_4 = 0\left\{ u \exp\left(-\frac{1}{3\zeta} \delta^2 u \right) \right\}. \tag{11}$$

Summarizing, from (10) and (11),

$$\limsup |u\{P(u; f(\zeta) - f(\zeta)\} - \frac{1}{2} \zeta f''(\zeta)| \leqq \delta.$$

But δ is arbitrarily small, hence the theorem:

Theorem 6. If $f(x)$ is bounded in every finite interval, if it is twice differentiable at a point $\zeta > 0$, and if for some $k > 0$ $f(x) = 0(x^k)$, $x \to \infty$, then

$$u\{P(u; f(\zeta)) - f(\zeta)\} \to \frac{1}{2} \zeta f''(\zeta), u \to \infty.$$

Analogous theorems for Bernstein's polynomials were given in [1] and [8].

8 In the terminology of probability distribution the Bernstein polynomial corresponds to the binomial distribution. The distribution function is

$$\sum_{v \leqq r} \binom{n}{v} t^v (1-t)^{n-v} = F_n(r);$$

UNIVERSITY OF MICHIGAN LIBRARIES

the linear functional $B_n(t;f)$ is

$$\int_0^1 f(r/n)dF_n(r)=\sum_{v=0}^{n} f(v/n)\binom{n}{v}t^v(1-t)^{n-v}.$$

Similarly, $P(u;f)$ corresponds to the Poisson distribution; the distribution function is

$$\sum_{v\le r}\frac{x^v}{v!}e^{-x}=G(r,x),$$

and

$$P(u;f)=\int_0^\infty f(r/u)dG(r,ux)=\sum_{v=0}^{\infty} e^{-ux}\frac{(ux)^v}{v!}f(v/u);$$

here the term with the largest weight has the index $v\sim ux$. In the Bernoulli polynomial the term with the largest weight has the index $v\sim tn$.

If instead of a function f we consider a sequence $S_0, S_1, S_2, \ldots$, then to the transform (1) corresponds

$$\sum_{v=0}^{n}\binom{n}{v}t^v(1-t)^{n-v}S_v, n\to\infty, \qquad (9)$$

which defines the generalized Euler summability, and to the transform (2) corresponds

$$e^{-x}\sum_{v=0}^{\infty}\frac{x^v}{v!}S_v, x\to\infty,$$

which gives Borel's summability method.

9. To approximate a function $f(x)$ over the whole real axis, we write

$$f(x)=\frac{f(x)+f(-x)}{2}+\frac{f(x)-f(-x)}{2}=f_1(x)+f_2(x), \text{ say};$$

obviously

$$f_1(-x)=f_1(x), f_2(-x)=-f_2(x).$$

Now

$$P(u;f)=P(u;f_1)+P(u;f_2);$$

here

$$P(u;f_1)=e^{-ux}\sum_{0}^{\infty}\frac{(ux)^v}{v!}f_1(v/u),$$

and if we change x into $-x$, u into $-u$, we get

$$P(-u;f_1(-x))=P(u;f_1(x)),$$

so that our previous results are directly applicable. Similarly,

$$P(-u;f_2(-x))=-P(u;f_2(x));$$

thus for negative values of x we need only change u into $-u$, and revert to our previous results.

10. It follows from a well-known property of the Beta function that

$$\binom{n}{v}\int_0^1 t^v(1-t)^{n-v}dt=\frac{1}{n+1}, v=0,1,\cdots,n;$$

hence

$$\int_0^1 B_n(t)dt=\frac{1}{n+1}\sum_{v=0}^{n} f(v/n),$$

so that for any Riemann integrable function

$$\int_0^1 B_n(t)dt\to\int_0^1 f(t)dt.$$

Similarly, at first formally

$$\int_0^\infty P(u;f)dx=\sum_0^\infty\frac{u^v}{v!}f(v/u)\int_0^\infty e^{-xu}x^v dx=$$

$$\frac{1}{u}\sum_0^\infty f(v/u);$$

the interchange of integration and summation is legitimate if the series $\sum f(v/u)$ is convergent. Thus, the formula

$$\int_0^\infty P(u;f)dx=\frac{1}{u}\sum_0^\infty f(v/u)$$

is valid if both sides exist. However, it is a delicate question under what conditions

$$\lim_{u\to\infty}\frac{1}{u}\sum_0^\infty f(v/u)\to\int_0^\infty f(x)dx.$$

An extensive literature deals with this question.

References

[1] S. Bernstein, Complément à l'article de E. Voronovskaja, Détermination de la forme, etc. Compt. Rend. l'acad. sci. URSS, **4,** 86 to 92 (1932).

[2] G. H. Hardy, Divergent series (Oxford Univ. Press., 1949).

[3] F. Herzog and J. D. Hill, The Bernstein polynomials for discontinuous functions, Am. J. Math., **68,** 109 to 124 (1946).

[4] M. Kac, Une remarque sur les polynomes de M. S. Bernstein, Studia Mathematica, **7,** 49 to 51, **8,** 170 (1938).

[5] G. Lorentz, Zur theorie der polynome von S. Bernstein, Mathematicheskii Sbornik (Recuil Mathematique), Nouvelle Serie, **2,** (44) 543 to 556 (1937).

[6] G. Pólya and G. Szegö, Aufgaben und Lehrsätze aus der Analysis, **1,** Berlin (1925).

[7] T. Popoviciu, Sur l'approximation de functions convexes d'ordre superieur, Mathematica, **10,** 49 to 54 (1935).

[8] E. Voronovskaja, Détermination de la forme asymptotique de l'approximation des fonctions par les polynômes de S. Bernstein, Compt. Rend. l' acad. sci. URSS, **4,** 79 to 85 (1932).

Attention is called to relevant work of Einar Hille (see Proc. Nat. Acad. Sci., p. 421 to 424 (Oct. 28, 1942), and his book: Functional analysis and semi-groups, Am. Math. Soc. Colloqu. publications **31,** 186 to 189, 323 to 325, 332 to 333 (1948), where transform (2) is dealt with as a special case of a more general transformation. It contains in particular some part of the results of this paper.

LOS ANGELES, November 9, 1949.

Journal of Research of the National Bureau of Standards Vol. 45, No. 3, September 1950 Research Paper 2132

Numerical Determination of Characteristic Numbers [1]

By W. E. Milne

This paper represents a contribution to the problem of characteristic values and characteristic solutions of ordinary linear differential equations. The problem is conceived as a vibration problem in x and t. The partial differential equation is then approximated by a difference equation in both entries. The problem is now to find those frequencies in which a separation in x and t takes place. This is done by finding the roots of a trigonometric expansion of certain order. The method is applied to a number of interesting cases that illustrate various types of situations encountered in problems of physics and engineering.

An improved method for obtaining the latent roots of a matrix has been devised by Cornelius Lanczos of this Bureau. He has shown further how this process may be used to secure the characteristic numbers (eigenwerte) belonging to a boundary value problem associated with an ordinary linear differential equation. The purpose of this note is to present a procedure for calculating characteristic numbers, based essentially on this method of Lanczos, but modified in such a way as to provide a simple numerical routine for the computation. A number of numerical examples, worked in full, illustrate the procedure and give an indication of the accuracy attained. The exposition is limited to the case of differential equations of the second order, but the method is capable of extension to cases of higher order.

1. *The problem.* Let

$$L(u)=P_0(x)\frac{d^2u}{dx^2}+P_1(x)\frac{du}{dx}+P_2(x)u.$$

The problem before us is to find those characteristic values of λ for which the differential system

$$\left.\begin{aligned} &L(u)+\lambda^2u=0\\ &u+g\frac{du}{dx}=0 \text{ at } x=a\\ &u+G\frac{du}{dx}=0 \text{ at } x=b \end{aligned}\right\} \qquad (1)$$

possesses nonzero solutions in the interval $a\leqq x\leqq b$.

Problems of this type arise in many different ways in mathematical physics. For example, they may occur in connection with the heat equation

$$\frac{\partial V}{\partial t}=L(V),$$

if we assume particular solutions of the form

$$V=u(x)e^{-\lambda^2t},$$

or in connection with the wave equation

$$\frac{\partial^2 V}{\partial t^2}=L(V),$$

[1] The preparation of this paper was sponsored (in part) by the Office of Naval Research.

UNIVERSITY OF MICHIGAN LIBRARIES

if we assume particular solutions of the form

$$V=u(x)\cos\lambda t,$$

or they may occur after separation of variables in more general partial differential equations.

The important fact is that the characteristic numbers are completely determined by the system 1, regardless of the particular physical problems from which 1 may have been derived. Consequently, in order to obtain numerical solution we may assume a fictitious partial differential system which leads to (1). The most satisfactory fictitious system for our purpose appears to be

$$\frac{\partial^2 V}{\partial t^2}=L(V), \tag{2}$$

with boundary conditions

$$\left.\begin{aligned} V+g\frac{\partial V}{\partial x}&=0 \text{ at } x=a,\\ V+G\frac{\partial V}{\partial x}&=0 \text{ at } x=b,\end{aligned}\right\} \tag{3}$$

and initial conditions

$$\left.\begin{aligned} V&=F(x) \text{ when } t=0,\\ \frac{\partial V}{\partial t}&=0 \text{ when } t=0.\end{aligned}\right\} \tag{4}$$

Following standard procedure, we assume that the solution of (2, 3, and 4) is

$$V=\sum_k c_k u_k(x)\cos\lambda_k t, \tag{5}$$

where the λ_k are the desired characteristic numbers, the $u_k(x)$ are the characteristic functions (normalized in some definite manner) and the c_k are constants depending on $F(x)$.

2. *Normalization of* $L(u)$. It will be assumed with respect to the coefficient functions in $L(u)$ that for all values of x in the interval $a\leqq x\leqq b$

(a) $P_0(x)>0$,

(b) $\frac{d}{dx}P_0(x)$ exists and is continuous,

(c) $P_1(x)$ and $P_2(x)$ are continuous.

We find it desirable to change the independent variable x to a new variable s by the relation

$$\frac{dx}{\sqrt{P_0(x)}}=ds.$$

This change of variable carries $L(u)$ into what we shall call the "normal form"

$$L(u)=\frac{d^2u}{ds^2}+p(s)\frac{du}{ds}+q(s)u,$$

where $p(s)$ and $q(s)$ are seen to be continuous in the interval $a'\leqq s\leqq b'$ corresponding to $a\leqq x\leqq b$. It will be assumed from now on that $L(u)$ has already been put in the normal form.

3. *The partial difference equation.* Let the interval $a\leqq x\leqq b$ be divided into $n+1$ equal subintervals of length

$$h=\frac{b-a}{n+1},$$

and let the value of $V(x,t)$ at the point $x=a+ih$ and at time $t=jh$, be designated by V_{ij}. Then in the differential equation

$$\frac{\partial^2 V}{\partial t^2}=\frac{\partial^2 V}{\partial x^2}+p(x)\frac{\partial V}{\partial x}+q(x)V$$

we make the substitutions

$$\frac{\partial^2 V}{\partial t^2}=\frac{V_{i,j+1}-2V_{ij}+V_{i,j-1}}{h^2},$$

$$\frac{\partial^2 V}{\partial^2 x}=\frac{V_{i+1,j}-2V_{ij}+V_{i-1,j}}{h^2},$$

$$\frac{\partial V}{\partial x}=\frac{V_{i+1,j}-V_{i-1,j}}{2h},$$

and after simplification obtain the *approximate* difference equation

$$V_{i,j+1}+V_{i,j-1}=V_{i+1,j}+V_{i-1,j}+\frac{hp_i}{2}[V_{i+1,j}-V_{i-1,j}]+h^2q_iV_{ij}, \tag{6}$$

in which

$$p_i=p(a+ih),\qquad q_i=q(a+ih).$$

If we assume the existence and continuity of the second derivatives of $p(x)$ and $q(x)$, and suppose that the error of eq 6 is expanded in powers of h, we find that the leading term of the error is

$$\frac{h^4}{12}\left[(p^2+2p'+2q)\frac{\partial^2 V}{\partial x^2}+(p''+pp'+2q'+2pq)\frac{\partial V}{\partial x}+(q''+pq'+q^2)V\right], \tag{7}$$

showing that the error of eq 6 is of fourth order in h.

4. *Derivation of the characteristic equation.* For simplicity in the following explanation, let us suppose that in the boundary conditions $g=G=0$, so that $V_{0j}=0$, $V_{n+1,j}=0$. For $t=0$ (or $j=0$) the values of V_{i0} are arbitrary (being equal to the arbitrary function $F(x)$). Hence we choose these in the most convenient manner, say $V_{10}\neq 0$, $V_{i0}=0$, $i>1$. Then we have for V_{ij} the array of values

j \ i	0	1	2	3	. . .	n	$n+1$
0	0	V_{10}	0	0	. . .	0	0
1	0	V_{11}	V_{21}	0		0	0
2	0	V_{12}	V_{22}	V_{32}	. . .	0	0
3	0	V_{13}	V_{23}	V_{33}		0	0
. . .	. . .	. . .	. . .	. . .	. . .	. . .	. . .
$n-1$	0	V_{1n-1}	V_{2n-1}	V_{3n-1}		V_{nn-1}	0
n	0	V_{1n}	V_{2n}	V_{3n}		V_{nn}	0

(8)

As just explained, the entries of the first row are arbitrary and are chosen as shown for convenience. To obtain the second row we use eq 6, together with the relation

$$V_{t,1}=V_{t,-1},$$

derived from the condition $\partial V/\partial t=0$ at $t=0$. All remaining rows are computed by eq 6.

So far no restriction has been placed on the magnitude of the interval h. We now impose the condition that h is chosen small enough that

$$|\tfrac{1}{2}hp_i|<1,$$

for all values of i.

It will then be seen from array 8, together with eq 6, that the entry in the principal diagonal in the second column is given by

$$V_{21}=\tfrac{1}{2}(1-\tfrac{1}{2}hp_2)\,V_{10},$$

whereas for subsequent columns the entries in the principal diagonal are

$$V_{32}=(1-\tfrac{1}{2}hp_3)\,V_{21},$$

$$V_{43}=(1-\tfrac{1}{2}hp_4)\,V_{32},$$

etc.

Since by our choice $V_{10}\neq 0$ no entry in the principal diagonal is zero, and the n-square matrix obtained from (8) by dropping the first and last columns and the last row is not singular. Then there will exist n constants $A_0, A_1, \ldots, A_{n-1}$ such that

$$\sum_{j=0}^{n}A_jV_{ij}=0 \text{ for } i=1, 2, \ldots, n,$$

(where $A_n=1$).

Now from eq 5 we have

$$V_{ij}=\sum_{k=1}^{n}c_ku_{ki}\cos\lambda_khj,$$

where $u_{ki}=u_k(a+ih)$. Therefore,

$$\sum_{k=1}^{n}c_ku_{ki}\sum_{j=0}^{n}A_j\cos\lambda_khj=0, \qquad i=1, 2, \ldots, n.$$

It can be shown that these equations imply

$$\sum_{j=0}^{n}A_j\cos\lambda_khj=0, \qquad k=1, 2, \ldots, n.$$

It is apparent, therefore, that the desired characteristic numbers λ_k are given by

$$\lambda_k=\mu_k/h, \qquad k=1, 2, \ldots, n,$$

where $\mu_1, \mu_2, \ldots, \mu_n$ are roots of the characteristic equation

$$\cos n\mu+A_{n-1}\cos(n-1)\mu+\cdots+A_1\cos\mu+A_0=0. \tag{9}$$

The λ_k thus found are correct for the *difference* equation with the given boundary conditions but in general are only approximations to the λ_k belonging to the differential system 1.

5. *The characteristic functions.* In order to obtain numerical values for the characteristic function u_{ki} associated with λ_k, we substitute

$$V_{ij}=u_{ki}\cos\mu_kj,$$

in eq 6. Since

$$V_{i,j+1}+V_{i,j-1}=2V_{ij}\cos\mu_k,$$

the result, after removal of the factor $\cos\mu_kj$, may be put in the form

$$(1+\tfrac{1}{2}hp_i)\;u_{k,i+1}=(2\cos\mu_k-h^2q_i)u_{ki}-(1-\tfrac{1}{2}hp_i)\;u_{k,i-1}. \tag{10}$$

This is an ordinary difference equation of second order. We may choose any nonzero value for u_{k1}, say

$$u_{k1}=1.$$

UNIVERSITY OF MICHIGAN LIBRARIES

Since $u_{k0}=0$ we obtain $u_{k,2}$ from eq 10, then $u_{k,3}$, etc. The fact that $u_{k,n+1}$ should turn out to be zero serves as a check on the calculations.

As a very simple example, let us take the system

$$\frac{d^2u}{dx^2}+\lambda^2u=0,$$

$$u=0 \qquad \text{at } x=0,$$

$$u=0 \qquad \text{at } x=1.$$

Let $h=1/6$. For this system eq 6 becomes

$$V_{i,j+1}+V_{i,j-1}=V_{i+1,j}+V_{i-1,i},$$

and if we take $V_{1,0}=2$ the array (8) turns out to be

0	2	0	0	0	0	0
0	0	1	0	0	0	0
0	−1	0	1	0	0	0
0	0	−1	0	1	0	0
0	0	0	−1	0	1	0
0	0	0	0	−1	0	0

From this we have immediately

$$A_0=A_2=A_4=0,$$

$$A_1=A_3=1,$$

and the characteristic equation is

$$\cos 5\mu+\cos 3\mu+\cos \mu=0,$$

or in factored form

$$\cos 3\mu\ (2\cos \mu+1)=0.$$

From the second form we read off the roots at once.

$$\mu_1=\frac{\pi}{6},\ \mu_2=\frac{2\pi}{6},\ \mu_3=\frac{3\pi}{6},\ \mu_4=\frac{4\pi}{6},\ \mu_5=\frac{5\pi}{6},$$

whence

$$\lambda_k=k\pi, \qquad k=1,\ 2,\ 3,\ 4,\ 5.$$

To obtain values of the characteristic functions, we resort to eq 10, which here becomes

$$u_{k,i+1}=2\ (\cos \mu_k)u_{k,i}-u_{k,i-1},$$

where $\cos \mu_1=\frac{1}{2}\sqrt{3}$, $\cos \mu_2=\frac{1}{2}$, $\cos \mu_3=0$, $\cos \mu_4=-\frac{1}{2}$, $\cos \mu_5=-\frac{1}{2}\sqrt{3}$.

Upon calculating the u_{ki} with this difference equation we have

i	=	0	1	2	3	4	5	6
u_{1i}	=	0	1	$\sqrt{3}$	2	$\sqrt{3}$	1	0
u_{2i}	=	0	1	1	0	−1	−1	0
u_{3i}	=	0	1	0	−1	0	1	0
u_{4i}	=	0	1	−1	0	1	−1	0
u_{5i}	=	0	1	$-\sqrt{3}$	2	$-\sqrt{3}$	1	0

This particular example is remarkable in that the values obtained for the λ_k and for the u_{ki} not only are exact for the difference equation but are also exact for the differential system from which we started. We know, of course, that the correct λ's are given by

$$\lambda_k=k\pi.$$

We readily see that the values obtained numerically for u_{ki} are also the values of the true characteristic functions

$$u_1(x)=2 \sin \pi x,$$

$$u_2(x)=\frac{2}{\sqrt{3}} \sin 2\pi x,$$

$$u_3(x)=\sin 3\pi x,$$

$$u_4(x)=\frac{2}{\sqrt{3}} \sin 4\pi x,$$

$$u_5(x)=2 \sin 5\pi x.$$

When $p(x)$ or $q(x)$ are different from zero, the results will no longer be exact but only approximate.

Several examples follow, showing the numerical calculations and comparing the values obtained with the correct values. Each of the examples illustrates a slightly different aspect of the process. Examples 1 and 2 differ only in the number of intervals employed. Example 3 illustrates the case of variable coefficients. In examples 1, 2, 3 the coefficients satisfy the conditions of continuity imposed in the foregoing discussion, whereas in 4 and 5 these conditions are not satisfied.

The values of the characteristic functions were also computed in the case of Example 4, and compared with the correct values.

Characteristic numbers: Example 1

Differential equation: $\frac{d^2u}{dx^2}+2\frac{du}{dx}+\lambda^2u=0$

Boundary conditions: $u=0$ at $x=0$ and at $x=1$

Interval: $h=1/8$

Difference equation: $V_{i,j+1}=\frac{1}{8}[7V_{i-1,j}+9V_{i+1,j}]-V_{i,j-1}$

Boundary conditions: $V_{0,j}=V_{8,j}=0$

0	1	2	3	4	5	6	7	8
0	2097152	0	0	0	0	0	0	0
0	0	917504	0	0	0	0	0	0
0	−1064960	0	802816	0	0	0	0	0
0	0	−946176	0	702464	0	0	0	0
0	512	0	−840448	0	614656	0	0	0
0	0	1120	0	−746368	0	537824	0	0
0	748	0	1764	0	−662676	0	470596	0
0	0	1519	0	2401	0	−588245	0	0

Characteristic equation:

$F(\mu)=\cos 7\mu+(1.09375)\cos 5\mu+(1.15869)\cos 3\mu+(1.19191)\cos \mu=0$

k	μ_k	[a]λ_k^*	[b]λ_k	Relative error
	Degrees			
1	23. 561	3. 2898	3. 2969	−0. 00215
2	45. 448	6. 3457	6. 3623	−0. 00261
3	67. 686	9. 4507	9. 4777	−0. 00285
4	90	12. 5664	12. 6061	−0. 00315
5	112. 314	15. 6820	15. 7398	−0. 00367
6	134. 552	18. 7870	18. 8761	−0. 00472
7	156. 439	21. 8430	22. 0139	−0. 00776

[a]λ_k^*=calculated value.
[b]λ_k=correct value.

UNIVERSITY OF MICHIGAN LIBRARIES

Characteristic numbers: Example 2

Differential equation: $\frac{d^2u}{dx^2}+2\frac{du}{dx}+\lambda^2u=0$

Boundary conditions: $u=0$ at $x=0$ and at $x=1$

Interval: $h=1/16$

Difference equation: $V_{i,j+1}=\frac{1}{16}[15V_{i-1,j}+17V_{i+1,j}]-V_{i,j-1}$

Boundary conditions: $V_{0,j}=V_{16,j}=0$

0	1	2	3	4	5	6	7	8	9	10	11	12	13	14	15	16
0	115292	0	0	0	0	0	0	0	0	0	0	0	0	0	0	0
0	0	54043	0	0	0	0	0	0	0	0	0	0	0	0	0	0
0	−57871	0	50665	0	0	0	0	0	0	0	0	0	0	0	0	0
0	0	−54465	0	47499	0	0	0	0	0	0	0	0	0	0	0	0
0	1.7592	0	−51259	0	44530	0	0	0	0	0	0	0	0	0	0	0
0	0	4.1232	0	−48241	0	41747	0	0	0	0	0	0	0	0	0	0
0	2.6216	0	6.9578	0	−45400	0	39138	0	0	0	0	0	0	0	0	0
0	0	5.7273	0	10.147	0	−42726	0	36692	0	0	0	0	0	0	0	0
0	3.4636	0	9.1926	0	13.590	0	−40208	0	34399	0	0	0	0	0	0	0
0	0	7.2869	0	12.910	0	17.199	0	−37838	0	32249	0	0	0	0	0	0
0	4.2787	0	11.356	0	16.788	0	20.902	0	−35608	0	30233	0	0	0	0	0
0	0	8.7900	0	15.573	0	20.748	0	24.634	0	−33508	0	28344	0	0	0	0
0	5.0606	0	13.431	0	19.856	0	24.723	0	28.344	0	−31532	0	26572	0	0	0
0	0	10.225	0	18.116	0	24.136	0	28.658	0	31.985	0	−29672	0	24.911	0	0
0	5.8035	0	15.403	0	22.772	0	28.354	0	32.508	0	35.522	0	−27921	0	23354	0
0	0	11.581	0	20.519	0	27.339	0	32.463	0	36.233	0	38.924	0	−26274	0	0

Characteristic equation:

$F(\mu)=\cos 15\mu+(1.05469)\cos 13\mu+(1.10275)\cos 11\mu+(1.14366)\cos 9\mu$
$+(1.17695)\cos 7\mu+(1.20225)\cos 5\mu+(1.21928)\cos 3\mu$
$+(1.22784)\cos \mu=0.$

k	μ_k	[a] λ_k^*	[b] λ_k	Relative error
	Degrees			
1	11.800	3.2952	3.2969	−0.00052
2	22.769	6.3583	6.3623	− .00063
3	33.917	9.4715	9.4777	− .00065
4	45.112	12.5976	12.6061	− .00067
5	56.325	15.7289	15.7398	− .00069
6	67.546	18.8625	18.8761	− .00072
7	78.772	21.9974	22.0139	− .00075
8	90	25.1327	25.1526	− .00079
9	101.228	28.2681	28.2920	− .00084
10	112.454	31.4030	31.4318	− .00092
11	123.675	34.5366	34.5720	− .00102
12	134.888	37.6679	37.7124	− .00118
13	146.083	40.7940	40.8529	− .00144
14	157.231	43.9072	43.9937	− .00197
15	168.200	46.9703	47.1345	− .00348

[a] λ_k^*=calculated value.
[b] λ_k=correct value.

Characteristic numbers: Example 3

Differential equation: $4x\frac{d^2u}{dx^2}+\lambda^2 u=0$

Boundary conditions: $u=0$ at $x=1$ and at $x=4$

Change variable: $x=s^2$

Normal equation: $\frac{d^2u}{ds^2}-\frac{1}{s}\frac{du}{ds}+\lambda^2 u=0$, $u=0$ at $s=1$ and at $s=2$

Interval: $h=1/8$

Difference equation: $V_{i,\,i+1}=\frac{1}{2i}\left[(2i+1)V_{i-1,\,i}+(2i-1)V_{i+1,\,i}\right]-V_{i,\,i-1}$

Boundary conditions: $V_{8,\,i}=V_{16,\,i}=0$

8	9	10	11	12	13	14	15	16
0	13178880	0	0	0	0	0	0	0
0	0	6918912	0	0	0	0	0	0
0	−6644352	0	7233408	0	0	0	0	0
0	0	−7023744	0	7534800	0	0	0	0
0	10816	0	−7384104	0	7824600	0	0	0
0	0	20202	0	−7728000	0	8104050	0	0
0	8263. 667	0	28497	0	−8057475	0	8374185	0
0	0	15547	0	35937. 5	0	−8374185	0	0

Characteristic equation:

$F(\mu)=\cos 7\mu+(1.03333)\cos 5\mu+(1.05506)\cos 3\mu+(1.06578)\cos\mu=0.$

k	μ_k	[a]λ_k^*	[b]λ_k	Relative error
	Degrees			
1	22. 873	3. 1936	3. 1966	−0. 00094
2	45. 164	6. 3060	6. 3124	−0. 00101
3	67. 568	9. 4343	9. 4445	−0. 00108
4	90	12. 5664	12. 5812	−0. 00118
5	112. 432	15. 6984	15. 7199	−0. 00137
6	134. 836	18. 8267	18. 8595	−0. 00174
7	157. 127	21. 9391	21. 9997	−0. 00275

[a] λ_k^* = calculated value.
[b] λ_k = correct value

UNIVERSITY OF MICHIGAN LIBRARIES

Characteristic numbers: Example 4

(Differential equation with singular point)

Differential equation: $\frac{d^2u}{dx^2}+\frac{1}{x}\frac{du}{dx}+\lambda^2u=0$

Boundary conditions: u finite at $x=0$, $u=0$ at $x=1$

Interval: $h=1/8$

Difference equation: $V_{i,j+1}=\frac{1}{2i}[(2i-1)V_{i-1,j}+(2i+1)V_{i+1,j}]=V_{i,j-1}$

Boundary conditions: $V_{0,j+1}=4V_{1,j}-2V_{0,j}-V_{0,j-1}$

$V_{8,j}=0$

0	1	2	3	4	5	6	7	8
1	0	0	0	0	0	0	0	0
−1	0. 25	0	0	0	0	0	0	0
2	−0. 5	0. 1875	0	0	0	0	0	0
−5	1. 03125	−0. 375	0. 15625	0	0	0	0	0
12. 125	−2. 5625	0. 78125	−0. 3125	0. 13672	0	0	0	0
−29. 5	6. 203125	−1. 9375	0. 65430	−0. 27344	0. 12305	0	0	0
71. 6875	−15. 09375	4. 68896	−1. 62109	0. 57422	−0. 24609	0. 11279	0	0
−174. 25	36. 67407	−11. 40918	3. 92310	−1. 421875	0. 51782	−0. 22558	0. 10473	0
423. 50879	−89. 14502	27. 72046	−9. 54541	3. 44104	−1. 28174	0. 47534	−0. 20947	0

Characteristic equation:

$F(\mu)=\cos 8\,\mu+2\cos 7\,\mu+(-0.21438)\cos 6\,\mu+(1.57126)\cos 5\,\mu+(-0.32580)\cos 4\,\mu+(1.41947)\cos 3\,\mu+(-0.35057)\cos 2\,\mu+(1.36154)\cos\mu+(-0.17790)=0$

k	μ_k	[a] λ_k^*	[b] λ_k	Relative error
	Degrees			
1	17. 212	2. 4032	2. 4048	−0. 00067
2	39. 518	5. 5178	5. 5201	−0. 00042
3	62. 000	8. 6568	8. 6537	+0. 00036
4	84. 623	11. 8156	11. 7915	0. 00204
5	107. 545	15. 0161	14. 9309	0. 00571
6	131. 028	18. 2950	18. 0711	0. 01239
7	155. 614	21. 7278	21. 2116	0. 02434

[a] λ_k^*=calculated value.
[b] λ_k=correct value.

Calculation of characteristic functions for example 4

$$V_{k,i-1}=\frac{1}{2i-1}\,[[4i\cos\mu_k]V_{ki}-(2i+1)V_{k,i+1}]$$

$V_{k8}=0,\ V_{k7}=1$ $\qquad\qquad$ $h=1/8$

k \ i	0	1	2	3	4	5	6	7	8
1	6. 06564	5. 94118	5. 54449	4. 90869	4. 07722	3. 10550	2. 05727	1	0
2	−4. 25902	−3. 78297	−2. 47048	−0. 77879	0. 73496	1. 61344	1. 66115	1	0
3	3. 78121	2. 76528	0. 47188	−1. 30444	−1. 38768	−0. 14450	1. 01194	1	0
4	−3. 81020	−1. 99290	1. 01301	1. 35254	−0. 49927	−1. 13784	0. 20836	1	0
5	4. 27565	1. 20726	−1. 89415	0. 15853	1. 27379	−0. 78300	−0. 62746	1	0
6	−5. 44631	−0. 14517	1. 93836	−1. 88249	0. 66491	0. 71347	−1. 36784	1	0
7	8. 51801	−1. 96624	−0. 52633	1. 92273	−2. 53211	2. 47611	−1. 90027	1	0

Normalized so that $V_{k,0}=1$

k \ i	0	1	2	3	4	5	6	7	8
1	1	0. 97948	0. 91408	0. 80926	0. 67218	0. 51198	0. 33917	0. 16486	0
2	1	0. 88823	0. 58006	0. 18286	−0. 17257	−0. 37883	−0. 39003	−0. 23480	0
3	1	0. 73132	0. 12480	−0. 34498	−0. 36699	−0. 03822	0. 26762	0. 26447	0
4	1	0. 52304	−0. 26587	−0. 35498	0. 13104	0. 29863	−0. 05468	−0. 26245	0
5	1	0. 28236	−0. 44301	0. 03708	0. 29792	−0. 18313	−0. 14675	0. 23388	0
6	1	0. 02665	−0. 35590	0. 34565	−0. 12208	−0. 13100	0. 25115	−0. 18361	0
7	1	−0. 23083	−0. 06179	0. 22573	−0. 29727	0. 29069	−0. 22309	0. 11740	0

True values: $J_0(j_{0k}x)$

k \ i	0	1	2	3	4	5	6	7	8
1	1	0. 97754	0. 91166	0. 80679	0. 66993	0. 51014	0. 33788	0. 16421	0
2	1	0. 88447	0. 57765	0. 18368	−0. 16840	−0. 37274	−0. 38424	−0. 23137	0
3	1	0. 72818	0. 13078	−0. 33158	−0. 35628	−0. 03825	0. 25859	0. 25597	0
4	1	0. 52632	−0. 24188	−0. 33776	0. 12078	0. 28180	−0. 05069	−0. 24713	0
5	1	0. 30138	−0. 40077	0. 02667	0. 27086	−0. 16394	−0. 13336	0. 21102	0
6	1	0. 07789	−0. 31640	0. 29149	−0. 09897	−0. 11348	0. 21266	−0. 15483	0
7	1	−0. 12066	−0. 07480	0. 18221	−0. 22704	0. 21788	−0. 16591	0. 08703	0

UNIVERSITY OF MICHIGAN LIBRARIES

Characteristic numbers: Example 5

Partial differential equation: $\frac{1}{x}\frac{\partial^2 u}{\partial t^2}=\frac{\partial}{\partial x}\left(\frac{1}{x}\frac{\partial u}{\partial x}\right)$

Boundary conditions: u finite at $x=0$, $u=0$ at $x=1$

Ordinary differential equation: $\frac{d^2u}{dx^2}-\frac{1}{x}\frac{du}{dx}+\lambda^2 u=0$

Difference equation: $V_{i,j+1}=\frac{1}{2i}\left[(2i+1)V_{i-1,j}+(2i-1)V_{i+1,j}\right]-V_{i,j-1}$

Boundary conditions: $V_{0,j}=V_{8,j}=0$

0	1	2	3	4	5	6	7	8
0	40320	0	0	0	0	0	0	0
0	0	25200	0	0	0	0	0	0
0	−27720	0	29400	0	0	0	0	0
0	0	−37800	0	33075	0	0	0	0
0	8820	0	−45937. 5	0	36382. 5	0	0	0
0	0	14371. 875	0	−52820	0	39414. 375	0	0
0	−1634. 0625	0	18604. 6875	0	−59121. 5625	0	42229. 6875	0
0	0	−2460. 9375	0	22118. 90625	0	−64752. 1875	0	0

Characteristic equation:

$F(\mu)=\cos 7\mu+(1.64286)\cos 5\mu+(1.95982)\cos 3\mu+(2.10044)\cos \mu=0$

k	μ_k	[a] λ_k^*	[b] λ_k	Relative error
	Degrees			
1	27. 145	3. 7901	3. 8318	−0. 0109
2	49. 044	6. 8479	7. 0155	− . 0239
3	69. 928	9. 7638	10. 1735	− . 0403
4	90	12. 5664	13. 3237	− . 0568
5	110. 072	15. 3690	16. 4706	− . 0669
6	130. 956	18. 2849	19. 6158	− . 0678
7	152. 855	21. 3427	22. 7601	− . 0623

[a] λ_k^* = calculated value.
[b] λ_k = correct value.

Los Angeles, June 20, 1949.